Distress analysis of mice used for translational research （Reflection of a surgeon on animal welfare）

Cumulative dissertation

To obtain the academic degree

Doctor of Medicine (Dr. med.)

From the Rudolf-Zenker-Institute for Experimental Surgery

Rostock University Medical Center

Director: Prof. Dr. med. Brigitte Vollmar

Submitted by Wentao Xie

Born on 11/10/1984, Hunan, China

Rostock, 2022

https://doi.org/10.18453/rosdok_id00004344

Dieses Werk ist lizenziert unter einer
Creative Commons Namensnennung 4.0 International Lizenz.

Reviewers

PD Dr. rer. nat. Dietmar Zechner, Universitätsmedizin Rostock, Rudolf-Zenker-Institut für Experimentelle Chirurgie

PD Dr. rer. nat. Hugo Murua Escobar, Universitätsmedizin Rostock, Medizinische Klinik III für Hämatologie, Onkologie und Palliativmedizin

Univ.-Prof. Dr. med. vet. Ute Lindauer, RWTH Aachen, Klinik für Neurochirurgie

Date of submission: 17.07.2022

Date of defense: 02.05.2023

Studies of the cumulative dissertation

Study I:

Wentao Xie, Marcel Kordt, Rupert Palme, Eberhard Grambow, Brigitte Vollmar, Dietmar Zechner. Diagnostic Ability of Methods Depicting Distress of Tumor-Bearing Mice. Animals. 2021;1:2155. (IF: 3.231)

Study II:

Wentao Xie, Rupert Palme, Clemens Schafmayer, Dietmar Zechner, Brigitte Vollmar, Eberhard Grambow. Distress Analysis of Mice with Cervical Arteriovenous Fistulas. Animals. 2021;11:3051. (IF: 3.231)

Study III:

Wentao Xie, Matthias Lorenz, Friederike Poosch, Rupert Palme, Dietmar Zechner, Brigitte Vollmar, Eberhard Grambow, Daniel Strüder. 3D-printed lightweight dorsal skin fold chambers from PEEK reduce chamber-related animal distress. Sci Rep. 2022;12:11599. (IF: 4.996)

Table of Contents

1. Abstract

The assessment and improvement of animal welfare is not only an ethical requirement, but also a guarantee of efficient and high quality translational research. In recent years, sophisticated animal models were created to study human diseases. However, the assessment of distress in these animal models is scarce. In order to provide a solid basis for optimizing animal welfare in future studies, body weight, burrowing, nesting activity, faecal corticosterone metabolites (FCMs), and distress scores were analyzed in several animal models. In the first study, a frequently used subcutaneous tumor model was analyzed. Only adjusted body weight change and FCMs have a high diagnostic ability to define distress caused by large tumors. However, all these non-invasive parameters did not predict the distress in mice with small tumors. In the second study, a novel cervical arteriovenous fistula (AVF) model was studied, and the distress of this model was described for the first time. This AVF is similar to the vascular access needed for hemodialysis patients in terms of anatomical and hemodynamic characteristics. Despite a difficult surgical intervention, only moderate distress score and no major reduction of body weight, burrowing activity or nesting behavior was observed. We not only attempted to analyze the distress of existing animal models, but also tried to refine one animal model to reduce distress. Therefore, we compared, in a dorsal skinfold chamber model, a novel lightweight chamber to heavier standard titanium chambers. This new lightweight chamber significantly reduced the distress of experimental mice and led to a higher survival rate. In conclusion, such evaluations can provide an objective basis to judge the distress caused by animal experiments. This might lead to refinement of future animal experiments and thereby improve future translational research.

2. Introduction

2.1 The relationship between surgeons and translational research

The role of a surgeon is not limited to clinical work, but should also include translational research. Translational research is a discipline that brings clinical problems into the laboratory to improve patient prognosis by improving basic understanding of the disease and providing solutions.[1] Surgeons made long-term and important contributions to translational research. Thus, the Nobel Prize in Physiology or Medicine was awarded to 10 trained surgeons.[2] It is important to rapidly and effectively translate the results of basic biomedical research into theories, techniques, methods and drugs in order to improve clinical practice.[3] However, this is a complex process, multidisciplinary teams are involved in it. A large number of *in vivo* experiments have led to a tremendous understanding of the basic molecular mechanisms underlying the development of various diseases, as well as providing a theoretical basis for improved treatment options, but only few experiments actually directly improved treatment options.[2] In order to make translational research more rapid and efficient, an academic surgeon must not be marginalized.[4,5] Surgeons can not only apply the bench results to the bedside, but also give feedback to the bench about problems in specific clinical applications.[6] Without this feedback, all hypotheses generated in a preclinical setting remains speculative.[7] Therefore, surgeons should have an active role in translational research.[8–10]

2.2 Translational research requires animal experiments

Over the past few decades, biomedical research has played a huge contribution to improving human health care. As an essential component of biomedical research, animal experiments play an important role in preventing, curing, and treating a vast range of ailments.[11] For example, modern anaesthetics, modern surgical techniques including hip replacement surgery, kidney transplants, heart transplants and blood transfusions were all relied on animal research in their development.[12] Medical devices and drugs need to be tested by animal experiments, more importantly, it is illegal and potentially disastrous to apply them directly to humans.[13] One example is the infamous thalidomide teratogenic incident. Due to the lack of systematic and

comprehensive animal experiments, serious teratogenic side effects have been observed after direct application of thalidomide to humans.[14]

Animal models should ideally mimic the human disease process and resemble the human physiology.[15] For this purpose, mammals are often used for *in vivo* experiments, particularly mice. Mice have many similarities to humans in terms of anatomy and physiology and thus are wildly used in biomedical research.[16] Nowadays, there are various mouse-based animal models in translational research, such as subcutaneous tumor models,[17] autologous arteriovenous fistula (AVF) models,[18] or the dorsal skinfold chamber (DSC) model.[19]

The subcutaneous tumor model in immunodeficient mice is one of the most frequently model for routine evaluation of cancer therapies.[17] Use of human tumor cells, a high take rate and continuous monitoring are advantages, which make this model an extensively used standard for validation and assessment in oncological studies.[20] In addition, due to an abundance of published data associated with subcutaneous tumor models, it is easy to access parameters and references needed for testing novel therapies.[21]

The murine AVF model is used to understand the involved mechanisms of vascular remodeling. By anastomosing the end of a branch of the external jugular vein to the side of the common carotid artery, a novel AVF model was created to mimic the anatomical and hemodynamic characteristics in hemodialysis patients.[18] Therefore, this model might improve the translation of experimental *in vivo* results into a clinical setting.

The DSC model is one of the most frequently used models for continuous *in vivo* analysis of microcirculation for up to three weeks.[19,22–25] It allows real-time visualization of morphological and dynamic changes of the microvascular network over the time. Therefore, this model is used to investigate inflammation,[26] thrombogenesis and thrombolysis,[27] wound healing,[28] vascularization of tissue as well as biomaterial transplants,[29] ischaemia-reperfusion,[30] tumour vascularization and respective therapies[31].

2.3 Animal welfare affects animal experiments

Appropriate animal models should strictly follow ethical standards. They should maximize the likelihood of obtaining the knowledge sought and minimize animal distress. Since the public awareness of the concept of animal rights grew over the last decades, animals are also protected by national laws and international guidelines.[32–34] It is the researchers' responsibility and obligation to comply with these laws and guidelines. In addition, it was quickly noticed that animal welfare also ensures a high quality in preclinical research.[35] The effects of distress on experimental animals are multifaceted and can manifest themselves in physiological and behavioural changes. For example, distress leads to chronic inflammation and intestinal leakage in rats, and this could add variables to confound the data.[36] Moreover, distress can affect the outcome of disease in human patients [37] as well as in animals.[38–40] For example, Tymvios et al. showed that reducing suffering makes data more reproducible and less variable.[41] In addition, to affect the accuracy of research results, distress can also affect the quality of an animal model. For example, Tymvios et al. showed that reducing the suffering of mice can better mimic the development and progression of thromboembolic diseases from a pharmacological or molecular perspective.[41] Although we know the importance of animal welfare in *in vivo* experiments, the present guidelines and publications only provide little data on distress for specific animal models and on the ability of methods to measure distress.[42]

2.4 Methods for distress assessment

Distress affects animals in three aspects: physiological, behavioural, and neuroendocrine.[43] It is commonly accepted that different distress response parameters must be included when evaluating distress. Therefore, this paper used a variety of parameters to assess distress in several animal models, covering physiological, behavioural and neuroendocrine responses.

A prominent physiological response to distress in experimental animals is the reduction of body weight. Body weight is a classical and essential indicator of animal distress. As early as 1985, it had been used as a key indicator to evaluate animal distress.[44] It was reported that the distress-induced decrease in body weight may be due to an decreased food intake, increased energy expenditure and increased body

temperature.[45] Nowadays, almost all guidelines use weight loss as a criterion for euthanasia.[17,33,34]

Burrowing and nesting activity are innate behaviours in rodents.[46] Since mice can remove pellets from artificial burrows and use proper materials to build dome-shaped, complex, multilayered nests, both activities were developed to monitor distress in a non-invasive manner.[47] Numerous studies have demonstrated that burrowing and nesting activity are reduced by distress.[48,49] Compared to classical indicator of animal distress, such as body weight, animal behaviours are more sensitive to reflect animal distress. For example, when mice were given analgesic drugs after laparotomy, the burrowing activity was reduced, but the body weight was increased.[50] While reduced burrowing and nesting activity may imply a negative affective state, these behaviours in mice are kind of genetically determined and thus strain differences in performance may occur.[51,52] For example, compared to C57BL/6, BALB/c showed lower nesting activity.[51]

Glucocorticoids (GCs) can be induced by distress, and are widely used as welfare indicators. However, taking blood for assessing hormones concentration can cause stress to animals.[43] For example, capture and handing as well as the pain caused by puncture can cause distress to mice.[53] Moreover, the loss of blood and frequent blood collection also can cause body weight loss, heart rate raise and high arterial pressure.[54,55] Since GCs are metabolized in the liver and partially excreted into the faeces via bile, it is possible to test the metabolites of GCs in faeces.[43] Faecal collection dose not disturb mice, and can be used to study changes in distress-related hormones over a certain period of time, thus avoiding the appearance of hasty generalization.[56] Increased FCM concentrations are, therefore, often used as indicator of high distress. However, induction of FCMs is also strongly strain-specific. For example, unpredictable chronic mild stress induced a significant FCMs change in BALB/c, C57BL/6, DBA and FVB but not in A/J, C3H and CBA mice.[57]

Due to the limitations of using only one single variable to measure distress, clinical score sheets were designed to systematically evaluate mice distress. Usually, scoring sheets consist of more than one factor, such as body weight, general condition, spontaneous behaviour or flight behaviour.[58,59] In contrast to single variable analysis, combining multiple factors to analyse distress in mice is more

sensitive.[60,61] Nowadays, score sheets are commonly used as a non-invasive method to assess distress in mice.[62,63]

2.5 Aim of this dissertation

The aim of the dissertation was to evaluate, if evidence-based distress assessment of animal models generates new knowledge, which can improve animal welfare as well as translational research. Specifically we wanted to answer the following three questions.

1. Which methods are sensitive enough to measure mild distress of mice? To answer this question a widely used animal model for subcutaneous tumors was chosen.
2. Can distress analysis support the use of a novel animal model? To address this question, a novel cervical AVF model with a difficult surgical intervention was selected.
3. Can evidence based assessment of distress be used to improve an animal experiment? To address this issue the distress of mice carrying a lightweight or a heavy weight chamber was evaluated using a DSC mouse model.

3. Methods

All methods used are described in detail in the corresponding publications of studies I-III that are listed in the appendix. The following text briefly summarizes the most important methods.

3.1 Subcutanous tumor model

The human malignant melanoma cells A-375 (CLS, Eppelheim, Germany) and the cutaneous squamous cell carcinoma cells SCL-2 (donated by Prof. Hahn, University Medical Center Goettingen) were mixed with the same volume of cold DPBS/Matrigel® High Concentration Growth Factor Reduced (Matrigel® HC GFR, Corning, New York, USA) on ice to prepare 100 µl 1 × 10^6 tumor cells. Eighteen male 9-11 weeks old NSG mice were anesthetized by 1.5-2.5% isoflurane (CP-pharma, Burgdorf, Germany). Then the fur at the flanks of the mice was removed, and the tumor cells were injected subcutaneously into the left and right flank, respectively. The longest diameter and the diameter perpendicular to this diameter were measured using a digital caliper (fortis, E/D/E, Wuppertal, Germany) with 0.01 mm precision. Assuming hemi-ellipsoidal shape of the tumors, the volume was derived using the formula: volume = 0.52 × length x $width^2$.[64] The tumor weight was derived using the formula: weight = 1.05 × volume.[64] Mice were euthanized on day 21 by intraperitoneal (ip) injection of ketamine (90 mg/kg bodyweight) and xylazine (25 mg/kg bodyweight).

3.2 Cervical arteriovenous fistula model

Twelve male C57Bl/6 mice were used at an age of 9-15 weeks. Mice were anesthetized by continuous isoflurane treatment (1.5% isoflurane; 0.8 L/min N_2O; 0.8-1.0 L/min O_2). After subcutaneous injection of heparin (1 U/kg bodyweight), the left dorsomedial branch of the external jugular vein and the ipsilateral common carotid artery were separated through ventral incision. The left sternocleidomastoid muscle was cauterized and the carotid artery was clamped. A 1 mm incision was made on the lateral side of the artery with microscissors followed by local rinse with heparin (200 U/ml). The distal end of the vein branch was ligated, cut and anastomosed to the common carotid artery in an end-to-side fashion using 10-0 Ethilon (Johnson & Johnson Medical GmbH, Norderstedt, Germany) by interrupted

sutures. The clamps were released in a distal to proximal order. Confirming no active bleeding, the neck incision was closed. For pain relief 1250 mg/l metamizol (Ratiopharm, Ulm, Germany) was provided daily in the drinking water after AVF creation. Mice were euthanized on day 21 by ip injection of ketamine (90 mg/kg bodyweight) and xylazine (25 mg/kg bodyweight).

3.3 Dorsal skinfold chamber model

Seventeen male homozygous SKH1-hr hairless mice at 12-29 weeks old were used in this study. Mice were anesthetized ip with a mixture of ketamine (90 mg/kg bodyweight) and xylazine (25 mg/kg bodyweight). Two symmetrical titanium or Polyetheretherketone (PEEK) frames were mounted to sandwich the dorsal skinfold. Cutis, subcutis, musculus panniculus carnosus, and the retractor muscles on the side of the observation window were completely removed. After the preparation, the chamber window was covered with a removable glass coverslip incorporated in one of the frames to prevent desiccation. The two PEEK frames were fixed by sutures to the skin and to each other, respectively. However, the fixation of titanium chambers required penetration of the base of the dorsal skinfold by screws. For pain relief 1250 mg/l metamizol (Ratiopharm, Ulm, Germany) was provided daily in the drinking water after chamber mounting. When examining the microcirculation by microscope, a picture of the mouse chamber was taken, and the tilt angles of the chamber was calculated. Mice were euthanized on day 21 by ip injection of ketamine (90 mg/kg bodyweight) and xylazine (25 mg/kg bodyweight).

3.4 Analysis of animal distress

According to the following evaluation methods, the distress of experimental animals was assessed at the indicated time points. (Figure 1)

3.4.1 Body weight and distress score analysis

The body weight was measured four times per week with a scale (EMB 200-2, KERN & SOHN, Balingen, Germany) in the morning at 9:00 - 9:30 am. At each time point, the percentage of body weight change was determined by comparison to the body weight before operation on day 0.

The score sheet was used in many publications.[59,61–63,65] It has a total of 66 points and evaluates body weight, general condition, spontaneous behaviour, flight

behaviour and process-specific criteria. One person assessed the distress score in a not blinded manner, according to the score sheet. In the first study, the distress score was assessed 30 ± 5 minutes after cell injection on day 0 (on all other days 09:00-09:30 am). In the other two studies, the distress score was assessed 09:00-09:30 am at each time point.

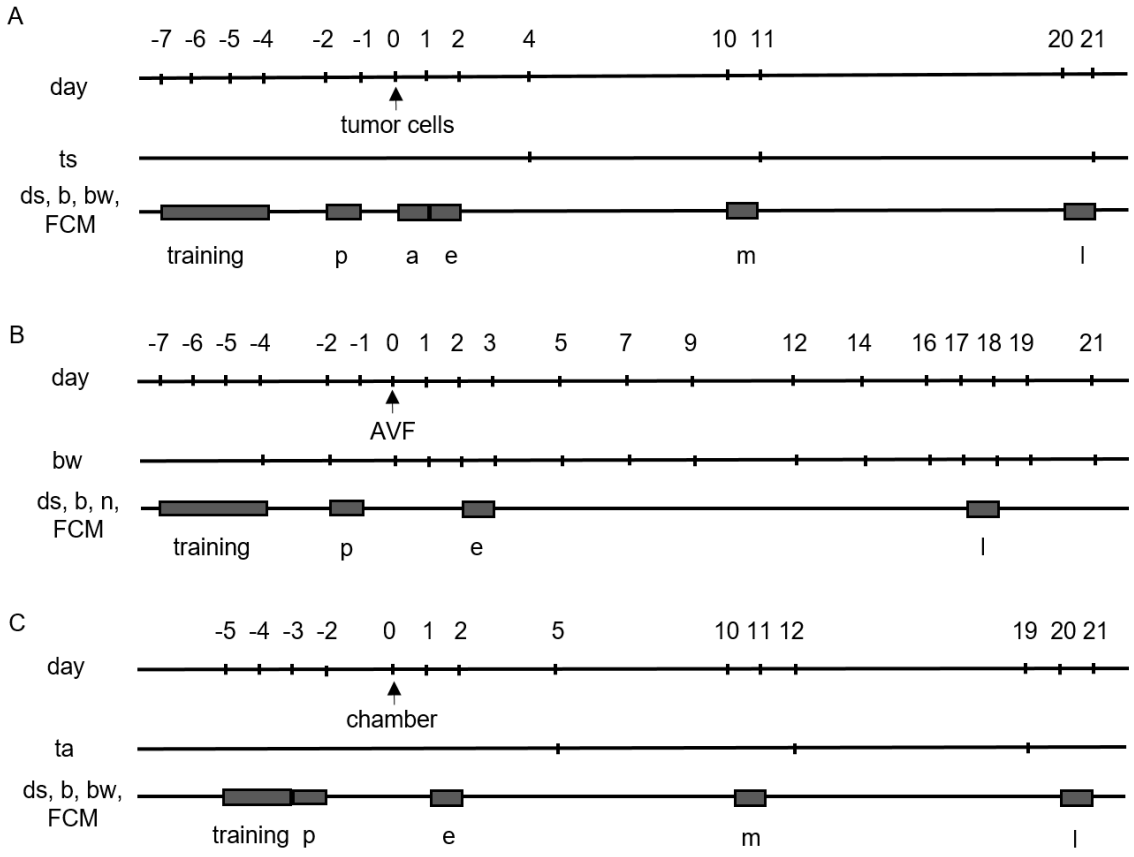

Figure 1. Experimental timelines for distress assessment. A. subcutaneous tumor growth model, B. cervical arteriovenous fistula (AVF) model, C. dorsal skinfold chamber model. Body weight (bw), the distress score (ds), burrowing (b) and/or nesting(n) activity, faecal corticosterone metabolites (FCMs), as well as tumor size (ts) or tilting angles (ta) were evaluated at pre-operative (p), acute (a), early (e), middle (m), late (l) phase in the respective models.

3.4.2 FCMs analysis

For analysis of FCMs, all bedding with old faeces was removed and fresh bedding was given into the cages 24 hours prior to the start of faeces collection. More than 400 mg fresh faeces were collected per mouse and dried for 4 hours at 65 °C. Until further processing, the faeces was stored at −20°C. Thereafter, 50 mg of dried faeces were extracted with 1 ml 80% methanol for further analysis by a 5α-pregnane-3β,11β,21-triol-20-one enzyme immunoassay.[56,66]

3.4.3 Assessment of burrowing and nesting activity

A burrowing tube (15 cm length × 6.5 cm diameter) which was filled with 200 ± 1 g food pellets (ssniff Spezialdiaeten GmbH) was placed in the left back corner of the cages 3 hours before the dark phase at 4:00 - 4:10 pm. Mice had free access to these pellets. Nesting material was left in the cages. The weight of the food pellets (g) that remained in the tube was measured after 2 hours or 17 hours, then the same tube was put back and measured on the next morning at 9:00 - 9:15 am and deducted from 200 g.

For evaluating nesting activity, a cotton nest building material (5 cm square of pressed cotton batting, Zoonlab GmbH, Castrop-Rauxel, Germany) was placed in the left front of the cage 3 hours before the dark phase at 4:00 - 4:15 pm. Pictures of the nests were taken, and nesting was scored at the next morning at 9:00 - 09:15 am. This score was previously described in detail.[49]

3.5 Statistical analysis

All data were graphed and analysed with GraphPad Prism (version 8.0.1, GraphPad Software Inc., San Diego, CA, USA) and were presented as single data points plus median and 95 % confidence interval. The characteristics of data were assessed by the Shapiro–Wilk test. In the case of non-parametric data, a one-way repeated measure ANOVA on ranks (Friedman Test) was performed, when analysing the influence of time on the dependent variables. When analysing the influence of the cell lines or chambers on the dependent variables, a Mann–Whitney rank sum test was used. In the case of parametric data a two-way repeated measure ANOVA with Geisser–Greenhouse was performed. Differences with $p \leq 0.05$ were considered to be significant.

In order to assess the diagnostic ability of each distress parameter in subcutanous tumor model, a ROC curve analysis was performed. To describe the performance of each readout parameter, the area under the curve, the 95% confidence interval and the P-value were calculated for each parameter. An area under the curve of 1.0 indicates that the parameter is perfect for discriminating between animals growing a tumor and animals not bearing a tumor, whereas a value of 0.5 suggests no discriminative power. More details are presented in the appendix.

4. Results

4.1 Subcutaneous tumor model

In all NSG mice the tumor cells were implanted successfully. However, on day 21 after cell injection, the volume of A-375 tumors was significantly larger than the volume of SCL-2 tumors (Figure 2A, 2B). Histological sections demonstrated different cell density in the tumors (Figure 2C, 2D). The A-375 tumors grew quickly, but the growth of SCL-2 tumors was relatively slow. In both the middle and late phase, the volume of A-375 tumors was significantly larger than the volume of SCL-2 tumors (Figure 2E).

There was no significant decrease in total body weight after cell injection or during tumor growth, and even a significant increase during A-375 tumor growth (Figure 2F). However, the adjusted body weight of the mice after subtracting the tumor weight showed a significant decrease in A-375 tumor bearing mice (Figure 2G). Throughout the experiment, only very low distress scores were observed (Figure 2H). Of the 66 points theoretically possible, the highest oberserved distress score was only 4 points. FCM concentrations in the feces of mice were significantly higher in the late phase of A-375 tumor growth compared to pre-phase or compared to mice in the late phase of SCL-2 tumor growth (Figure 2I). The mice also showed no significant differences when comparing burrowing before tumor injection to burrowing during tumor growth (Figure 2J).

Considering the differences of each tumor cell line, the diagnostic ability of each distress parameter was analyzed separately. The diagnostic ability to distinguish tumor-bearing and tumor-free mice was low for total body weight change (Figure 2K), burrowing activity (Figure 2L) and distress score (Figure 2M) after injection of A-375 tumor cells. However, FCMs concentration (Figure 2N) and adjusted body weight (Figure 2O) can well distinguish between mice with and without tumors. After injection of SCL-2 tumor cells, all distress parameters including percentage change of body weight (Figure 2P), burrowing activity (Figure 2Q), distress score (Figure 2R), FCM (Figure 2S) and adjusted body weight (Figure 2T) failed to distinguish between mice with and without tumors.

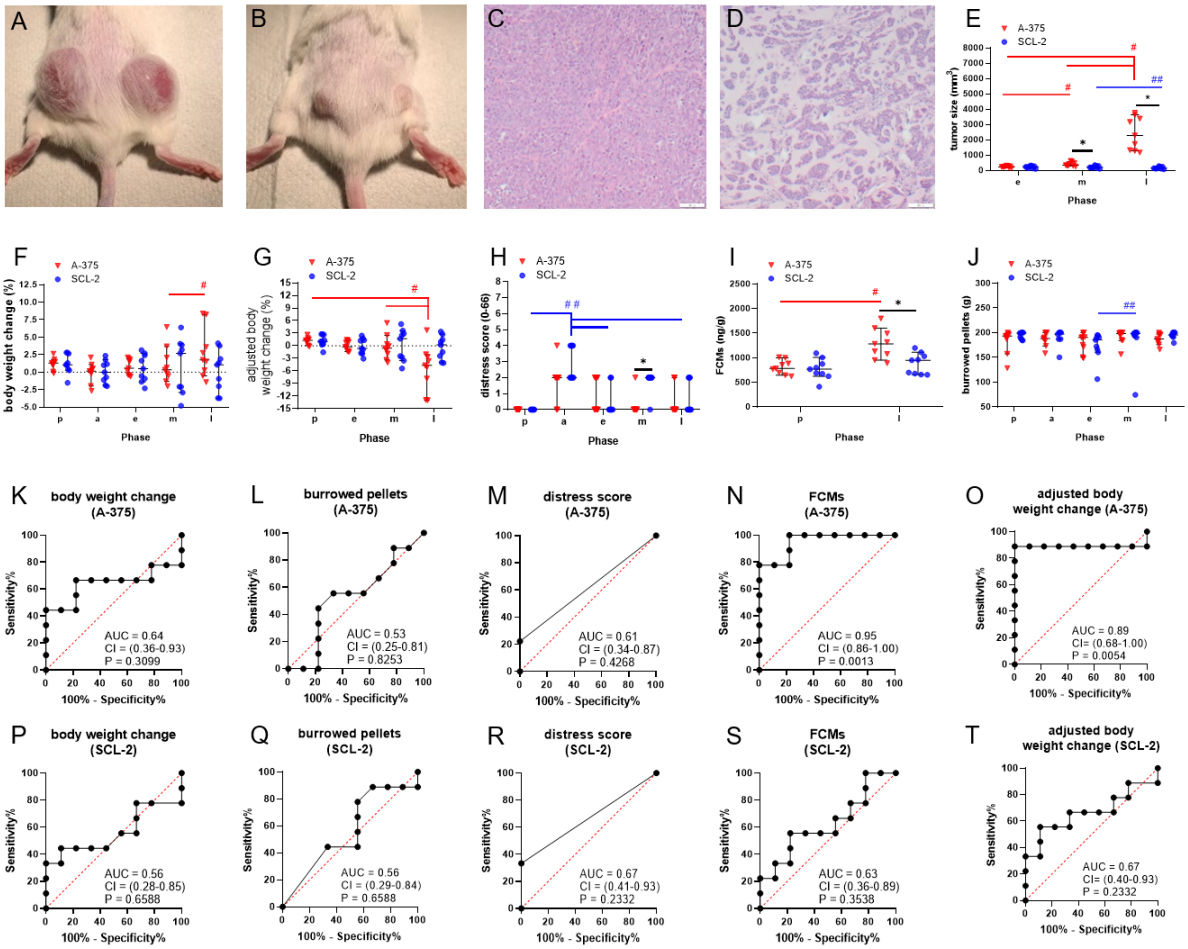

Figure 2. The characteristic of tumors and distress assessment of tumor bearing mice. Morphology of A-375 cell (A) and SCL-2 cell (B) induced tumors in the late phase after cell injection. Histology of A-375 cell (C) and SCL-2 cell tumors (D) after hematoxylin and eosin staining; scale bar =50 μm. The tumor size (E) , percentage of body weight change (F), percentage of adjusted body weight change (G), distress score (H) , FCMs (I) and burrowing activity (J) were analyzed at the indicated phases. Median with 95%CI. E:*p≤0.0116, #p≤0.0091, ##p=0.0003; F: #p=0.0366; G: #p≤0.0315; H: *p=0.0034, ##p≤0.0175; I: *p=0.0013, #p<0.0001; J: ##p=0.0287. A-375: n=9, SCL-2: n=9. Diagnostic ability of parameters in differentiating between mice before cancer cells were injected and identical mice bearing A-375 tumors (K-O) or SCL-2 tumors (P-T) in the late phase via ROC curve analysis. The area under the curve (AUC), the 95 % confidence interval (CI) and the p value (P) for testing the AUC to be 0.5 are presented in each graph.

4.2 Cervical arteriovenous fistula model

A total of twelve mice were used to create a cervical AVF (Figure 3A). Two mice were euthanized due to severe bleeding during the surgery, but ten AVF were created successfully. At the time when the tissue was harvested, six of ten fistulas matured sufficiently (Figure 3B), as defined by an increased diameter (Figure 3C) compared to the contralateral vein (Figure 3D). The other four fistulas were not mature and showed occlusion with no blood flow inside.

All mice showed body weight loss after AVF creation, but started to recover from day 3. However, there was no significant difference compared to day -2 (Figure 3E). It is worth pointing out that nine of the ten mice lost less than 10% of their body weight after the creation of AVF, and only one mouse lost more than 10% of its body weight. There was a mild but non-significant increase in FCM concentrations on day 2 and day 17 after AVF creation (Figure 2F). The mouse with a significant decrease in body weight also exhibited a significant increase in FCMs concentration. Analysis of burrowing activity after 2 hours showed no reduction in burrowing activity during the early and late phase after AVF creation (Figure 4G). In fact, the burrowing activity was even more intense on day 17 compared to day -2. When mice were given a longer time to burrow, almost all mice exhibited active burrowing behaviour. No significant difference was observed between each phase (Figure 3H). However, the mouse with more than 10% reduction in body weight showed a strong decrease in burrowing activity on day 2. There was no reduction in nesting activity (Figure 3I). Notably, although mice showed mild distress in the early phase, the distress scores were only 2/0-2 (median/95% confidence interval) on day 2, and even less on day 17 (Figure 3K).

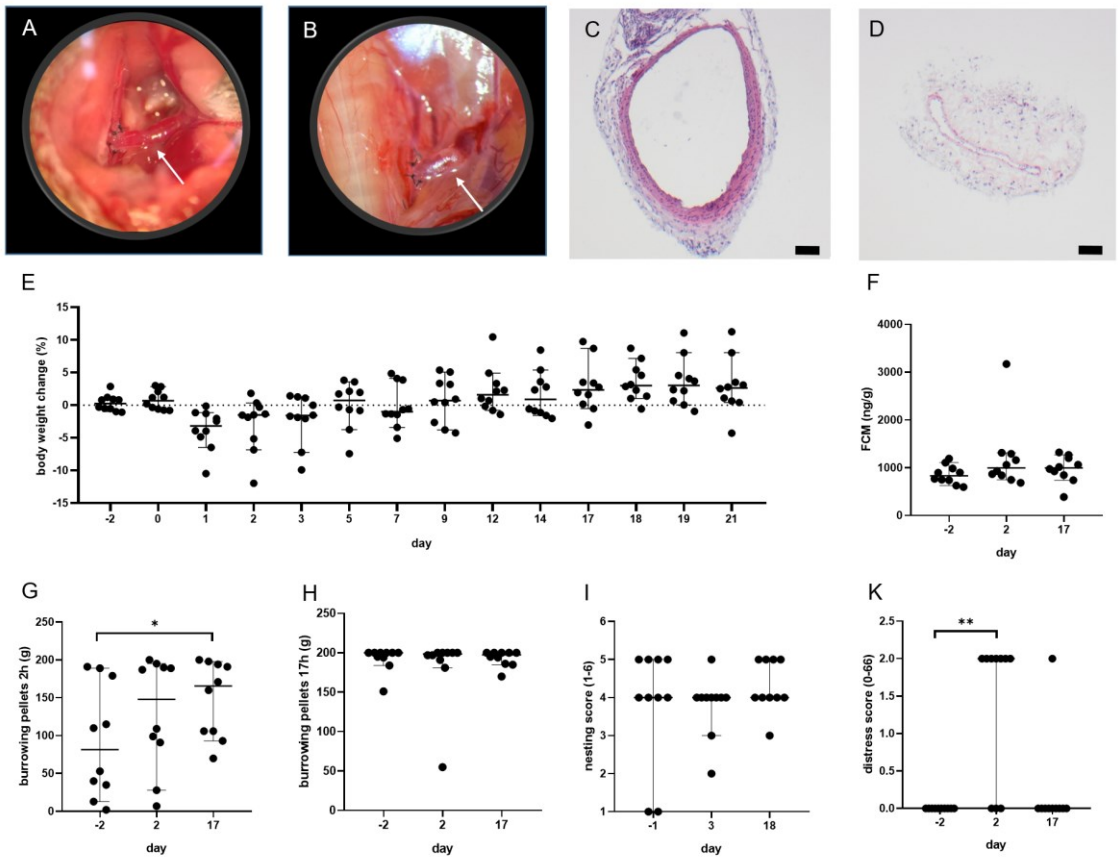

Figure 3. Characteristics of arteriovenous fistula (AVF) and the evaluation of distress parameters during the AVF maturation. Morphology of AVF (white arrows) immediately after fistula creation (A) and day 21 (B) after creation of the AVF. Magnification = 40x. Hematoxylin-eosin stained cross sections from of a respective fistula vein (C) and a control vein (D) on day 21 after fistula creation. Scale bar = 50 µm. Percentage of body weight change (E), faecal corticosterone metabolites (FCM) (F), 2h burrowing activity (G), 17h burrowing activtiy (H), nesting activity (I) and the distress score (K) were assessed on the indicated days. Median with 95%CI.*p = 0.0073. **p = 0.0378. n = 10.

4.3 Dorsal skinfold chamber model

During the observation period, all six mice carrying a PEEK chamber survived. However, five from a total of 11 mice carrying a titanium chamber did not survive. This was due to a loss of more than 20% body weight in the first week in one mouse. A suddenly death happened in another mouse on day 12 without any known reason. Euthanasia needed to be done in the other three mice because of a significant tilt of the chamber in the second week. Despite this observed obvious difference in survival rates, the statistical analysis using Log-rank test showed no significant difference between this two groups (Figure 4A). In the PEEK group, the tilting angle of the chamber did not increase, whereas the tilting angle of chamber increased in the titanium group (Figure 4B). However, in the titanium group this difference was statistically not significant. Moreover, there was also no significant difference in the tilting angles between the two groups at the end of the experiment.

Both the PEEK and titanium groups showed significant body weight loss in the early phase after operation (Figure 4C). However, the titanium chamber caused more body weight loss compared to the PEEK chamber in the early phase. As the observations progressed, almost all mice gained body weight compared to the early phase, but the average body weight of the mice in the titanium group remained lower than the weight during the pre-operative phase. In the early and middle phases of the experiment, the percentage of body weight loss in the PEEK group was significantly lower than that in the titanium group.

Analysis of burrowing activity showed significant reduction in the early phase after operation (Figure 4D). However, the burrowing activity of the PEEK group mice increased in the middle phase, while the titanium group still had significantly lower activity compared to the pre-operative phase. As the mice adapted to the chamber, there was a non-significant slight increase in the burrowing activity at the end of the experiment compared to the early and middle phase.

The multifactorial clinical score revealed that the distress in mice carrying a PEEK chamber was significantly increased in the early phase (Figure 4E). The distress score in the titanium group, however, was significantly increased not only in the early phase, but also in the middle and late phase.

Similar to other parameters, FCM concentrations were increased after operation in the early phase (Figure 4F). However, there was only a significant increase in the titanium group. Since the mice recovered from the operation, the FCM concentrations decreased in the middle and late phase, with no significant difference compared to the pre-operative phase.

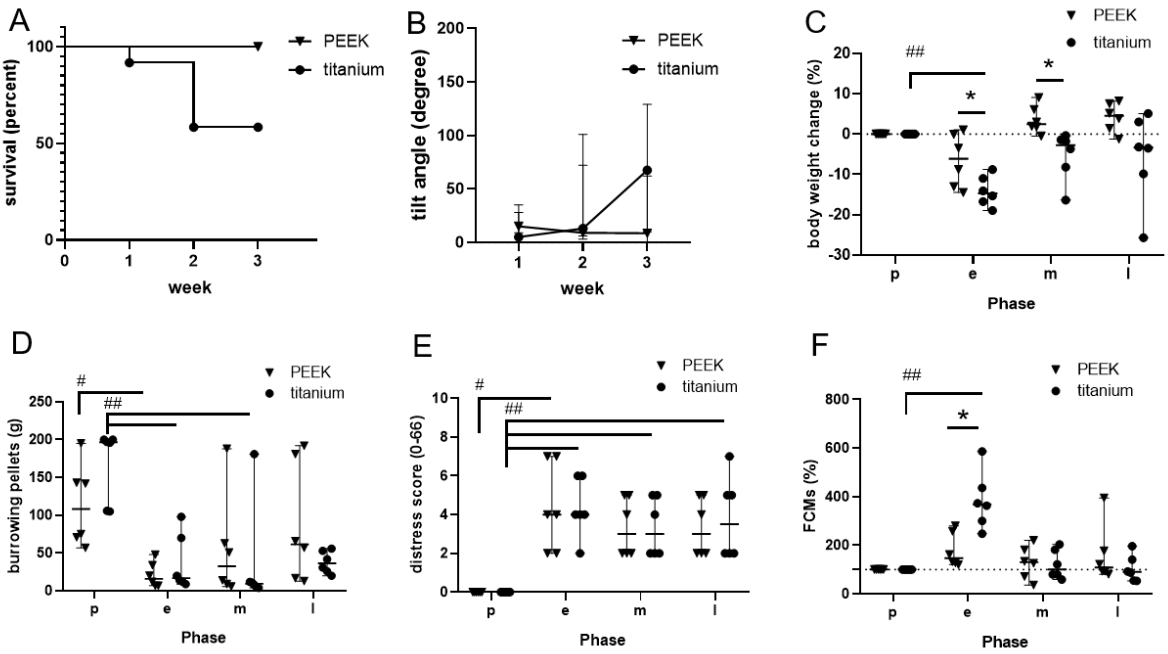

Figure 4. General and distress assessment of dorsal skinfold chamber mice. (A) survival curve and (B) titling angles were assessed on the indicated weeks. Percentage of body weight change (C), burrowing activity (D), distress score (E) and percentage of faecal corticosterone metabolites (FCMs) concentrations (F) were assessed on the indicated days. C: ##p=0.0024, *p≤0.0329; D: #p=0.0219, ##p≤0.0417; E: #p=0.0024, ##p≤0.0417; F: ##p=0.0417, *p=0.0046. Polyetheretherketone (PEEK): n=6, titanium: n=6.

5. Discussion

5.1 Subcutaneous tumor model

As a result of the performed study, we could demonstrate that adjusted body weight change and FCMs have a high diagnostic ability to define distress caused by large subcutaneous tumors.

The total body weight, however, had no diagnostic ability to differentiate between mice with or without subcutaneous tumors in this performed study. This seems to contradict the literature, since many murine tumor models use total body weight as readout parameter for distress analysis.[67–69] Indeed, it is widely recognized that tumor growth can result in severe body weight loss.[69,70] However, some studies have revealed that the total body weight of the mice did not decrease during the growth of the tumors.[58,63,71–73] For example, when tumor cells were intratibially injected in SCID mice and grew for 20 days, the total body weight was not reduced, although the mice exhibited pain responses such as ruffled fur or hunched back.[72] Similar findings were also observed in a subcutaneous tumor model.[73] Moreover, one study of mice with subcutaneous tumors found that the adjusted body weight better reflects the cachexia status compared to the total body weight.[70] Therefore, some publications support the conclusion of this study that adjusted body weight provides a better prediction of distress than total body weight in tumor-bearing mice. Actually, several articles have mentioned that the tumor itself can effect total body weight.[32,58,73,74] For example, Narver mentioned that the weight of the tumor itself and intraperitoneal effusion may mask the body weight loss.[74] Han et al. pointed out that the size of subcutaneous tumors increased the total body weight of tumor bearing mice.[70] Therefore, the adjusted body weight should be used in the subsequent assessment of distress in tumor-bearing mice.

FCM concentration is a common parameter for assessing distress of animals, and was used to assess distress in tumor-bearing mice.[63,65,75,76] Only few publications describe that FCM levels were not elevated in the tumor-bearing mice.[63,75] However, these mice only beared small tumors. For example, one of these study found that the FCM concentrations were not significantly increased in an orthotopic breast tumor mouse model, when tumors were smaller than 600 mm^3.[75] This is in line with our findings. When mice had a small SCL-2 tumors (< 300 mm^3), the FCM

concentrations did not increase significantly. However, when mice had large A-375 tumors (>1000 mm^3), the FCM were significant higher. One study, however, contradicts our findings, because they published a negative correlation between FCM concentration and tumor size in SCID mice after subcutaneous injection of prostate tumor cells.[76] However this study used a different mouse strain and different methods to assess FCMs. This might explain the observed differences.[57]

Burrowing activity and clinical distress scores are commonly used to assess distress in mice,[48,58,59,62] but this study failed to depict an increase in distress during tumor growth by these methods. A possible reason for this is that tumor growth in subcutaneous tumor models causes only mild distress, which cannot be measured by burrowing activity or distress scores.[63,77] However, these methods were still valid for evaluating distress, when cancer induces symptoms such as bone pain or cachexia.[72,78,79] In addition, the distress score is often considered to be a subjective readout parameter, which can be influenced by the perception of the researcher and might, therefore, not be a very reliable method, especially for mild distress.

5.2 Cervical arteriovenous fistula model

The presented AVF is similar to the vascular access needed for hemodialysis patients in terms of anatomical and hemodynamic characteristics. Our analysis demonstrated that the mice suffered only moderate distress during the early phase of fistula maturation.

Before this cervical AVF model was created, multiple mouse AVF models were tested to study hemodialysis access. For example, the inferior vena cava-abdominal aortic fistula model,[80] or the tail median artery-collateral vein fistula model were developed.[81] Although there were several carotid-jugular vein fistula models [82–84] created, most of these models do not reflect the anatomical and flow characteristics of AVF in humans.[18] The obvious neointimal hyperplasia in this novel cervical AVF confirmed that this model is valid to study the mechanism of fistula maturation for hemodialysis access in patients and might also be used to test various treatment options to prevent lack of correct maturation.[85]

Surgery and anesthesia are both particularly potent stressors,[54,86] and thus post-surgical body weight reduction is common in mice.[59–63,71] In our research, the surgery also caused a body weight loss in the early phase. Numerous factors

including the degree of tissue trauma, proficiency of the surgeon, surgery duration and degree of aseptic technique may influence the physiological response to the surgery.[55] Although the AVF were created by a skilled surgeon, body weight loss was inevitable. Compared to the carotid artery cannulation procedure in mice, which is generally classified as a procedure of moderate severity, the percentage of body weight loss was similar after operation (around 10% body weight lost on day 1).[55] As expected, mice that lost more blood volume during the operation showed noticeable weight loss after operation. Correspondingly, the burrowing activity decreased and the FCM level increased. This is a good illustration of the consistent physiological, behavioural and neuroendocrine effects of distress.[43] Burrowing activity is significantly reduced when the animal suffers severe distress such as bile duct ligation.[61] However, there is no reduction observed in our study. In contrast to liver injury caused by bile duct ligation, AVF did not cause any physical disease in the experimental animals. Moreover, the novel model uses a smaller diameter vein, a branch of the external jugular vein, as a venous fistula. This, possibly, reduces the cardiac load and the risk of heart failure,[18] which might also explain that less reduction in burrowing activity was observed compared to bile duct ligation.

C57Bl/6 mice usually show a high motivation in nesting behaviour.[62,63] This was also observed in the present study, but no significant difference between each time point was observed. However, it has to be noted that we evaluated nesting during the early phase 2 days after surgery. Thus, we did not evaluate the distress caused by surgical intervention but distress during an early phase of fistula maturation. This assumption is supported by a publication, which demonstrated that nesting activity recovers on the second postoperative day after surgical interventions.[63] However, when animals suffered serious physical diseases such as chronic pancreatitis, nesting activity was significantly reduced.[60] This indicates that AVF causes less distress than chronic pancreatitis. All mice also showed low distress scores during the study. However, clinical scores were originally developed to cover several mouse models of gastrointestinal disease,[63] and perhaps the distress score is not sensitive enough to assess distress of mice during AVF maturation.

5.3 Dorsal skinfold chamber model

This study revealed that the titanium chamber, which is widely used for the DSC model caused distress to mice. In addition, several mice carrying this titanium chamber had to be euthanized, because the chamber was tilted. This tilting of the chamber, the mortality and distress was significantly improved by using a new lightweight PEEK chamber.

PEEK is broadly used as medical material.[87] It causes similar to titanium barely any biological responses, but has a much lower density. While the traditional titanium chamber weights 3.6 grams, the novel PEEK chamber only weights 1.5 grams. This may cause less chamber tilting and also less distress to mice. Chamber tilting is a critical issue to avoid in dorsal skinfold chamber model, because it significantly affects the animal welfare of the mice.[23] Normally, the DSC model allows up to three weeks of observation.[19,24,22] However, often a severe chamber tilt is observed during the last two weeks shortening the potential observation time. In order to address this issue, some studies used modified chambers.[19,23,88–90] Consistent with our observation these chambers prolong the observation time in mice.[23,88] However, none of these studies explicitly assessed the difference in distress between the traditional and the modified chamber.

Body weight is the only parameter that was published to describe the distress of DSC mice in most studies.[88,91,92,28,93,94] For example, Leunig et al. observed a 15% weight loss in mice within the first 48 hours after a traditional chamber was mounted.[92] This is in line with our observation using titanium chambers. However, a PEEK chamber only caused average 6% body weight lost in our study, which may indicate the improvement in animal welfare. After three weeks observation, the mice in the PEEK group had an average weight gain, while the titanium group had a reduction. Several studies support our findings, they revealed a 10%-20% weight loss after two weeks of carrying a titanium chamber.[91,93,94] However, no reduction of body weight was observed in mice with a plastic chamber.[88]

The conclusion, that the PEEK chamber causes less distress than the titanium chamber was supported by the assessment of FCM concentrations. In the early phase, the titanium group showed a significantly higher FCM levels compared with the PEEK group and the preoperative phase. Thus two read out parameters, body

weight and FCMs, demonstrate that the PEEK chamber causes less distress than the titanium chamber. However, two other methods, evaluation of a distress score and measuring burrowing activity, did not demonstrate a significant difference between these two groups. Possibly, these methods are not sensitive enough to measure moderate changes in distress.

5.4 Improvement for preclinical research

The lack of validity of animal models has been described as an important reason why animal models often do not predict clinical outcomes.[16,95,96] Therefore, improvement the validity of an animal models are important for the success of future preclinical research.

A careful evaluation of improved animal models has been done within study II (cervical AVF) and study III (DSC). In study II, we describe several advantages of the cervical AVF model, such as the anatomical configuration and blood flow characteristics.[18] This model was characterized by neointimal hyperplasia, which is a common pathological change during fistula maturation.[97] This finding suggests that this model can be used to study the mechanisms of fistula maturation by means of histological, immunohistochemical or biomolecular analysis. Moreover, 40% of the fistulas in our study did not mature by the third postoperative week. Wong et al also found a 50% immaturation rate in the same AVF model.[18] Since the maturation rate is lower than 100%, this animal model can also be used to evaluate therapeutic approaches to improve fistula maturation. However, the creation of AVF needs experienced microsurgical skills. Wong et al., who introduced this model, presented the model as challenging for scientific researchers. However, after sufficient training, the success rate of the procedure increased from 67% to 97%.[18] For this study 33.3% (2/6) of mice had to be euthanized during the first experiment, whereas none of mice had to be euthanized in the last experiment. Therefore, continuous training can reduce the number of used mice and minimise animal distress.

In study III, we use a lightweight PEEK chamber to reduce the suffering of mice. This can extend the observation duration. Although DSC is widely used in studies related to microcirculation, the serious distress caused by traditional titanium chambers have limited its application. A significant chamber tilt of more than 90 degrees is often found during a two weeks observation,[23] and thus letting these

mice live is unkind. However, long-term observation is demanded for evaluation of the long-term compatibility of new biomaterials.[98] In our study, the use of PEEK chambers significantly improved the severe tilt caused by titanium chambers. Three mice were euthanized due to severe chamber tilting in the titanium group, but none was euthanized in the PEEK group. This suggests that long-term observation using PEEK chambers can reduce the number of used mice. In addition, the high survival rate also ensures the authenticity and validity of the experimental data, and that no data are lost due to the accidental death of mice. Actually, several articles found that the use of a lightweight chamber in the DSC model could prolong the observation time and might reduce distress, however, none of them compared the differences between them by quantifying them. [19,88,99] Our study is the first study to provide data demonstrating an improvement of animal welfare by using a lightweight chamber.

6. Conclusion and outlook

This dissertation provides three specific examples how animal distress can be evaluated and how this assessment can provide a basis for improving animal welfare as well as translational research. As shown in this dissertation, non-invasive distress analysis methods are simple and easy to perform. Integrating such an analysis in translational research, will therefore, alleviate the suffering of animals in future experiments and help science to develop better animal models with an ethically justifications that are based on objective data. Thus, I hope that this dissertation will encourage surgeons and other scientists to integrate an evaluation of animal distress in their preclinical research.

7. References

1. Cesario A, Galetta D, Russo P, et al. The role of the surgeon in translational research. *The Lancet* 2003; 362: 1082.
2. Stein SL. Scholarship in academic surgery: history, challenges, and ideas for the future. *Clin Colon Rectal Surg* 2013; 26: 207–211.
3. Littman BH, Di Mario L, Plebani M, et al. What's next in translational medicine? *Clinical Science* 2007; 112: 217–227.
4. Rosengart TK, Mason MC, LeMaire SA, et al. The seven attributes of the academic surgeon: Critical aspects of the archetype and contributions to the surgical community. *The American Journal of Surgery* 2017; 214: 165–179.
5. Eric J. Charles and Irving L. Kron. Bedside-to-Bench and Back Again: Surgeon-Initiated Translational Research. *The Annals of Thoracic Surgery* 2018; 105: 10–11.
6. Marincola FM. Translational Medicine: A two-way road. *J Transl Med* 2003; 1: 1.
7. Barré-Sinoussi F and Montagutelli X. Animal models are essential to biological research: issues and perspectives. *Future Science OA* 2015; 1.
8. Carrel T. The relationship between surgeon and basic scientist. *Transplant Immunology* 2002; 9: 331–337.
9. Kibbe MR and Velazquez OC. The Extinction of the Surgeon Scientist. *Annals of Surgery* 2017; 265: 1060–1061.
10. Goldstein AM, Blair AB, Keswani SG, et al. A Roadmap for Aspiring Surgeon-Scientists in Today's Healthcare Environment. *Annals of Surgery* 2019; 269: 66–72.
11. Faggion CM. Animal research as a basis for clinical trials. *Eur J Oral Sci* 2015; 123: 61–64.
12. Institute of Medicine. *Science, Medicine, and Animals*. Washington, D.C.: National Academies Press, 1991.

13. Carlson RV, Boyd KM and Webb DJ. The revision of the Declaration of Helsinki: past, present and future. *Br J Clin Pharmacol* 2004; 57: 695–713.

14. Ray Greek, Niall Shanks, Mark J. Rice. The History and Implications of Testing Thalidomide on Animals. *The Journal of Philosophy, Science & Law* 2011; 11: 1–32.

15. Prabhakar S. Translational Research Challenges. *J Investig Med* 2012; 60: 1141–1146.

16. Perrin S. Preclinical research: Make mouse studies work. *Nature* 2014; 507: 423–425.

17. Workman P, Aboagye EO, Balkwill F, et al. Guidelines for the welfare and use of animals in cancer research. *Br J Cancer* 2010; 102: 1555–1577.

18. Wong CY, Vries MR de, Wang Y, et al. A Novel Murine Model of Arteriovenous Fistula Failure: The Surgical Procedure in Detail. *J Vis Exp* 2016: e53294.

19. Schreiter J, Meyer S, Schmidt C, et al. Dorsal skinfold chamber models in mice. *GMS Interdiscip Plast Reconstr Surg DGPW* 2017; 6: Doc10.

20. Jung J. Human tumor xenograft models for preclinical assessment of anticancer drug development. *Toxicol Res* 2014; 30: 1–5.

21. Valcourt DM, Kapadia CH, Scully MA, et al. Best Practices for Preclinical In Vivo Testing of Cancer Nanomedicines. *Adv Healthc Mater* 2020; 9: e2000110.

22. Sorg H, Krueger C and Vollmar B. Intravital insights in skin wound healing using the mouse dorsal skin fold chamber. *J Anat* 2007; 211: 810–818.

23. Ushiyama A, Yamada S and Ohkubo C. Microcirculatory parameters measured in subcutaneous tissue of the mouse using a novel dorsal skinfold chamber. *Microvasc Res* 2004; 68: 147–152.

24. Laschke MW and Menger MD. The dorsal skinfold chamber: A versatile tool for preclinical research in tissue engineering and regenerative medicine. *Eur Cell Mater* 2016; 32: 202–215.

25. Michael S, Sorg H, Peck C-T, et al. The mouse dorsal skin fold chamber as a means for the analysis of tissue engineered skin. *Burns* 2013; 39: 82–88.

26. Hillgruber C, Steingräber AK, Pöppelmann B, et al. Blocking von Willebrand factor for treatment of cutaneous inflammation. *J Invest Dermatol* 2014; 134: 77–86.

27. Kram L, Grambow E, Mueller-Graf F, et al. The anti-thrombotic effect of hydrogen sulfide is partly mediated by an upregulation of nitric oxide synthases. *Thromb Res* 2013; 132: e112-7.

28. Gelaw B and Levin S. Wound-induced angiogenesis and its pharmacologic inhibition in a murine model. *Surgery* 2001; 130: 497–501.

29. Dau M, Volprich L, Grambow E, et al. Collagen membranes of dermal and pericardial origin-In vivo evolvement of vascularization over time. *J Biomed Mater Res A* 2020; 108: 2368–2378.

30. Hightower CM and Intaglietta M. The Use of Diagnostic Frequency Continuous Ultrasound to Improve Microcirculatory Function After Ischemia–Reperfusion Injury. *Microcirculation* 2007; 14: 571–582.

31. Boucher Y, Leunig M and Jain RK. Tumor angiogenesis and interstitial hypertension. *Cancer Res* 1996; 56: 4264–4266.

32. P. Workman, A. Balmain, J. A. Hickman, et al. United Kingdom Co-ordinating Committee on Cancer Research (UKCCCR) Guidelines for the Welfare of Animals in Experimental Neoplasia (Second Edition). *Br J Cancer* 1998; 77: 1–10.

33. National Research Council. *Guide for the Care and Use of Laboratory Animals.* 8th. Washington (DC), 2011.

34. The European Parliament and the Council of the European Union. Directive 2010/63/EU of the European Parliament and of the Council of 22 September 2010 on the protection of animals used for scientific purposes. *Official Journal of the European Union* 2010; 53: 33–79.

35. Prescott MJ and Lidster K. Improving quality of science through better animal welfare: the NC3Rs strategy. *Lab Anim (NY)* 2017; 46: 152–156.

36. Akhtar A. The flaws and human harms of animal experimentation. *Camb Q Healthc Ethics* 2015; 24: 407–419.

37. Batty GD, Russ TC, Stamatakis E, et al. Psychological distress in relation to site specific cancer mortality: pooling of unpublished data from 16 prospective cohort studies. *BMJ* 2017; 356: j108.

38. Page GG, McDonald JS and Ben-Eliyahu S. Pre-operative versus postoperative administration of morphine: impact on the neuroendocrine, behavioural, and metastatic-enhancing effects of surgery. *Br J Anaesth* 1998; 81: 216–223.

39. Ragan AR, Lesniak A, Bochynska-Czyz M, et al. Chronic mild stress facilitates melanoma tumor growth in mouse lines selected for high and low stress-induced analgesia. *Stress* 2013; 16: 571–580.

40. Taylor DK. Influence of Pain and Analgesia on Cancer Research Studies. *Comp Med* 2019; 69: 501–509.

41. Tymvios C, Jones S, Moore C, et al. Real-time measurement of non-lethal platelet thromboembolic responses in the anaesthetized mouse. *Thromb Haemost* 2008; 99: 435–440.

42. European Commission. Directorate-General for Environment. *Caring for animals aiming for better science: Directive 2010/63/EU on protection of animals used for scientific purposes education and training framework.* Luxembourg: Publications Office of the European Union, 2018.

43. Palme R. Non-invasive measurement of glucocorticoids: Advances and problems. *Physiol Behav* 2019; 199: 229–243.

44. D.B. Morton PHMG. Guidelines on the recognition of pain, distress and discomfort in experimental animals and an hypothesis for assessment. *Veterinary Record* 1985; 16: 431–436.

45. Jeong JY, Lee DH and Kang SS. Effects of Chronic Restraint Stress on Body Weight, Food Intake, and Hypothalamic Gene Expressions in Mice. *Endocrinol Metab* 2013; 28: 288.

46. Jirkof P. Burrowing and nest building behavior as indicators of well-being in mice. *J Neurosci Methods* 2014; 234: 139–146.

47. Jirkof P, Rudeck J and Lewejohann L. Assessing Affective State in Laboratory Rodents to Promote Animal Welfare—What Is the Progress in Applied Refinement Research? *Animals* 2019; 9: 1026.

48. Jirkof P, Cesarovic N, Rettich A, et al. Burrowing behavior as an indicator of post-laparotomy pain in mice. *Front Behav Neurosci* 2010; 4: 165.

49. Deacon R. Assessing burrowing, nest construction, and hoarding in mice. *J Vis Exp* 2012: e2607.

50. Jirkof P, Tourvieille A, Cinelli P, et al. Buprenorphine for pain relief in mice: repeated injections vs sustained-release depot formulation. *Lab Anim* 2015; 49: 177–187.

51. Gaskill BN, Gordon CJ, Pajor EA, et al. Heat or Insulation: Behavioral Titration of Mouse Preference for Warmth or Access to a Nest. *PLoS ONE* 2012; 7: e32799.

52. Deacon RMJ. Burrowing in rodents: a sensitive method for detecting behavioral dysfunction. *Nat Protoc* 2006; 1: 118–121.

53. Balcombe JP, Barnard ND and Sandusky C. Laboratory routines cause animal stress. *Journal of the American Association for Laboratory Animal Science* 2004; 43: 42–51.

54. McGuill MW and Rowan AN. Biological Effects of Blood Loss: Implications for Sampling Volumes and Techniques * Commentary: H. Richard Adams. *ILAR J* 1989; 31: 5–20.

55. Teilmann AC, Kalliokoski O, Sørensen DB, et al. Manual versus automated blood sampling: impact of repeated blood sampling on stress parameters and behavior in male NMRI mice. *Lab Anim* 2014; 48: 278–291.

56. Touma C, Palme R and Sachser N. Analyzing corticosterone metabolites in fecal samples of mice: a noninvasive technique to monitor stress hormones. *Hormones and Behavior* 2004; 45: 10–22.

57. Ibarguen-Vargas Y, Surget A, Touma C, et al. Multifaceted strain-specific effects in a mouse model of depression and of antidepressant reversal. *Psychoneuroendocrinology* 2008; 33: 1357–1368.

58. Paster EV, Villines KA and Hickman DL. Endpoints for mouse abdominal tumor models: refinement of current criteria. *Comp Med* 2009; 59: 234–241.

59. Kumstel S, Tang G, Zhang X, et al. Grading Distress of Different Animal Models for Gastrointestinal Diseases Based on Plasma Corticosterone Kinetics. *Animals (Basel)* 2019; 9: 145.

60. Abdelrahman A, Kumstel S, Zhang X, et al. A novel multi-parametric analysis of non-invasive methods to assess animal distress during chronic pancreatitis. *Sci Rep* 2019; 9: 14084.

61. Tang G, Seume N, Häger C, et al. Comparing distress of mouse models for liver damage. *Sci Rep* 2020; 10: 19814.

62. Tang G, Nierath W-F, Palme R, et al. Analysis of Animal Well-Being When Supplementing Drinking Water with Tramadol or Metamizole during Chronic Pancreatitis. *Animals (Basel)* 2020; 10: 2306.

63. Kumstel S, Vasudevan P, Palme R, et al. Benefits of non-invasive methods compared to telemetry for distress analysis in a murine model of pancreatic cancer. *Journal of Advanced Research* 2020; 21: 35–47.

64. Jensen MM, Jørgensen JT, Binderup T, et al. Tumor volume in subcutaneous mouse xenografts measured by microCT is more accurate and reproducible than determined by 18F-FDG-microPET or external caliper. *BMC Med Imaging* 2008; 8: 16.

65. Kumstel S, Wendt EHU, Eichberg J, et al. Grading animal distress and side effects of therapies. *Ann N Y Acad Sci* 2020; 1473: 20–34.

66. Touma C, Sachser N, Möstl E, et al. Effects of sex and time of day on metabolism and excretion of corticosterone in urine and feces of mice. *General and Comparative Endocrinology* 2003; 130: 267–278.

67. Zhang X, Kumstel S, Tang G, et al. A rational approach of early humane endpoint determination in a murine model for cholestasis. *ALTEX* 2020; 37: 197–207.

68. Talbot SR, Biernot S, Bleich A, et al. Defining body-weight reduction as a humane endpoint: a critical appraisal. *Lab Anim* 2020; 54: 99–110.

69. Wallace J. Humane endpoints and cancer research. *ILAR J* 2000; 41: 87–93.

70. Han Y-H, Mun J-G, Jeon HD, et al. The Extract of Arctium lappa L. Fruit (Arctii Fructus) Improves Cancer-Induced Cachexia by Inhibiting Weight Loss of Skeletal Muscle and Adipose Tissue. *Nutrients* 2020; 12: 3195.

71. Lofgren J, Miller AL, Lee CCS, et al. Analgesics promote welfare and sustain tumour growth in orthotopic 4T1 and B16 mouse cancer models. *Lab Anim* 2018; 52: 351–364.

72. Husmann K, Arlt MJE, Jirkof P, et al. Primary tumour growth in an orthotopic osteosarcoma mouse model is not influenced by analgesic treatment with buprenorphine and meloxicam. *Lab Anim* 2015; 49: 284–293.

73. Miller A, Burson H, Söling A, et al. Welfare Assessment following Heterotopic or Orthotopic Inoculation of Bladder Cancer in C57BL/6 Mice. *PLoS ONE* 2016; 11: e0158390.

74. Narver HL. Care and monitoring of a mouse model of melanoma. *Lab Anim (NY)* 2013; 42: 92–98.

75. Baier J, Rix A, Drude NI, et al. Influence of MRI Examinations on Animal Welfare and Study Results. *Invest Radiol* 2020; 55: 507–514.

76. Jacobsen KR, Jørgensen P, Pipper CB, et al. The utility of fecal corticosterone metabolites and animal welfare assessment protocols as predictive parameters of tumor development and animal welfare in a murine xenograft model. *In Vivo* 2013; 27: 189–196.

77. Chartier LC, Howarth GS, Lawrance IC, et al. Emu Oil Improves Clinical Indicators of Disease in a Mouse Model of Colitis-Associated Colorectal Cancer. *Dig Dis Sci* 2018; 63: 135–145.

78. Sliepen SHJ, Diaz-Delcastillo M, Korioth J, et al. Cancer-induced Bone Pain Impairs Burrowing Behaviour in Mouse and Rat. *In Vivo* 2019; 33: 1125–1132.

79. Chartier LC, Hebart ML, Howarth GS, et al. Affective state determination in a mouse model of colitis-associated colorectal cancer. *PLoS ONE* 2020; 15: e0228413.

80. Kuwahara G, Hashimoto T, Tsuneki M, et al. CD44 Promotes Inflammation and Extracellular Matrix Production During Arteriovenous Fistula Maturation. *Arterioscler Thromb Vasc Biol* 2017; 37: 1147–1156.

81. Lin T, Horsfield C and Robson MG. Arteriovenous fistula in the rat tail: a new model of hemodialysis access dysfunction. *Kidney Int* 2008; 74: 528–531.

82. Yang B, Shergill U, Fu AA, et al. The mouse arteriovenous fistula model. *J Vasc Interv Radiol* 2009; 20: 946–950.

83. Castier Y, Lehoux S, Hu Y, et al. Characterization of neointima lesions associated with arteriovenous fistulas in a mouse model. *Kidney Int* 2006; 70: 315–320.

84. Skartsis N, Martinez L, Duque JC, et al. c-Kit signaling determines neointimal hyperplasia in arteriovenous fistulae. *Am J Physiol Renal Physiol* 2014; 307: F1095-104.

85. Roy-Chaudhury P, Arend L, Zhang J, et al. Neointimal Hyperplasia in Early Arteriovenous Fistula Failure. *American Journal of Kidney Diseases* 2007; 50: 782–790.

86. Desborough JP. The stress response to trauma and surgery. *Br J Anaesth* 2000; 85: 109–117.

87. Panayotov IV, Orti V, Cuisinier F, et al. Polyetheretherketone (PEEK) for medical applications. *J Mater Sci Mater Med* 2016; 27: 118.

88. Axelsson H, Bagge U, Lundholm K, et al. A one-piece plexiglass access chamber for subcutaneous implantation in the dorsal skin fold of the mouse. *Int J Microcirc Clin Exp* 1997; 17: 328–329.

89. Gu J-M, Yuan S, Sim D, et al. Blockade of placental growth factor reduces vaso-occlusive complications in murine models of sickle cell disease. *Experimental Hematology* 2018; 60: 73-82.e3.

90. DeGeorge BR, Ning B, Salopek LS, et al. Advanced Imaging Techniques for Investigation of Acellular Dermal Matrix Biointegration. *Plastic and Reconstructive Surgery* 2017; 139: 395–405.

91. Leunig M, Yuan F, Gerweck LE, et al. Effect of basic fibroblast growth factor on angiogenesis and growth of isografted bone: quantitative in vitro-in vivo analysis in mice. *Int J Microcirc Clin Exp* 1997; 17: 1–9.

92. Leunig M, Yuan F, Menger MD, et al. Angiogenesis, microvascular architecture, microhemodynamics, and interstitial fluid pressure during early growth of human adenocarcinoma LS174T in SCID mice. *Cancer Res* 1992; 52: 6553–6560.

93. Cernaianu G, Frank S, Erbstösser K, et al. TNP-470 fails to block the onset of angiogenesis and early tumor establishment in an intravital minimal disease model. *Int J Colorectal Dis* 2006; 21: 143–154.

94. Shan S, Flowers C, Peltz CD, et al. Preferential extravasation and accumulation of liposomal vincristine in tumor comparing to normal tissue enhances antitumor activity. *Cancer Chemother Pharmacol* 2006; 58: 245–255.

95. Varga OE, Hansen AK, Sandøe P, et al. Validating Animal Models for Preclinical Research: A Scientific and Ethical Discussion. *Altern Lab Anim* 2010; 38: 245–248.

96. Begley CG and Ellis LM. Raise standards for preclinical cancer research. *Nature* 2012; 483: 531–533.

97. Hu H, Patel S, Hanisch JJ, et al. Future research directions to improve fistula maturation and reduce access failure. *Semin Vasc Surg* 2016; 29: 153–171.

98. Nitesh R. Patel, Piyush P. Gohil. A review on biomaterials: scope, applications & human anatomy significance. *International Journal of Emerging Technology and Advanced Engineering* 2012; 2: 91–101.

99. Leung HM, Schafer R, Pagel MM, et al. Multimodality pH imaging in a mouse dorsal skin fold window chamber model. *Proc SPIE Int Soc Opt Eng* 2013; 8574: 85740L.

8. Acknowledgement

I would like to express my gratitude to all the people who accompanied and supported me during my studies.

My deepest gratitude is to my boss Prof. Dr. Brigitte Vollmar for allowing me to do my doctoral thesis at your institute. Thanks to your support in both scientific and personal matters.

I would like to express my sincere thanks to my supervisor PD Dr. med. habil. Eberhard Grambow. Without his help, I would not have been able to completed my studies.

Another thanks goes to PD. Dr. Dietmar Zechner for his expert support, critical advice and constructive discussions during the work.

I am also deeply indebted to the entire team of the Rudolf-Zenker-Institut für Experimentelle Chirurgie. I would like to thank PD Dr. Angela Kuhla, Dr. Tobias Linder, Anna Schildt, Johanna Förster, Berit Blendow, Eva Lorbeer, Maren Nerowski, Dorothea Frenz and Christin Schlie for their professional work and support in the laboratory. Many thanks also to Anja Gellert for their administrative support. I would also like to thank my colleagues Marcel Kordt, Wiebke-Felicitas Nierath, Tim Schreiber, Benjamin Schulz and Nicole Guerra-Power for their support and friendship.

Special thanks to my family, who have supported me in all situation and have always been supportive of my decisions.

9. List of abbreviations

Arteriovenous fistula	AVF
Dorsal skinfold chamber	DSC
Glucocorticoids	GSs
Faecal corticosterone metabolites	FCMs
Intraperitoneal	ip
Polyetheretherketone	PEEK

10. Eidesstattliche Versicherung

Ich erkläre an Eides statt, dass ich die vorliegende Dissertation selbstständig und nur unter der Verwendung der angegebenen Quellen und Hilfsmittel erstellt habe. Die aus anderer Literatur verwendeten Inhalte sind als solche kenntlich gemacht. Die Regeln zur Sicherung guter wissenschaftlicher Praxis wurden beachtet. Ich versichere, dass ich für die inhaltliche Erstellung der vorliegenden Arbeit nicht die entgeltliche Hilfe von Vermittlungs- und Beratungsdiensten (Promotionsberater oder andere Personen) in Anspruch genommen habe. Ich bestätige, dass diese Arbeit an keiner anderen als der Universität Rostock zur Erlangung des Grades Doktor der Medizin vorgelegt wurde.

Wenting Xie

Rostock, 26.07.2022 ……

Ort, Abgabedatum Vollständige Unterschrift

11. Thesen

1. The effects of distress on experimental animals can lead to high mortality and affect the outcome of the experiment.
2. In order to analyse distress, the body weight, faecal corticosterone metabolites, burrowing activity, nesting behaviour and a distress score were evaluated.
3. Until now, it has not been studied, if these parameters can assess distress in mice bearing subcutaneous tumors.
4. This study demonstrates that adjusted body weight and faecal corticosterone metabolites are useful parameters to depict distress of mice bearing large subcutaneous tumors.
5. In some research areas, for example for studying hemodialysis access, it is necessary to improve animal models.
6. In order to improve hemodialysis access by studying fistula maturation or vascular remodelling, arteriovenous fistulas are often generated in mice.
7. The mice used for the cervical arteriovenous fistula model suffered only moderate distress during fistula maturation, which implies that this model should be used for future preclinical studies.
8. The traditional dorsal skinfold chamber model, frequently used for microvascular research, causes severe distress making it difficult to study mice for longer than three weeks.
9. A novel lightweight (PEEK) chamber increased the survival rate, was well tolerated, and reduced animal distress compared to titanium chambers.
10. Thus, distress assessment of animal models generates new knowledge, which can improve animal welfare as well as translational research.

12. Curriculum vitae

PERSONAL DETAIL

Name: Wentao Xie

Email: toxwt101@gmail.com

Address: No. 7#2402, Huangshan Road 639, Hefei, 230069 China

Date/place of birth 11.10.1984 in Hunan, China

CURRENT POSITION

PhD student, Institute of Experimental Surgery, University Rostock

EDUCATION

04/2019 - PhD student of Experimental Surgery, University Rostock, Germany

09/2003 - 07/2010 Bachelor and Master of Medicine in Surgery, Anhui Medical University, China

WORK EXPERIENCE

07/2010 - 04/2019 Department of General Surgery, the First Affiliated Hospital of Anhui Medical University, China

PUBLICATIONS

1. Grambow, E., Klee, G., Xie, W., Schafmayer, C., Vollmar, B.. Hydrogen sulfide reduces the activity of human endothelial cells. Clinical hemorheology and microcirculation. 2020;76:513–523. https://doi.org/10.3233/CH-200868
2. Xie, W., Kordt, M., Palme, R., Grambow, E., Vollmar, B., Zechner, D. Diagnostic Ability of Methods Depicting Distress of Tumor-Bearing Mice. Animals (Basel). 2021;11:2155. https://doi.org/10.3390/ani11082155
3. Xie, W., Palme, R., Schafmayer, C., Zechner, D., Vollmar, B., Grambow, E. Distress Analysis of Mice with Cervical Arteriovenous Fistulas. Animals (Basel). 2021;11: 3051. https://doi.org/10.3390/ani11113051

4. Xie W, Lorenz M, Poosch F, Palme R, Zechner D, Vollmar B, Grambow E, Strüder D. 3D-printed lightweight dorsal skin fold chambers from PEEK reduce chamber-related animal distress. Sci Rep. 2022;12:11599. https://doi: 10.1038/s41598-022-13924-5.

13. Appendix

Die folgenden Publikationen sind Teil des Appendix:

Wentao Xie, Marcel Kordt, Rupert Palme, Eberhard Grambow, Brigitte Vollmar, and Dietmar Zechner. Diagnostic Ability of Methods Depicting Distress of Tumor-Bearing Mice. Animals. 2021; 11(8):2155.

Wentao Xie, Rupert Palme, Clemens Schafmayer, Dietmar Zechner, Brigitte Vollmar, and Eberhard Grambow. Distress Analysis of Mice with Cervical Arteriovenous Fistulas. Animals. 2021; 11(11):3051.

Wentao Xie, Matthias Lorenz, Friederike Poosch, Rupert Palme, Dietmar Zechner, Brigitte Vollmar, Eberhard Grambow, Daniel Strüder. 3D-printed lightweight dorsal skin fold chambers from PEEK reduce chamber-related animal distress. Sci Rep. 2022 Jul 8;12(1):11599.

animals

MDPI

Article

Diagnostic Ability of Methods Depicting Distress of Tumor-Bearing Mice

Wentao Xie [1,2,*], Marcel Kordt [1], Rupert Palme [3], Eberhard Grambow [1,4], Brigitte Vollmar [1] and Dietmar Zechner [1]

1 Rudolf-Zenker-Institute for Experimental Surgery, University Medical Center Rostock, 18057 Rostock, Germany; marcel.kordt@uni-rostock.de (M.K.); eberhard.grambow@med.uni-rostock.de (E.G.); brigitte.vollmar@med.uni-rostock.de (B.V.); dietmar.zechner@uni-rostock.de (D.Z.)
2 Department of Vascular and Thyroid Surgery, Department of General Surgery, The First Affiliated Hospital of Anhui Medical University, Hefei 230022, China
3 Unit of Physiology, Pathophysiology and Experimental Endocrinology, Department of Biomedical Sciences, University of Veterinary Medicine Vienna, 1210 Vienna, Austria; Rupert.Palme@vetmeduni.ac.at
4 Department of General, Visceral, Thoracic, Vascular and Transplantation Surgery, University Medical Center Rostock, 18057 Rostock, Germany
* Correspondence: toxwt101@gmail.com; Tel.: +49-381-494-2513; Fax: +49-381-494-2502

Simple Summary: Experiments on animals can provide important information for improving the life expectancy and life quality of patients. At the same time, the welfare of these animals is a growing public concern. Therefore, many laws and international guidelines were established with the goal of minimizing the harm inflicted on these animals. A prerequisite of improving animal welfare is to correctly measure how much distress the experiments cause to these animals. However, it is often unknown as to which methods are appropriate to assess distress. Mice bearing subcutaneous tumors are the most frequently used animal model to study the therapeutic effects of drugs. We evaluated if body weight, faecal corticosterone metabolites concentration, burrowing activity and a distress score were capable of differentiating between mice before cancer cell injection and mice bearing large tumors. We observed that only adjusted body weight change and faecal corticosterone metabolites concentration were capable of measuring distress caused by large subcutaneous tumors. Therefore, these two methods are appropriate to assess the welfare of mice with subcutaneous tumors. This knowledge provides a solid basis to optimize animal welfare in future studies. For example, both methods can define the ideal time point when an experiment should end by finding a good compromise between minimal distress for the animals and maximal knowledge gain for mankind.

Abstract: Subcutaneous tumor models in mice are the most commonly used experimental animal models in cancer research. To improve animal welfare and the quality of scientific studies, the distress of experimental animals needs to be minimized. For this purpose, one must assess the diagnostic ability of readout parameters to evaluate distress. In this study, we evaluated different noninvasive readout parameters such as body weight change, adjusted body weight change, faecal corticosterone metabolites concentration, burrowing activity and a distress score by utilising receiver operating characteristic curves. Eighteen immunocompromised NOD.Cg-Prkdcscid Il2rgtm1Wjl/SzJ mice were used for this study; half were subcutaneously injected with A-375 cells (human malignant melanoma cells) that resulted in large tumors. The remaining mice were inoculated with SCL-2 cells (cutaneous squamous cell carcinoma cells), which resulted in small tumors. The adjusted body weight and faecal corticosterone metabolites concentration had a high diagnostic ability in distinguishing between mice before cancer cell injection and mice bearing large tumors. All other readout parameters had a low diagnostic ability. These results suggest that adjusted body weight and faecal corticosterone metabolites are useful to depict the distress of mice bearing large subcutaneous tumors.

Keywords: animal model; animal welfare; xenograft models; in vivo; 3Rs

check for updates

Citation: Xie, W.; Kordt, M.; Palme, R.; Grambow, E.; Vollmar, B.; Zechner, D. Diagnostic Ability of Methods Depicting Distress of Tumor-Bearing Mice. *Animals* **2021**, *11*, 2155. https://doi.org/10.3390/ani11082155

Received: 11 June 2021
Accepted: 17 July 2021
Published: 21 July 2021

Publisher's Note: MDPI stays neutral with regard to jurisdictional claims in published maps and institutional affiliations.

Copyright: © 2021 by the authors. Licensee MDPI, Basel, Switzerland. This article is an open access article distributed under the terms and conditions of the Creative Commons Attribution (CC BY) license (https://creativecommons.org/licenses/by/4.0/).

1. Introduction

According to the World Health Organization, cancer has become the leading cause of death worldwide [1]. Thus, it is necessary to pursue research focusing on this issue. Indeed, many experiments have led to an extraordinary increase in our knowledge of the fundamental molecular mechanisms involving cancer development and improved therapy regimens [2,3]. For example, Trastuzumab, a novel targeted therapeutic regimen, was proven to significantly improve disease-free survival among women with human epidermal growth factor receptor 2 positive breast cancer [4,5]. Furthermore, since 1997, the U.S. Food and Drug Administration has approved many novel drugs for the treatment of several cancers [6]. However, before new treatments for diseases can be developed and introduced into clinical practice, preclinical trials, often using animal experiments, must be conducted [7].

Subcutaneous tumor models using mice are the simplest model for routine evaluation of cancer therapies [2]. The use of human tumor cells, high taking rates, and continuous monitoring are advantages, which make this model an extensively used standard for validation and assessment in oncological studies [8]. In addition, due to an abundance of published data associated with subcutaneous tumor models, it is easy to access the parameters and references needed for testing novel therapies [7].

However, animal experiments are often associated with distress for animals, which has scientific as well as ethical implications [9,10] Distress can affect the results and the conclusions of experiments. For example, it has been proven that distress can affect the outcome of cancer in human patients [11] as well as in animals [12–14]. In addition, it is a moral imperative to minimise pain, suffering, distress and harm in experimental animals. These moral issues are addressed by publications, national laws and international guidelines [15–19]. Researchers do have the responsibility and obligation to comply with these laws and guidelines. Unfortunately, the present guidelines and publications only provide little data on distress for specific animal models and on the ability of methods to measure distress. This requires that researchers describe the distress caused by specific cancer models. This might also provide a basis for alleviating the suffering of animals in future experiments. One important first step is to analyse which readout parameters are useful to describe the distress of animals.

Assessing body weight, burrowing activity, faecal corticosterone metabolites (FCMs) and distress scores are commonly used non-invasive methods to quantify distress in mice [20–24]. Body weight loss as an important indicator of distress is used by guidelines as a criterion for euthanasia [2,18,19]. Distress leads to body weight loss and also influences instinctive behaviours in mice, such as burrowing activity [21]. FCMs are a measurement for adrenocortical activity in experimental mice and increased concentration suggests distress [23–25]. Moreover, distress scores based on general condition and behaviour can also reflect reduced well-being in mice [17,22,26,27].

The goal of this study was to assess which readout parameters can measure the distress of tumor-bearing mice. In order to assess the diagnostic ability of these readout parameters, we used receiver operating characteristic (ROC) curves.

2. Materials and Methods

2.1. Cell Culture

The human malignant melanoma cells A-375 (CLS, Eppelheim, Germany) and the cutaneous squamous cell carcinoma cells SCL-2 (donated by Prof. Hahn, University Medical Center Goettingen) were cultured in Dulbecco's modified Eagle's medium with high glucose, GlutaMax and pyruvate (Thermo Fisher Scientific, Waltham, MA, USA) supplemented with10% foetal bovine serum (Biochrom GmbH, Berlin, Germany), 100 U/mL penicillin and 100 mg/mL streptomycin (Sigma-Aldrich, Taufkirchen, Germany) in an incubator at 37 °C with 5% CO_2.

2.2. Establishment and Evaluation of the Tumor Model

This study was conducted in accordance with the European directive 2010/63/EU and national law. All experiments were approved by the local ethics committee and the public authority (Landesamt für Landwirtschaft, Lebensmittelsicherheit und Fischerei Mecklenburg-Vorpommern, 7221.3-1-057/18). For this study, 18 male 9–11-week-old NOD.Cg-Prkdcscid Il2rgtm1Wjl/SzJ (NSG) mice were bred in the central animal facility of the Rostock University Medical Center (initially purchased from Jackson Laboratory). The health of the animal stock is routinely checked according to FELASA guidelines (Helicobacter sp., Rodentibacter pneumotropicus, murine Norovirus and rat Theilovirus were detected within the last two years in few animals; these animals were not used for any experiments).

Although we are aware of the debate that the single-housing of mice may cause distress [28,29], we decided that all mice would be single-housed in a Eurostandard Type II L clear plastic cage with a light/dark cycle of 12 h/12 h (dawn: 6:30–7:00 am) and at a temperature of 21 ± 2 °C, with a relative humidity of 60 ± 20%. This was necessary because we needed to assess the burrowing activity and FCM concentrations of single mice. We also provided autoclaved bedding (Bedding Espe Max 3–5 mm granulate, H 0234–500, Abedd, Vienna, Austria), shredded tissue paper (PZN03058052, FSMED Verbandmittel GmbH, Frankenberg, Germany), one paper tunnel (75 × 38 mm, H 0528–151, ssniff, Spezialdiaeten GmbH, Soest, Germany), a wooden enrichment tool (Espe size S, 40 × 16 × 10 mm, H0234.NSG, Abedd, Vienna, Austria), food (pellets, V1534.000, 10 mm, ssniff, Spezialdiaeten GmbH, Soest, Germany) and tap water ad libitum. The bedding material was changed every week.

On day 0, the mice were anaesthetized by 1.5–2.5% isoflurane (CP-pharma, Burgdorf, Germany) in oxygen and placed on a heating plate (37 °C). Then the fur at the flanks of the mice was removed by asid-med (ASID BONZ, Herrenberg, Germany), and 1×10^6 tumor cells mixed on ice with 100 µL 1:1 cold DPBS/Matrigel® High Concentration Growth Factor Reduced (Matrigel® HC GFR, Corning, New York, NY, USA) were injected subcutaneously into the left and right flank, respectively. In order to reduce observer bias, the tumor size was evaluated by scientists during the early (day 4), middle (day 11), and late phase (day 21) in a blinded manner. The longest diameter and the diameter perpendicular to this diameter were measured using a digital caliper (fortis, E/D/E, Wuppertal, Germany) with 0.01 mm precision. Assuming the hemi-ellipsoidal shape of the tumors, the volume was derived using the formula: Volume = 0.52 × Length × Width^2 [30]. The tumor weight was derived using the formula: Weight = 1.05 × Volume [30]. On day 22, the mice were euthanized by quick anaesthesia with 5 vol % isoflurane, killed with cervical dislocation and the tumors were removed, fixed and embedded in paraffin. Histological sections were then stained with haematoxylin and eosin.

2.3. Evaluation of Animal Distress

Before cell injection (data presented as pre-phase), body weight, burrowing activity, faecal corticosterone metabolites (FCMs), and distress scores were assessed on all mice. Throughout the manuscript, we refer to data assessed at this time point as baseline data.

The percentage of body weight change was assessed before cell injection (day 0, pre-phase), after cell injection (day 1, acute phase) and during the early (day 2), middle (day 11) as well as late phase (day 21) of tumor growth (each time point the percentage of body weight change was determined by comparison to the body weight at day –1 before cell injection).

To evaluate the burrowing activity of mice, a tube (length: 15 cm, diameter: 6.5 cm) filled with 200 ± 1 g of food pellets was placed into the cage 3 h before the dark phase (at 04:00–04:10 pm). The mice had free access to these pellets, and the nesting material was left in the cages. The remaining pellets in the burrowing tube were weighed after 17 ± 2 h and the weight of the burrowed pellets was calculated. The burrowing activity was measured

before cell injection (day –2, pre-phase), after cell injection (day 0, acute phase) and during the early (day 1), middle (day 10), as well as the late phase (day 20) of tumor growth.

The distress score considers body weight, general condition, spontaneous behaviour, flight behaviour and process-specific criteria as previously published (for details also see Supplementary Tables S1 and S2) [22]. The score was assessed by only one person according to a scoring sheet before cell injection (day –2, pre-phase), after cell injection (day 0, acute phase) and during the early (day 1), middle (day 10) as well as the late phase (day 20) of tumor growth. The distress score was assessed 30 ± 5 min after cell injection on day 0 (on all other days, 09:00–09:30 am).

In order to measure faecal corticosterone metabolites, the bedding with old faeces was removed and replaced by fresh bedding before cell injection (on day −1, pre-phase) and during the late phase of tumor growth (day 20). After 24 h, more than 400 mg fresh faeces were collected. The faeces were dried for 4 h at 65 °C and kept at −20 °C until further processing. Thereafter, 50 mg of dried faeces were extracted with 1 mL 80% methanol and FCMs analysed with a 5α-pregnane-3β,11β,21-triol-20-one enzyme immunoassay [23,31].

2.4. Data Presentation and Statistical Analysis

All data were graphed and analysed with GraphPad Prism (version 8.0.1, GraphPad Software Inc., San Diego, CA, USA) and were presented as single data points plus median and 95% confidence interval. The characteristics of data were assessed by the Shapiro–Wilk test. In the case of nonparametric data (distress score, burrowing activity), a one-way repeated measure ANOVA on ranks (Friedman Test) was performed (corrections of multiple comparisons were done as suggested by GraphPad Prism: Dunn's correction), when analysing the influence of time on the dependent variables (readout parameters). When analysing the influence of the cell lines on the dependent variables, a Mann–Whitney rank sum test (plus Bonferroni correction for multiple time points) was used. In the case of parametric data (tumor size, percentage of body weight change, FCMs, percentage of adjusted body weight change) a two-way repeated measure ANOVA with Geisser–Greenhouse correction (corrections of multiple comparisons were done as suggested by GraphPad Prism: either Sidak test or Tukey test) was performed. Differences with $p \leq 0.05$ were considered to be significant.

In order to assess the diagnostic ability of each distress parameter, when differentiating between mice with and without tumors, a ROC curve analysis was performed (using data before cell injection and during the late phase of tumor progression). To describe the performance of each readout parameter, the area under the curve, the 95% confidence interval and the P-value were calculated for each parameter. An area under the curve of 1.0 indicates that the parameter is perfect for discriminating between animals growing a tumor and animals not bearing a tumor, whereas a value of 0.5 suggests no discriminative power.

3. Results

All tumors were implanted successfully, but the subcutaneous injection of A-375 or SCL-2 cells in mice yielded tumors with completely distinct characteristics. In particular, the volume of A-375 tumors was noticeably larger than the volume of the SCL-2 tumors on day 21 after cell injection (Figure 1a,b). Histological sections of the tumors demonstrated that A-375 cells were densely packed, while in SCL-2 tumors only a few cells were loosely interspersed within the extracellular matrix (Figure 1c,d). After the injection of A-375 cells, the tumor volume significantly increased between the early and middle phase as well as between the middle and late phase of tumor growth (Figure 1e). After injection of the SCL-2 cells, the tumor volume actually decreased between the middle and late phases in all nine mice (Figure 1e). Thus, the volume of A-375 tumors was significantly larger than the volume of the SCL-2 tumors in the middle as well as in the late phase of tumor growth.

larger than the volume of the SCL-2 tumors in the middle as well a
tumor growth.

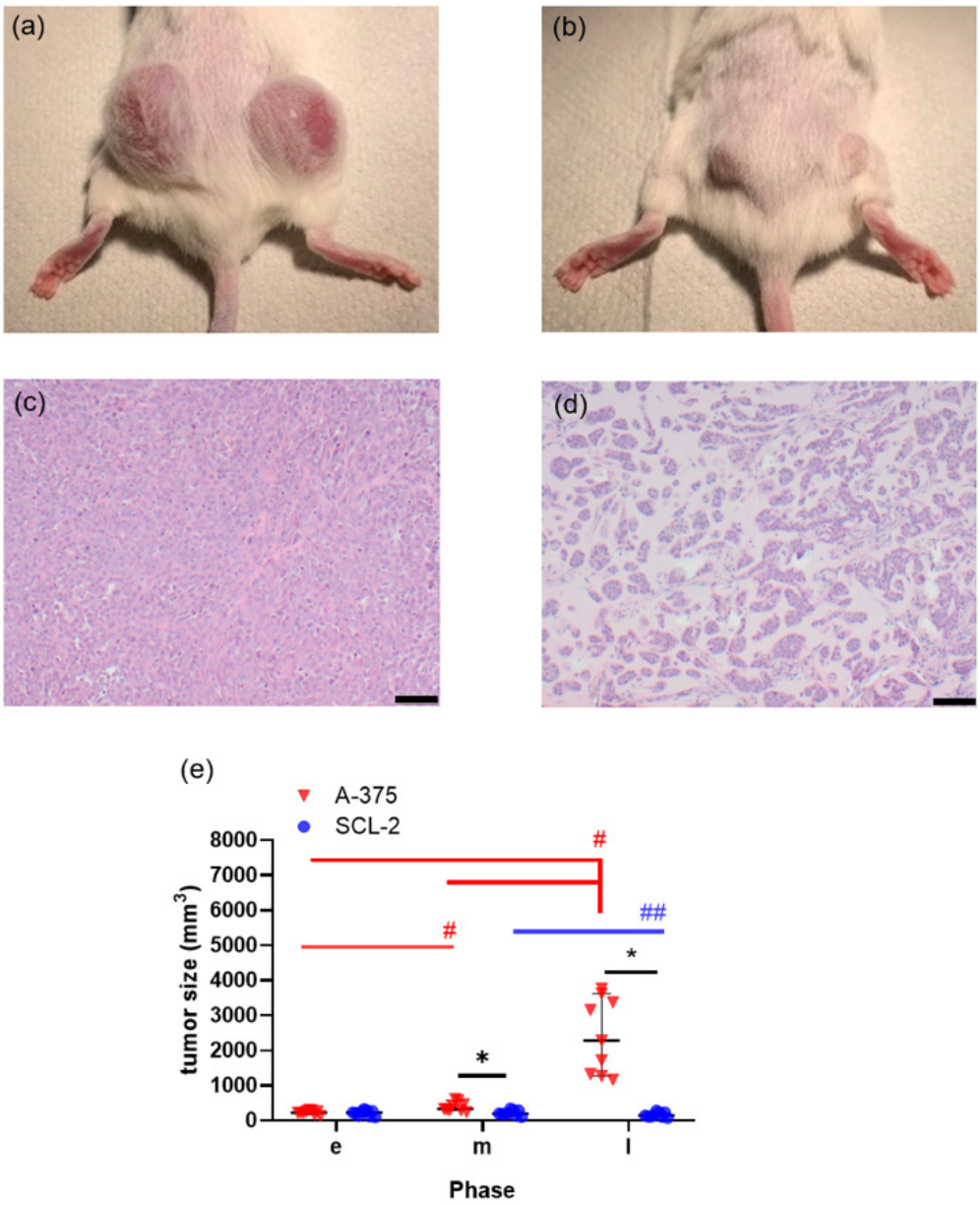

Figure 1. Characterization of A-375 and SCL-2 cell-induced tumors. Morphology of A-375 cell (**a**) and SCL-2 cell (**b**) induced tumors in the late phase after cell injection. Histology of A-375 cell (**c**) and SCL-2 cell tumors (**d**) after hematoxylin and eosin staining; scale bar = 50 µm. (**e**) The sum of tumor size (left flank tumor + right flank tumor) during early (**e**), middle (m) and late (l) phase of tumor growth. * $p \leq 0.0116$, # $p \leq 0.0091$, ## $p = 0.0003$; A-375: n = 9, SCL-2: n = 9.

Figure 1. Characterization of A-375 and SCL-2 cell-induced tumors. Morp
and SCL-2 cell (b) induced tumors in the late phase after cell injection. His
and SCL-2 cell tumors (d) after hematoxylin and eosin staining; scale bar =
tumor size (left flank tumor + right flank tumor) during early (e), middle (
tumor growth. * $p \leq 0.0116$, # $p \leq 0.0091$, ## $p = 0.0003$; A-375: n = 9, SCL-2: n = 9

In order to evaluate whether mice experience distress after ce
the growth of subcutaneous tumors, body weight change, burrowi
distress score and FCMs were analysed. No loss in body weight c
were noticed after cell injection or during tumor growth (Figure 2a,b
tress scores (maximal distress score of 4 out of 66 theoretically poss
served during the entire experiment (Figure 2c). A moderate increas
after injection of the A-375 cells and a significant increase in the di
SCL-2 injection was noticed (Figure 2c). Mice had a significantly hi

In order to evaluate whether mice experience distress after cell injection or during the growth of subcutaneous tumors, body weight change, burrowing activity, distress score and FCMs were analysed. No loss in body weight or burrowing activity were noticed after cell injection or during tumor growth (Figure 2a,b). Only very low distress scores (maximal distress score of 4 out of 66 theoretically possible points) were observed during the entire experiment (Figure 2c). A moderate increase in the distress score after injection of the A-375 cells and a significant increase in the distress score after the SCL-2 injection was noticed (Figure 2c). Mice had a significantly higher FCM concentration in the faeces in the late phase of A-375 tumor growth when compared to mice before cell injection or compared to mice in the late phase of SCL-2 tumor growth (Figure 2d).
Due to the distinct characteristics of each tumor cell line, the diagnostic ability of each distress parameter was analysed separately. After A-375 cell injection, the diagnostic ability

to differentiate between mice with and without tumor was low for body weight change (Figure 3a), burrowing activity (Figure 3b) and distress scores (Figure 3c). However, FCM concentrations (Figure 3d) could differentiate very well between mice with and without tumors. After SCL-2 cell injection, all distress parameters, percentage of body weight change (Figure 4a), burrowing activity (Figure 4b), distress scores (Figure 4c) and FCMs (Figure 4d), could not differentiate between mice with and without a tumor.

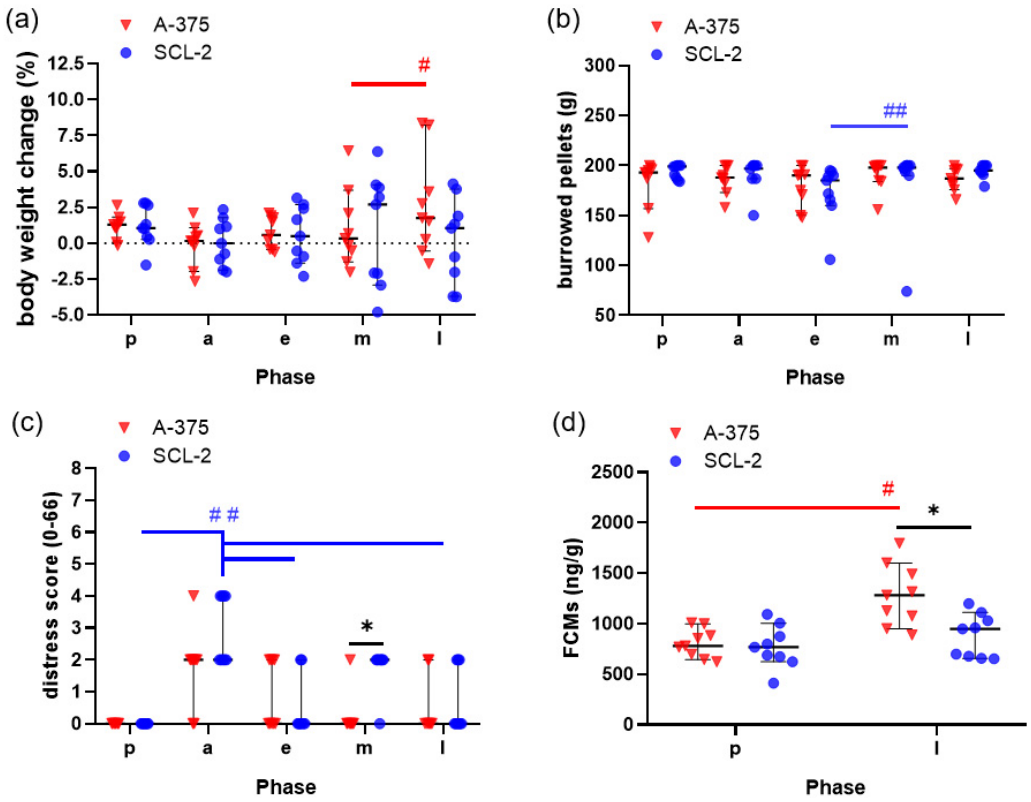

Figure 2. Evaluation of distress during the growth of the A-375 and SCL-2 tumors in mice during pre- (p), acute (a), early (e), middle (m) and late (l) phase. (**a**) Percentage of body weight change, (**b**) burrowing activity, (**c**) distress score and (**d**) concentration of faecal corticosterone metabolites (FCMs). Graph (a): $^{\#}p = 0.0366$; (b): $^{\#\#}p = 0.0287$; (c): $^{**}p = 0.0034$, $^{\#\#}p < 0.0175$; (d): $^{*}p = 0.0013$; $^{\#}p < 0.0001$; A-375: n = 9, SCL-2: n = 9.

Figure 2. Evaluation of distress during the growth of the A-375 and SCL-2 tumors in mic
pre- (p), acute (a), early (e), middle (m) and late (l) phase. (**a**) Percentage of body weight cha
burrowing activity, (**c**) distress score and (**d**) concentration of faecal corticosterone me

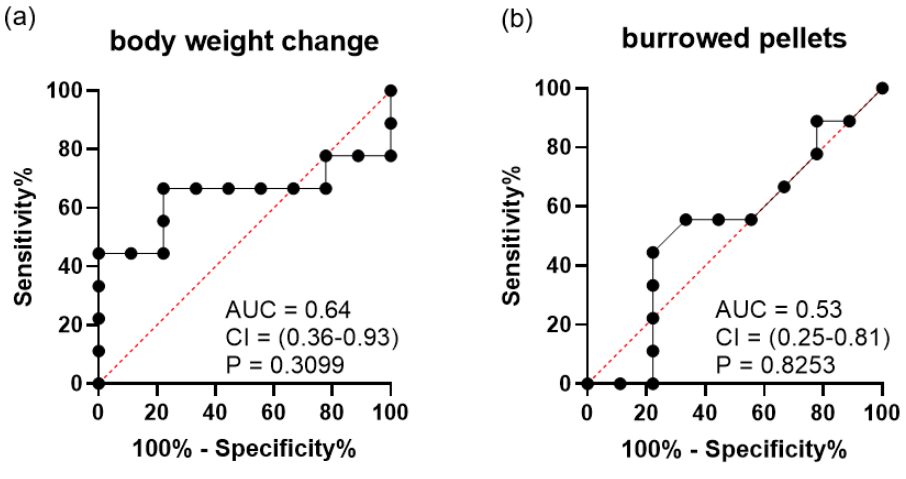

Figure 3. *Cont.*

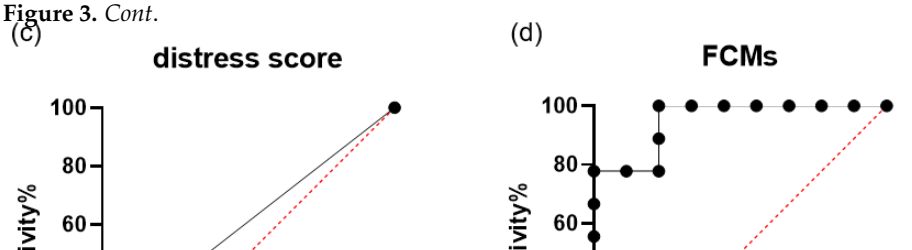

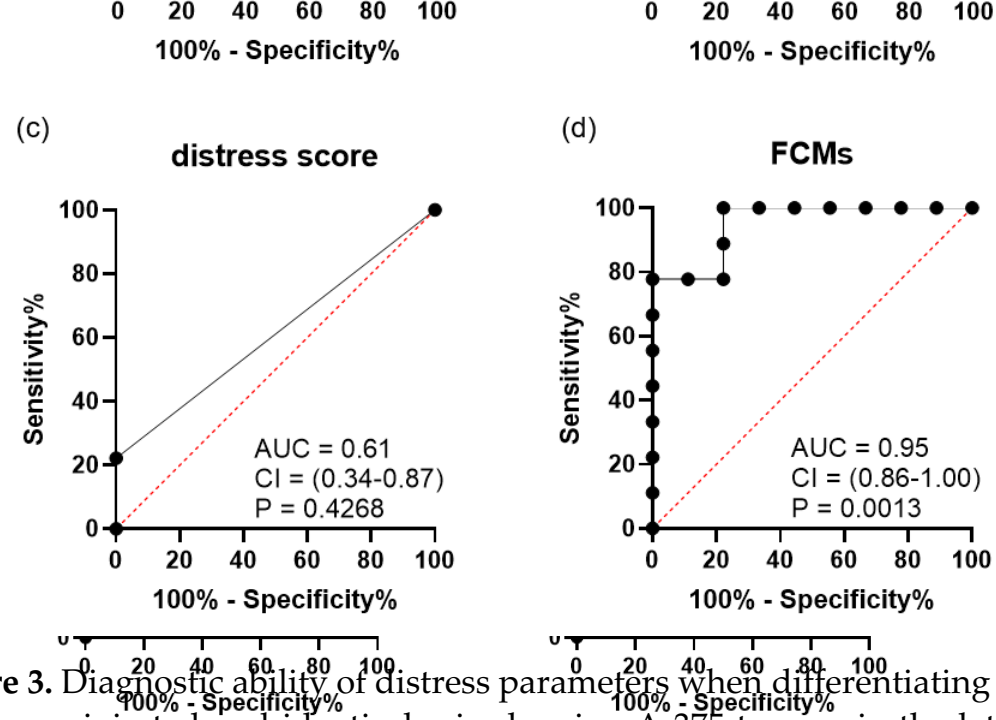

Figure 3. Diagnostic ability of distress parameters when differentiating between mice before cancer cells were injected and identical mice bearing A-375 tumors in the late phase (n = 9). ROC curve analysis of (**a**) percentage of body weight change, (**b**) burrowing activity, (**c**) distress score, and (**d**) concentration of faecal corticosterone metabolites (FCMs). The area under the curve (AUC), the 95% confidence interval (CI) and the P-value (P) for testing the AUC to be 0.5 are presented in each graph.

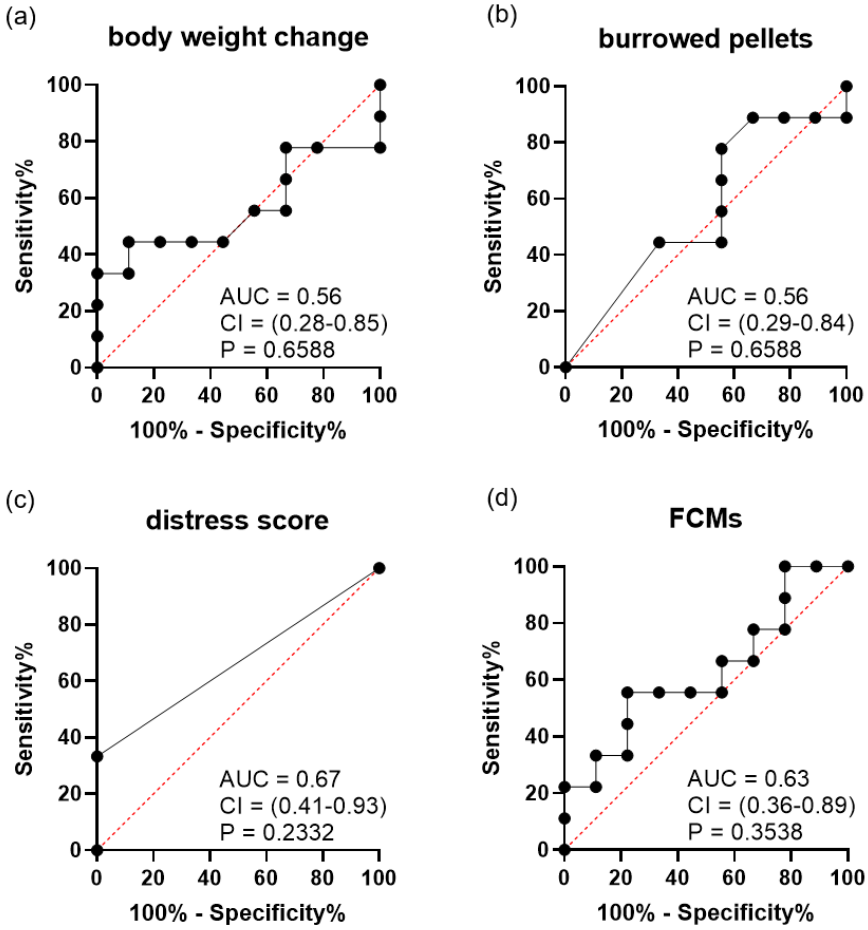

Figure 4. Diagnostic ability of distress parameters when differentiating between the mice before cancer cells were injected and identical mice bearing SCL-2 tumors in the late phase (n = 9). ROC curve analysis of (**a**) percentage of body weight change, (**b**) burrowing activity, (**c**) distress score, and (**d**) concentration of faecal corticosterone metabolites (FCMs). The area under the curve (AUC), the 95% confidence interval (CI) and the P-value (P) for testing the AUC to be 0.5 are presented in each graph.

Animals **2021**, *11*, x FOR PEER REVIEW 8 of 12
Animals **2021**, *11*, x FOR PEER REVIEW 8 of 12

Because of the significant volume growth of the A-375 tumors (Figure 1a), adjusted body weight was calculated by subtracting the tumor weight from the body weight (Figure 2). At the late phase of tumor growth, the A-375-injected mice showed a significant adjusted body weight loss (Figure 3a) rather than a body weight gain (Figure 2a). This adjusted body weight had a high diagnostic ability in distinguishing between baseline data and data derived from mice bearing a large A-375 tumor at the late phase (Figure 5b). Adjusted body weight had, however, barely any diagnostic ability in distinguishing between the baseline data and data derived from mice bearing a SCL-2 tumor at the late phase of tumor progression (Figure 5c).

Because of the significant volume growth of the A-375 tumors (Figure 1a), adjusted body weight was calculated by subtracting the tumor weight from the body weight (Figure 2). At the late phase of tumor growth, the A-375-injected mice showed a significant adjusted body weight loss (Figure 3a) rather than a body weight gain (Figure 2a). This adjusted body weight had a high diagnostic ability in distinguishing between baseline data and data derived from mice bearing a large A-375 tumor at the late phase (Figure 5b). Adjusted body weight had, however, barely any diagnostic ability in distinguishing between the baseline data and data derived from mice bearing a SCL-2 tumor at the late phase of tumor progression (Figure 5c).

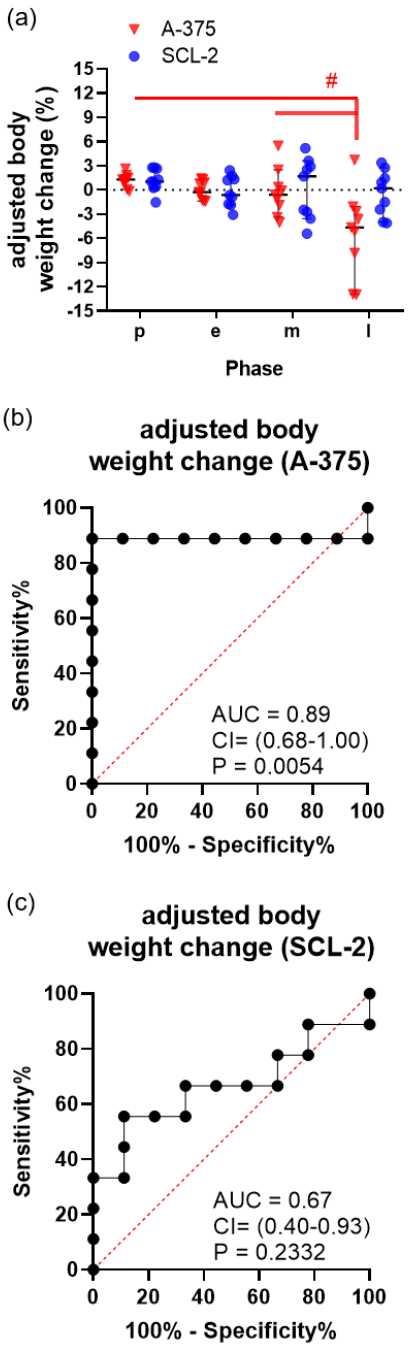

Figure 5. Assessment of adjusted body weight after subtracting the tumor weight from the body weight. (**a**) Percentage of adjusted body weight change of mice during the growth of A-375 and SCL-2 tumors. The area under the curve (AUC), the 95% confidence interval (CI) and the *p*-value (P) for testing the AUC to be 0.5 are presented in each graph. # $p \leq 0.0315$; A-375: n = 9, SCL-2: n = 9.

Figure 5. Assessment of adjusted body weight after subtracting the tumor weight from the body weight. (**a**) Percentage of adjusted body weight change of mice during the growth of A-375 and SCL-2 tumors. The area under the curve (AUC), the 95% confidence interval (CI) and the *p*-value (P) for testing the AUC to be 0.5 are presented in each graph. # $p \leq 0.0315$; A-375: n = 9, SCL-2: n = 9.
Figure 5. Assessment of adjusted body weight after subtracting the tumor weight from the body weight. (**a**) Percentage of adjusted body weight change of mice during the growth of A-375 and SCL-2 tumors. The area under the curve (AUC), the 95% confidence interval (CI) and the *p*-value (P) for testing the AUC to be 0.5 are presented in each graph. # $p \leq 0.0315$; A-375: n = 9, SCL-2: n = 9.

4. Discussion

In this study, we could demonstrate that the adjusted body weight change and FCMs have a high diagnostic ability to define distress caused by large subcutaneous tumors. Other readout parameters such as the distress score, burrowing activity or total body weight were not useful to differentiate between mice before cell injection and mice bearing such tumors.

Many studies used total body weight as readout parameter when assessing distress in various animal models [20,26,32]. In our study, this readout parameter was uninformative for differentiating between baseline data and data derived from tumor-bearing mice. This is inconsistent with the widely published concept that severe weight loss can be observed in some animal models during tumor growth [20,33]. However, several other publications also describe that the total body weight was not reduced in tumor-bearing mice [34–38]. For example, no loss of body weight was reported by Husmann et al. when analysing an osteosarcoma mouse model, although metastasis was observed in these mice [38].

However, when we calculated an adjusted body weight, by subtracting the tumor weight from the total body weight, this method could differentiate between mice with and without large tumors. This observation supports the recommendations of some guidelines and is consistent with data presented in some publications. For example, the UKCCCR guidelines emphasize that it is important to focus not only on body weight but also on the weight of the tumor itself [17]. Some authors also mention that the weight of the tumor itself and intraperitoneal effusion may mask the body weight loss [39]. Another study on a mouse xenograft model demonstrated that the size of subcutaneous tumors increased the total body weight of tumor-bearing mice [33]. However, these studies did not compare the adjusted body weight to other readout parameters for distress and did not address the issue if adjusted body weight change has the diagnostic ability to differentiate between mice with and without a tumor.

Please note that we evaluated the body weight changes twice—once as a single parameter and once as part of the distress score. Interestingly, we noticed that the adjusted body weight change has a better diagnostic ability than evaluating a distress score containing body weight change in addition to other parameters (please compare Figure 5b to Figure 3c). This suggests that single readout parameters can have a higher diagnostic ability than complex clinical scores.

FCMs can assess the distress of various animal models and have also been used to evaluate the distress of tumor-bearing mice [35,40–42]. In our study, FCM concentrations were not significantly increased when mice had relatively small SCL-2 tumors (<300 mm^3), but were significantly higher when mice had relatively large A-375 tumors (>1000 mm^3). In addition, we observed that tumor size moderately correlated with FCM concentration at the late phase of tumor progression (Pearson correlation coefficient of 0.6266, data not shown). We, therefore, conclude that FCMs might only be sensitive enough to indicate distress when mice bear large tumors.

However, it is a limitation of this study that this conclusion is based on analysing only one mouse strain and two cell lines. One study contradicts our conclusion because it reported that FCM concentrations negatively correlated with tumor size in mice after subcutaneously injecting prostate tumor cells; however, the method to measure FCMS was not validated for use in mice [41]. Our conclusion is supported by several other studies. For example, FCM concentrations were not significantly increased in an orthotopic breast tumor mouse model, when tumors were smaller than 600 mm^3 [40]. In a mouse model for pancreatic cancer, it was also observed that FCM concentrations did not significantly change when the tumors were small [35]. Thus, our data are consistent with several publications in the literature and support the concept that large subcutaneous tumors can increase FCM concentrations.

Although burrowing activity and clinical distress scores are commonly used as non-invasive methods to assess distress in mice [21,22,27,34], this study failed to define increased distress with these methods during the growth of subcutaneous tumors. Notably,

the distress score is often considered to be a subjective readout parameter, which can be influenced by the perception of the researcher. This might be a limitation of this method. However, we also want to mention that similar observations have been published in tumor models for pancreatic cancer and colon cancer [35,43,44]. Possibly, tumor growth in many tumor models causes only mild distress, which cannot be measured by burrowing activity [44] or a distress score [35]. However, it is important to note that some types of cancer can induce, for example, bone pain or severe cachexia [38,45]. Therefore, it cannot be concluded that these methods are uninformative for all cancer models. Indeed, some publications suggest that a clinical distress score or an activity index can be a good indicator to show distress in certain cancer models [34,43].

5. Conclusions

Cancer is a general term for a large group of diseases, and the biological characteristics of various types of cancer are quite diverse. Consequently, different cancer models might cause completely different levels of distress. Thus, each cancer model should be carefully evaluated [46]. This study succeeded in defining, that two methods, adjusted body weight and FCMs could define the distress of mice bearing large subcutaneous tumors.. Future studies will have to clarify if these methods are also useful to describe distress caused by cancer in other animal models.

Supplementary Materials: The following are available online at https://www.mdpi.com/article/10.3390/ani11082155/s1, Table S1: Distress score on mice, Table S2: Consequences according to distress score.

Author Contributions: Individual author contributions were as follows: D.Z. and B.V. acquired the funding. E.G., D.Z. and B.V. developed the study concept. W.X., E.G. and D.Z. developed the concept for experiments and data evaluation. W.X. and M.K. carried out the experiments. R.P. was responsible for analysing FCMs. W.X. and D.Z. analysed the data. W.X. and D.Z. wrote the manuscript. All authors have read and agreed to the published version of the manuscript.

Funding: This study was supported by the Deutsche Forschungsgemeinschaft (DFG research group FOR 2591, ZE 712/1-1, ZE 712/1-2, VO 450/15-1 and VO 450/15-2) and European Social Fund (ESF, grant numbers ESF/14-BM-A55-0003/18).

Institutional Review Board Statement: All experiments were approved by the local ethics committee and the public authority (Landesamt für Landwirtschaft, Lebensmittelsicherheit und Fischerei Mecklen-burg-Vorpommern, 7221.3-1-057/18).

Data Availability Statement: The data presented in this study are available on request from the corresponding author. The data are not publicly available to preserve privacy of the data.

Acknowledgments: The authors kindly thank Berit Blendow, Dorothea Frenz, Christin Schlie, (Institute for Experimental Surgery, Rostock University Medical Center) and Edith Klobetz-Rassam (Department of Biomedical Sciences, University of Veterinary Medicine Vienna) for their excellent technical assistance.

Conflicts of Interest: The authors declare no conflict of interest.

References

1. Ferlay, J.; Ervik, M.; Lam, F.; Colombet, M.; Mery, L.; Piñeros, M.; Znaor, A.; Soerjomataram, I.; Bray, F. Global Cancer Observatory, Cancer Today. Lyon, International Agency for Research on Cancer. 2020. Available online: https://gco.iarc.fr/today (accessed on 21 May 2021).
2. Workman, P.; Aboagye, E.O.; Balkwill, F.; Balmain, A.; Bruder, G.; Chaplin, D.J.; Double, J.A.; Everitt, J.; Farningham, D.A.; Glennie, M.J.; et al. Guidelines for the welfare and use of animals in cancer research. *Br. J. Cancer* **2010**, *102*, 1555–1577. [CrossRef] [PubMed]
3. Polson, A.G.; Fuji, R.N. The successes and limitations of preclinical studies in predicting the pharmacodynamics and safety of cell-surface-targeted biological agents in patients. *Br. J. Pharmacol.* **2012**, *166*, 1600–1602. [CrossRef] [PubMed]
4. Piccart-Gebhart, M.J.; Procter, M.; Leyland-Jones, B.; Goldhirsch, A.; Untch, M.; Smith, I.; Gianni, L.; Baselga, J.; Bell, R.; Jackisch, C.; et al. Trastuzumab after adjuvant chemotherapy in HER2-positive breast cancer. *N. Engl. J. Med.* **2005**, *353*, 1659–1672. [CrossRef] [PubMed]

5. Baselga, J.; Norton, L.; Albanell, J.; Kim, Y.M.; Mendelsohn, J. Recombinant humanized anti-HER2 antibody (Herceptin) enhances the antitumor activity of paclitaxel and doxorubicin against HER2/neu overexpressing human breast cancer xenografts. *Cancer Res.* **1998**, *58*, 2825–2831. [PubMed]
6. Gharwan, H.; Groninger, H. Kinase inhibitors and monoclonal antibodies in oncology, clinical implications. *Nat. Rev. Clin. Oncol.* **2016**, *13*, 209–227. [CrossRef]
7. Valcourt, D.M.; Kapadia, C.H.; Scully, M.A.; Dang, M.N.; Day, E.S. Best Practices for Preclinical In Vivo Testing of Cancer Nanomedicines. *Adv. Healthc. Mater.* **2020**, *9*, e2000110. [CrossRef]
8. Jung, J. Human tumor xenograft models for preclinical assessment of anticancer drug development. *Toxicol. Res.* **2014**, *30*, 1–5. [CrossRef]
9. Osborne, N.J.; Payne, D.; Newman, M.L. Journal editorial policies, animal welfare, and the 3Rs. *Am. J. Bioeth.* **2009**, *9*, 55–59. [CrossRef]
10. Littlewood, S. Cruelty to Animals Act, 1876. *Br. Med. J.* **1963**, *2*, 256. [CrossRef]
11. Batty, G.D.; Russ, T.C.; Stamatakis, E.; Kivimäki, M. Psychological distress in relation to site specific cancer mortality, pooling of unpublished data from 16 prospective cohort studies. *BMJ* **2017**, *356*, j108. [CrossRef]
12. Taylor, D.K. Influence of Pain and Analgesia on Cancer Research Studies. *Comp. Med.* **2019**, *69*, 501–509. [CrossRef] [PubMed]
13. Ragan, A.R.; Lesniak, A.; Bochynska-Czyz, M.; Kosson, A.; Szymanska, H.; Pysniak, K.; Gajewska, M.; Lipkowski, A.W.; Sacharczuk, M. Chronic mild stress facilitates melanoma tumor growth in mouse lines selected for high and low stress-induced analgesia. *Stress* **2013**, *16*, 571–580. [CrossRef] [PubMed]
14. Page, G.G.; McDonald, J.S.; Ben-Eliyahu, S. Pre-operative versus postoperative administration of morphine, impact on the neuroendocrine, behavioural, and metastatic-enhancing effects of surgery. *Br. J. Anaesth.* **1998**, *81*, 216–223. [CrossRef] [PubMed]
15. Mellor, D.J.; Reid, C.S.W. Concepts of animal well-being and predicting the impact of procedures on experimental animals. In *Improving the Well-Being of Animals in the Research Environment*; WellBeing International: Potomac, MD, USA, 1994; pp. 3–18.
16. The European Parliament and the Council of the European Union. Directive 2010/63/EU of the European Parliament and of the Council of 22 September 2010 on the protection of animals used for scientific purposes. *Off. J. Eur. Union* **2010**, *53*, 33–79.
17. United Kingdom Co-ordinating Committee on Cancer Research (UKCCCR) Guidelines for the Welfare of Animals in Experimental Neoplasia (Second Edition). *Br. J. Cancer* **1998**, *77*, 1–10. [CrossRef]
18. National Research Council (US) Committee for the Update of the Guide for the Care and Use of Laboratory Animals. *Guide for the Care and Use of Laboratory Animals*, 8th ed.; National Academies Press (US): Washington, DC, USA, 2011.
19. European Commission. Directorate-General for Environment. In *Caring for Animals Aiming for Better Science, Directive 2010/63/EU on Protection of Animals Used for Scientific Purposes Education and Training Framework*; Office of the European Union: Luxembourg, 2018.
20. Wallace, J. Humane endpoints and cancer research. *ILAR J.* **2000**, *41*, 87–93. [CrossRef] [PubMed]
21. Jirkof, P.; Cesarovic, N.; Rettich, A.; Nicholls, F.; Seifert, B.; Arras, M. Burrowing behavior as an indicator of post-laparotomy pain in mice. *Front. Behav. Neurosci.* **2010**, *4*, 165. [CrossRef] [PubMed]
22. Kumstel, S.; Tang, G.; Zhang, X.; Kerndl, H.; Vollmar, B.; Zechner, D. Grading distress of different animal models for gastrointestinal diseases based on plasma corticosterone kinetics. *Animals* **2019**, *9*, 145. [CrossRef] [PubMed]
23. Touma, C.; Palme, R.; Sachser, N. Analyzing corticosterone metabolites in fecal samples of mice, a noninvasive technique to monitor stress hormones. *Horm. Behav.* **2004**, *45*, 10–22. [CrossRef]
24. Palme, R. Non-invasive measurement of glucocorticoids, Advances and problems. *Physiol. Behav.* **2019**, *199*, 229–243. [CrossRef]
25. Möstl, E.; Palme, R. Hormones as indicators of stress. *Domest. Anim. Endocrinol.* **2002**, *23*, 67–74. [CrossRef]
26. Zhang, X.; Kumstel, S.; Tang, G.; Talbot, S.R.; Seume, N.; Abshagen, K.; Vollmar, B.; Zechner, D. A rational approach of early humane endpoint determination in a murine model for cholestasis. *ALTEX* **2020**, *37*, 197–207. [CrossRef] [PubMed]
27. Tang, G.; Nierath, W.-F.; Palme, R.; Vollmar, B.; Zechner, D. Analysis of animal well-being when supplementing drinking water with tramadol or metamizole during chronic pancreatitis. *Animals* **2020**, *10*, 2306. [CrossRef]
28. Zidar, J.; Weber, E.M.; Ewaldsson, B.; Tjäder, S.; Lilja, J.; Mount, J.; Svensson, C.I.; Svensk, E.; Udén, E.; Törnqvist, E. Group and Single Housing of Male Mice, Collected Experiences from Research Facilities in Sweden. *Animals* **2019**, *9*, 1010. [CrossRef] [PubMed]
29. Lidster, K.; Owen, K.; Browne, W.J.; Prescott, M.J. Cage aggression in group-housed laboratory male mice, an international data crowdsourcing project. *Sci. Rep.* **2019**, *9*, 15211. [CrossRef] [PubMed]
30. Jensen, M.M.; Jørgensen, J.T.; Binderup, T.; Kjaer, A. Tumor volume in subcutaneous mouse xenografts measured by microCT is more accurate and reproducible than determined by 18F-FDG-microPET or external caliper. *BMC Med. Imaging* **2008**, *8*, 16. [CrossRef]
31. Touma, C.; Sachser, N.; Möstl, E.; Palme, R. Effects of sex and time of day on metabolism and excretion of corticosterone in urine and feces of mice. *Gen. Comp. Endocrinol.* **2003**, *130*, 267–278. [CrossRef]
32. Talbot, S.R.; Biernot, S.; Bleich, A.; van Dijk, R.M.; Ernst, L.; Häger, C.; Helgers, S.; Koegel, B.; Koska, I.; Kuhla, A.; et al. Defining body-weight reduction as a humane endpoint, a critical appraisal. *Lab. Anim.* **2020**, *54*, 99–110. [CrossRef]
33. Han, Y.H.; Mun, J.G.; Jeon, H.D.; Yoon, D.H.; Choi, B.M.; Kee, J.Y.; Hong, S.H. The Extract of Arctium lappa L. Fruit (Arctii Fructus) Improves Cancer-Induced Cachexia by Inhibiting Weight Loss of Skeletal Muscle and Adipose Tissue. *Nutrients* **2020**, *12*, 3195. [CrossRef]

34. Paster, E.V.; Villines, K.A.; Hickman, D.L. Endpoints for mouse abdominal tumor models, refinement of current criteria. *Comp. Med.* **2009**, *59*, 234–241.
35. Kumstel, S.; Vasudevan, P.; Palme, R.; Zhang, X.; Wendt, E.; David, R.; Vollmar, B.; Zechner, D. Benefits of non-invasive methods compared to telemetry for distress analysis in a murine model of pancreatic cancer. *J. Adv. Res.* **2020**, *21*, 35–47. [CrossRef] [PubMed]
36. Lofgren, J.; Miller, A.L.; Lee, C.C.S.; Bradshaw, C.; Flecknell, P.; Roughan, J. Analgesics promote welfare and sustain tumour growth in orthotopic 4T1 and B16 mouse cancer models. *Lab. Anim.* **2017**, *52*, 351–364. [CrossRef] [PubMed]
37. Miller, A.; Burson, H.; Söling, A.; Roughan, J. Welfare Assessment following Heterotopic or Orthotopic Inoculation of Bladder Cancer in C57BL/6 Mice. *PLoS ONE* **2016**, *11*, e0158390. [CrossRef] [PubMed]
38. Husmann, K.; Arlt, M.J.E.; Jirkof, P.; Arras, M.; Born, W.; Fuchs, B. Primary tumour growth in an orthotopic osteosarcoma mouse model is not influenced by analgesic treatment with buprenorphine and meloxicam. *Lab. Anim.* **2015**, *49*, 284–293. [CrossRef] [PubMed]
39. Narver, H.L. Care and monitoring of a mouse model of melanoma. *Lab. Anim.* **2013**, *42*, 92–98. [CrossRef]
40. Baier, J.; Rix, A.; Drude, N.I.; Darguzyte, M.; Baues, M.; May, J.N.; Schipper, S.; Möckel, D.; Palme, R.; Tolba, R.; et al. Influence of MRI Examinations on Animal Welfare and Study Results. *Investig. Radiol.* **2020**, *55*, 507–514. [CrossRef]
41. Jacobsen, K.R.; Jørgensen, P.; Pipper, C.B.; Steffensen, A.M.; Hau, J.; Abelson, K.S. The utility of fecal corticosterone metabolites and animal welfare assessment protocols as predictive parameters of tumor development and animal welfare in a murine xenograft model. *In Vivo* **2013**, *27*, 189–196.
42. Kumstel, S.; Wendt, E.H.U.; Eichberg, J.; Talbot, S.R.; Häger, C.; Zhang, X.; Abdelrahman, A.; Schönrogge, M.; Palme, R.; Bleich, A.; et al. Grading animal distress and side effects of therapies. *Ann. N. Y. Acad. Sci.* **2020**, *1473*, 20–34. [CrossRef] [PubMed]
43. Chartier, L.C.; Hebart, M.L.; Howarth, G.S.; Whittaker, A.L.; Mashtoub, S. Affective state determination in a mouse model of colitis-associated colorectal cancer. *PLoS ONE* **2020**, *15*, e0228413. [CrossRef]
44. Chartier, L.C.; Howarth, G.S.; Lawrance, I.C.; Trinder, D.; Barker, S.J.; Mashtoub, S. Emu Oil Improves Clinical Indicators of Disease in a Mouse Model of Colitis-Associated Colorectal Cancer. *Dig. Dis. Sci.* **2018**, *63*, 135–145. [CrossRef]
45. Sliepen, S.H.J.; Diaz-Delcastillo, M.; Korioth, J.; Olsen, R.B.; Appel, C.K.; Christoph, T.; Heegaard, A.M.; Rutten, K. Cancer-induced Bone Pain Impairs Burrowing Behaviour in Mouse and Rat. *In Vivo* **2019**, *33*, 1125–1132. [CrossRef] [PubMed]
46. Examples to Illustrate the Process of Severity Classification, Day-to-Day Assessment and Actual Severity Assessment. Available online: https://ec.europa.eu/environment/chemicals/lab_animals/pdf/examples.pdf (accessed on 9 July 2021).

animals

MDPI

Article

Distress Analysis of Mice with Cervical Arteriovenous Fistulas

Wentao Xie [1,2,*], Rupert Palme [3], Clemens Schafmayer [4], Dietmar Zechner [1], Brigitte Vollmar [1] and Eberhard Grambow [1,4]

1 Rudolf-Zenker-Institute for Experimental Surgery, University Medical Center Rostock, 18057 Rostock, Germany; dietmar.zechner@uni-rostock.de (D.Z.); brigitte.vollmar@med.uni-rostock.de (B.V.); eberhard.grambow@med.uni-rostock.de (E.G.)
2 Department of Vascular and Thyroid Surgery, Department of General Surgery, The First Affiliated Hospital of Anhui Medical University, Hefei 230022, China
3 Unit of Physiology, Pathophysiology and Experimental Endocrinology, Department of Biomedical Sciences, University of Veterinary Medicine Vienna, 1210 Vienna, Austria; Rupert.Palme@vetmeduni.ac.at
4 Department for General, Visceral, Thoracic, Vascular and Transplantation Surgery, University Medical Center Rostock, 18057 Rostock, Germany; clemens.schafmayer@med.uni-rostock.de
* Correspondence: toxwt101@gmail.com

Simple Summary: Functional hemodialysis access is essential for the survival of patients with end-stage renal disease. Although various guidelines recommend autologous arteriovenous fistula as the first choice for hemodialysis, it is still the Achilles heel for patients. Several in vivo models have been used to study and improve the mechanisms of vascular remodeling of arteriovenous fistula. However, some models have the disadvantage of having anatomical features or a hemodynamic profile different from that of the arteriovenous fistula in humans. In the presented cervical arteriovenous fistula model, these disadvantages were eliminated. It resembles the human physiology and is an ideal animal model for arteriovenous fistula research. Moreover, in order to understand the impact of this model on animal welfare, the distress of this new animal model was analyzed. Body weight, faecal corticosterone metabolites, burrowing activity, nesting behaviour and distress scores were analysed after fistula creation and during the following three weeks. The physiological, behavioural, and neuroendocrine assessments all indicated that this model causes only moderate distress to the animals. This not only meets the need for animal ethics but also improves the quality of scientific research. Therefore, this cervical model is suitable for arteriovenous fistula research and should be used more frequently in the future.

Abstract: The welfare of laboratory animals is a consistent concern for researchers. Its evaluation not only fosters ethical responsibility and addresses legal requirements, but also provides a solid basis for a high quality of research. Recently, a new cervical arteriovenous model was created in mice to understand the pathophysiology of arteriovenous fistula, which is the most commonly used access for hemodialysis. This study evaluates the distress caused by this new animal model. Ten male C57B6/J mice with cervical arteriovenous fistula were observed for 21 days. Non-invasive parameters, such as body weight, faecal corticosterone metabolites, burrowing activity, nesting activity and distress scores were evaluated at each time point. Six out of ten created arteriovenous fistula matured within the observation time as defined by an increased diameter. The body weight of all animals was reduced after surgery but recovered within five days. In addition, the distress score was significantly increased during the early time point but not at the late time point after arteriovenous fistula creation. Neither burrowing activity nor nesting behaviour were significantly reduced after surgical intervention. Moreover, faecal corticosterone metabolite concentrations did not significantly increase. Therefore, the cervical murine arteriovenous fistula model induced moderate distress in mice and revealed an appropriate maturation rate of the fistulas.

Keywords: hemodialysis access; animal model; distress; animal welfare; 3R rule

check for updates

Citation: Xie, W.; Palme, R.; Schafmayer, C.; Zechner, D.; Vollmar, B.; Grambow, E. Distress Analysis of Mice with Cervical Arteriovenous Fistulas. *Animals* **2021**, *11*, 3051. https://doi.org/10.3390/ani11113051

Academic Editor: Sylvia García-Belenguer

Received: 23 September 2021
Accepted: 22 October 2021
Published: 26 October 2021

Publisher's Note: MDPI stays neutral with regard to jurisdictional claims in published maps and institutional affiliations.

Copyright: © 2021 by the authors. Licensee MDPI, Basel, Switzerland. This article is an open access article distributed under the terms and conditions of the Creative Commons Attribution (CC BY) license (https://creativecommons.org/licenses/by/4.0/).

1. Introduction

As vascular access for hemodialysis, all academic guidelines suggest autologous arteriovenous fistula (AVF) as the first option [1,2]. Although native AVF show the lowest risk of complications, the lowest need for intervention and the best long-term patency [1], it is still the Achilles' heel for patients [3]. After fistula creation, there are several factors that can cause fistula dysfunction, such as immaturation, thrombosis or neointimal hyperplasia [4]. In order to understand the involved mechanisms, researchers have attempted to find an effective animal model to study the underlying mechanisms.

Animal models are crucial to study physiology and pathophysiology for almost all diseases in humans and in animals as well as to develop new therapies in all fields of medicine. Appropriate animal models should strictly follow ethical standards to maximise the likelihood of obtaining the knowledge sought balanced against minimising animal discomfort. Over the past few decades, various rodent animal models have been used to study AVF maturation. For example, AVFs were created between the aorta and the inferior cava vein in a side-to-side manner [5] or by anastomosis of the common carotid artery to the jugular vein in an end-to-end manner [6]. However, none of these models mimics the anatomical characteristics of AVF in hemodialysis patients, which determines the hemodynamic profile within the fistula. This is very important because the blood flow dynamics have an important impact on AVF maturation and dysfunction [7]. Recently, researchers have created a murine AVF model in which the end of a branch of the external jugular vein was anastomosed to the side of the common carotid artery [7]. It mimics similar hemodynamic properties to classical AVF in humans, in which the anastomosis is also created in a side-to-end fashion. This improves the translation of experimental in vivo results in clinical settings. Because the new cervical model uses a small vein for AVF, the volume stress on the heart is expected to be reduced as well. However, it is not known what distress the model induces in the experimental animals.

In order to quantify the distress of animals in different experimental models, several parameters can be assessed. Body weight is a classical and essential indicator of animal distress, and all committees use body weight as an important experimental animal welfare indicator [8]. Faecal corticosterone metabolites (FCMs) reflect adrenocortical activity and are used increasingly often as a non-invasive assessment of distress [9,10]. Burrowing and nesting activity are innate behaviours in rodents. These behaviours are often affected by pain or suffering [11]. Therefore, it is possible to assess animal welfare by analysing changes in burrowing and nesting activity. This study was conducted to assess whether the cervical AVF causes a significant increase in distress for the animals and to provide objective evidence to support the use of this new animal model in future AVF studies.

2. Materials and Methods

2.1. Animals

All experiments were conducted in accordance with the European Directive (2010/63/EU). Twelve male C57BL/6 mice were used at an age of 9–15 weeks and a body weight of 20–30 g. Mice were bred in standard laboratories with a 12:12 h light-dark cycle, constant temperature (21 $\pm$ 2 °C) and humidity (60 $\pm$ 20%) and provided free access to chow and water ad libitum.

2.2. Experimental Design

It is known that burrowing behaviour can be affected by learning and is enhanced by social facilitation [12]. Therefore, a group training with two to four mice per cage was performed on three days in a row, starting on day −7 (shown in Figure 1). Although single housing of mice may cause distress, we decided to separate mice into single cages from day −4 because group housed male mice can show aggressive behaviour [13]. The separation also allowed us to assess burrowing activity, nesting activity and FCM concentrations for individual mice. These data were assessed from unaffected mice before AVF creation (pre-operative phase) and at various time points after AVF creation. Please note that data

from the pre-operative phase served as control to data assessed after AVF creation. Faeces were collected on days −2, 2 and 17. On days −2, 2 and 17, burrowing behaviour and distress score were assessed. One day later, nesting activity was studied respectively. The time points of data assessment were described as pre-operative phase (day −2/−1), early phase (day 2/3) and late phase (day 17/18). In order to analyse continuous body weight change, the body weight was assessed on days −4, −2, 0, 1, 2, 3, 5, 7, 9, 12, 14, 16, 17, 18, 19 and 21. On day 21, the patency of the fistula was checked directly by opening the wound, and the mice were euthanized.

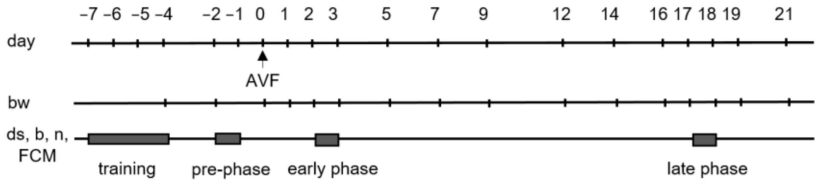

Figure 1. Experimental timeline for assessment of animal distress. The fistulas were created on day 0 and mice euthanized on day 21. The mice had a training phase to learn burrowing. Body weight (bw), distress score (ds), burrowing (b) as well as nesting (n) activity and faecal corticosterone me tabolites (FCMs) were evaluated as indicated.

2.3. AVF Model and Tissue Harvest

AVF creation was performed as previously described [7]. In brief, mice were anaesthetised by continuous isoflurane treatment (1.5% isoflurane; 0.8 L/min N_2O; 0.8–1.0 L/min O_2). After subcutaneous (s.c.) injection of heparin (1 U/kg bw), the left dorsomedial branch of the external jugular vein and the ipsilateral common carotid artery were separated through ventral incision. The left sternocleidomastoid muscle was cauterized, and the carotid artery was clamped. An incision of the same diameter as the artery was made on the lateral side of the artery with micro scissors, followed by local rinse with heparin (200 U/mL). The distal end of the vein branch was ligated, cut and anastomosed to the common carotid artery in a side-to-end fashion using 10-0 Ethilon (Johnson & Johnson Medical GmbH, Norderstedt, Germany) interrupted sutures. The clamps were then released in a distal to proximal order. Confirming no active bleeding, the neck incision was closed with 5–0 Prolene (Johnson & Johnson Medical GmbH, Norderstedt, Germany). Finally, 0.5 mL of saline and 5 mg/kg bw of carprofen were injected s.c. for volume institution and pain relief, respectively. For pain relief, 1250 mg/L metamizol (Ratiopharm, Ulm, Germany) was provided daily in the drinking water after AVF creation. Mice were euthanized on day 21 by intraperitoneal (i.p.) injection of ketamine (90 mg/kg bw) and xylazine (25 mg/kg bw). To harvest the fistula vein and the contralateral dorsomedial branch of the external jugular vein as control, first 0.9% NaCl was injected intracardially in order to flush the blood out of the veins. Then, 4% formalin (Formafix, Grimm med. Logistik GmbH, Torgelow, Germany) was injected in the same way and also flushed around the veins to fixate the tissue. For histological analysis, 4-µm-thick cross-sections of both the fistula and the control vein were stained by haematoxylin-eosin (HE).

2.4. Body Weight and FCM Analysis

The body weight of the mice was measured four times per week with a scale (EMB 200-2, KERN & SOHN, Balingen, Germany) in the morning at 9:00–9:30 a.m. At each time point, the percentage of body weight change was determined by comparison to the body weight before AVF creation on day −4.

For analysing FCMs, all bedding with old faeces was removed, and fresh bedding was added to the cages 24 h prior to the start of faeces collection. More than 400 mg of fresh faeces were collected per mouse and dried for 4 h at 65 °C. Until further processing, the faeces was stored at −20 °C. Thereafter, 50 mg of dried faeces were extracted with 1 mL

of 80% methanol for further analysis by a 5α-pregnane-3β,11β,21-triol-20-one enzyme immunoassay [10,14].

2.5. Assessing Burrowing and Nesting Activity

A burrowing tube (15 cm length × 6.5 cm diameter) which was filled with 200 ± 1 g food pellets (ssniff Spezialdiaeten GmbH) was placed in the left back corner of the cages 3 h before the dark phase at 4:00–4:10 pm. Mice had free access to these pellets. Nesting material was left in the cages. The weight of the food pellets (g) that remained in the tube was measured after 2 h at 6:00–6:10 pm. Then, the same tube was put back and measured on the next morning at 9:00–9:15 am and deducted from 200 g.

For evaluating nesting activity, a cotton nest-building material (5 cm square of pressed cotton batting, Zoonlab GmbH, Castrop-Rauxel, Germany) was placed in the left front of the cage 3 h before the dark phase at 4:00–4:15 pm. Pictures of the nests were taken, and nesting was scored the next morning at 9:00–09:15 a.m. This score was previously described in detail [12].

2.6. Distress Score Analysis

Based on the distress score sheet designed by Paster et al. [15], our working group made some modifications (for details also see Supplementary Tables S1 and S2) [16]. In brief, the scoring sheet has a total of 66 points and consists of five parts, body weight, general condition, spontaneous behaviour, flight behaviour and process-specific criteria. The distress score was assessed by only one person in a not blinded manner, according to the scoring sheet. All scores were assessed in the morning at 9:00–9:30 a.m.

2.7. Statistical Analysis

Data were graphed and analysed with GraphPad Prism8 (version 8.0.1, GraphPad Software Inc., San Diego, CA, USA). They were presented as single data points plus median and 95% confidence interval. Since the data describing percentage of body weight, FCM, burrowing activity, nesting score and distress score were non-parametric (as assessed by Shapiro Wilk test), one-way repeated measure ANOVA on ranks (Friedman Test) were performed by comparing each time point to the pre-operative phase (day −2 or day −1) and by correcting for multiple comparisons (Dunn's method). Overall, statistical significance was set at $p < 0.05$.

3. Results

3.1. Mortality of Mice and Maturation of Fistulas

One AVF was created in every mouse. Two mice were euthanized during surgical intervention due to severe bleeding, while in the other ten mice, AVF was created successfully (shown in Figure 2a). On day 21, six of ten fistulas matured sufficiently (shown in Figure 2b) as defined by patency and an increased diameter compared to the contralateral jugular vein. Four fistulas did not mature and were found occluded on day 21. Compared to control veins, HE staining of patent fistulas revealed a marked increase in both diameter and thickness of the vein wall as a sign of sufficient maturation (shown in Figure 2d).

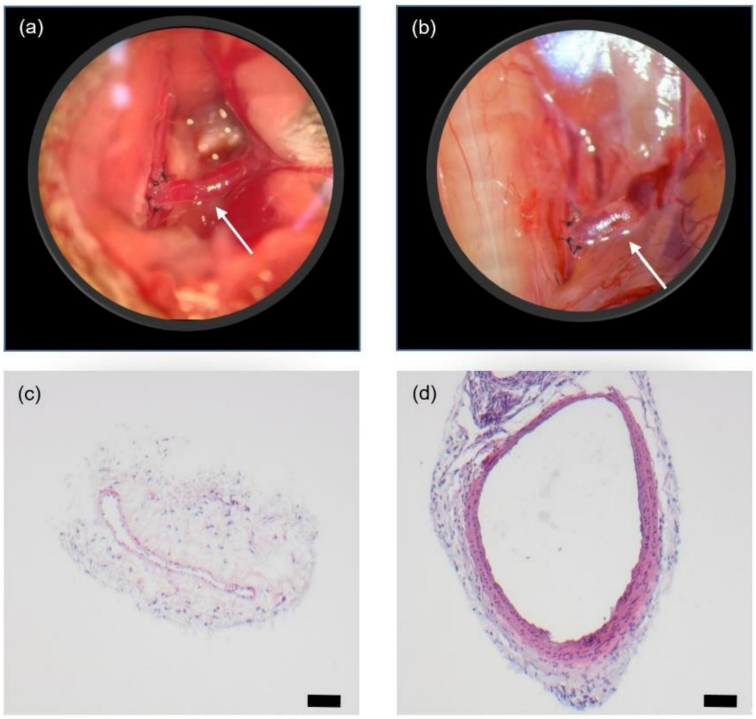

Figure 2. Characteristics of AVF. Morphology of AVF (white arrows) immediately after fistula creation (**a**) and on day 21 (**b**). Magnification = 40×. Haematoxylin-eosin stained cross-sections from of a control vein (**c**) and a respective fistula vein on day 21 after creation of the arteriovenous anastomosis (**d**). Scale bar = 50 µm.

3.2. Analysis of Animal Distress

The body weight decreased after AVF creation but recovered at day 5 after surgical intervention and steadily increased until day 21. However, there was no significant difference compared to the pre-operative phase, on day −2 (shown in Figure 3). It is worth pointing out that in this early phase, nine mice lost weight in the range of 10% or less, only one mouse lost more than 10% of its body weight.

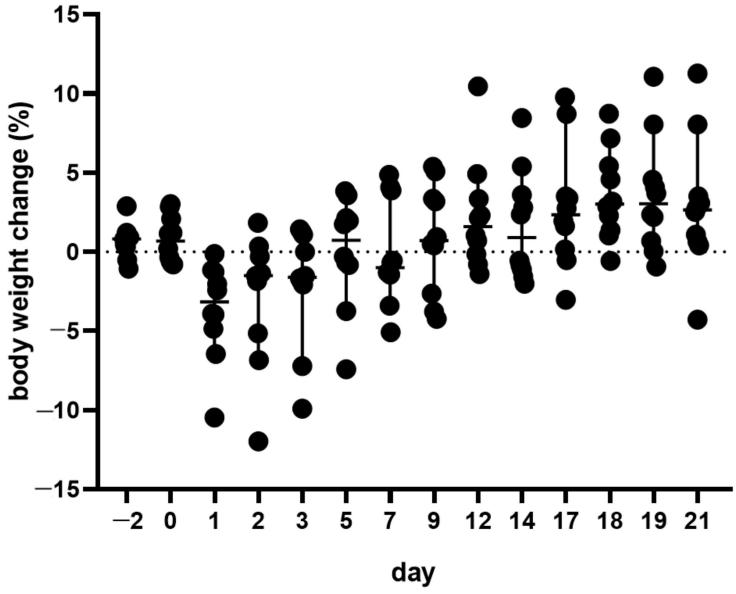

Figure 3. Body weight change of mice before and after creation of an AVF on day 0. Median with 95% CI. *n* = 10.

There was a slight, but not significant ($p = 0.1473$) increase in FCM concentrations on day 2 after completion of the AVF creation, from 831/628–1106 on day −2 to 993/746–1312 ng/g (median/95% confidence interval) on day 2 (shown in Figure 4a). Notably, one mouse that lost over 10% of its body weight revealed an increase of FCMs to 3170 ng/g on day 2. In this mouse, FCM level decreased noticeably on day 17.

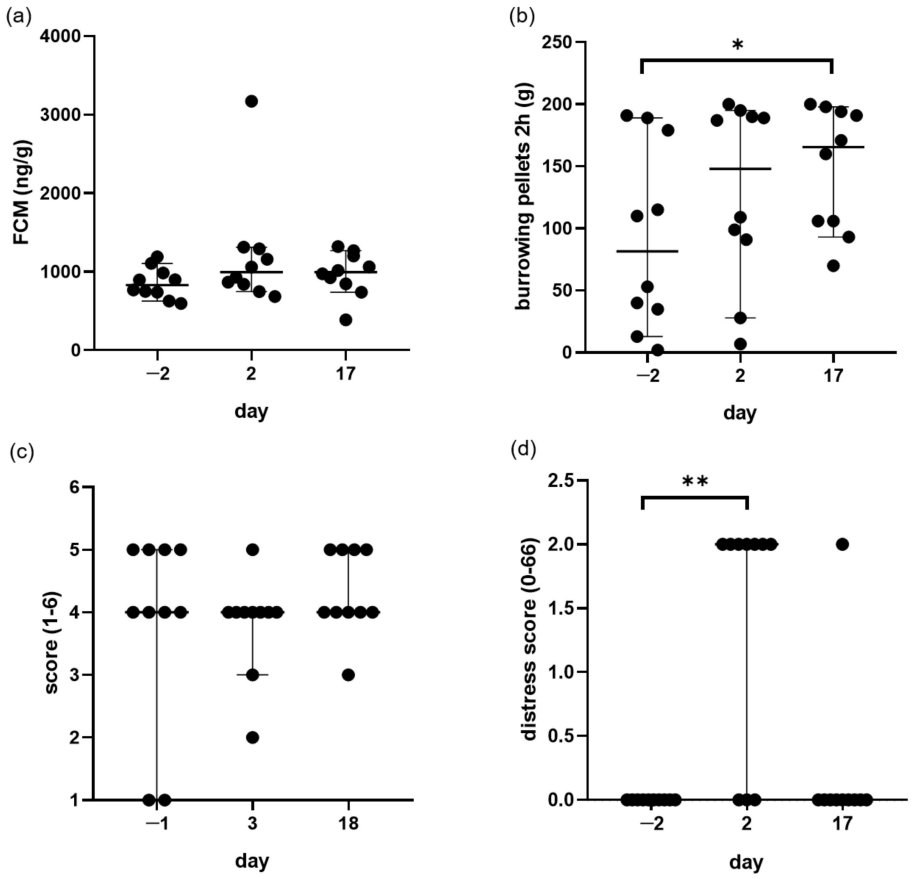

Figure 4. Evaluation of distress parameters during the maturation of AVF. FCM concentrations (**a**), 2-h burrowing activity (**b**), nesting activity (**c**) and the distress score (**d**) were assessed on the indicated days during pre-operative phase (day −2 or day−1), at the early time point (day 2 or day 3) or late time point (day 17 or 18) after AVF creation. Median with 95% CI. * $p = 0.0073$. ** $p = 0.0378$. $n = 10$. Each circle mean one animal.

Analysis of burrowing activity after 2 h showed no reduction of burrowing activity during the early and late phase after AVF creation (shown in Figure 4b). Indeed, compared to day −2, the burrowing behaviour was actually significantly more intense on day 17 ($p = 0.0073$). When mice were allowed to burrow the entire night, almost all mice burrowed all pellets out of the tube. Thus, no significant difference was observed when comparing the two time points after AVF creation to the pre-operative phase (data not shown). It is noteworthy that one mouse showed a decreased burrowing activity on day 2, but that the burrowing behaviour recovered on day 17 (data not shown). This was the identical mouse, which lost more than 10% of its body weight and revealed an increased FCM concentration of 3170 ng/g on day 2.

At the different time points, all mice were similarly active in building their nests (shown in Figure 4c). The nesting scores were 4/1–5, 4/3–4 and 4/4–5 (median/95% confidence interval) on day −1, day 3 and day 18, respectively.

Notably, in the early phase, the distress of some mice increased (shown in Figure 4d). The distress scores were 0/0–0 (median/95% confidence interval) on day −2 and 2/0–2 on day 2. On day 17, the distress score returned to 0 for most mice.

4. Discussion

This study demonstrates that cervical AVF matures successfully and that mice after AVF experience only suffered moderate distress. Therefore, it might be stated that the cervical murine AVF model is a suitable animal model for studying vascular remodelling of an arteriovenous hemodialysis access.

C57BL/6 is the most common inbred mouse strain and has been widely used as a genetic background for studying genetically modified mice to evaluate the molecular mechanisms underlying human disorders. The purpose of the animal model presented here was to create an AVF in C57BL/6 mice to facilitate research on the molecular mechanism of AVF maturation. Although the learning curve for the challenging microsurgical creation of this cervical AVF model is long and needs continuous training, this mouse model has its own advantages compared to large animal AVF models, in which AVF creation is technically easier. For example, fistulas of this mouse model showed significant pathophysiological changes within 4 weeks [7]. This allows scientists to study fistula maturation within a fairly short period of time.

Although the vessels are much smaller in the cervical AVF model in mice compared to humans, the anatomical configuration and blood flow characteristics of the fistula are similar to AVF for hemodialysis access in humans. In addition to anatomical consistency with the clinical condition, this animal model also has a similar clinical success rate. In this study, 40% of the fistulas did not mature and were occluded three weeks after the operation. This is in line with the description of Wang et al. [7]. Since the patency rate is lower than 100%, this animal model also allows researchers to assess therapeutic approaches for an improvement of fistula maturation. In addition, the immature fistulas provide an opportunity to study the mechanism of AVF immaturity by means of histological, immunohistochemical or biomolecular analysis. Compared to native veins, patent fistulas showed increased diameter and thicker vessel walls. These characteristics are also found in human fistulas. In humans, neointimal hyperplasia is a common pathological manifestation during fistula maturation [4]. HE staining revealed markedly neointimal hyperplasia compared to contralateral native veins. These findings suggest that this model can be used to study the mechanisms of fistula maturation as well as different treatment options. It is notable that all successfully created AVF mice survived to the end of experiment. No mouse died due to complications, such as heart failure, which is a main cause of distress after AVF creation [17,18]. The novel model uses a smaller diameter vein, a branch of the external jugular vein, as a venous fistula. This may reduce the cardiac load and the risk of heart failure, which might explain the moderate level of distress. Thus, this animal model might reduce the number of animals needed for pursuing research in this field without causing severe distress to animals.

Improvement in animal welfare is important for pursuing basic as well as preclinical research [19]. In order to quantify the distress of this animal model, body weight, FCMs, burrowing activity and nesting behaviour as well as distress score were chosen as distress indicators.

Body weight is the most common parameter for assessing distress. As early as 1985, it had been used as a key indicator to evaluate animal distress [20]. Because weighing is non-invasive and objective, almost daily weight had been done to see the dynamics of weight change. Before operation, without AVF stressor, all mice showed good health status and progressive weight gain. Continuous observation of body weight revealed that there was a weight loss in the early phase, which could be explained by surgery. Surgery and anesthesia are both particularly potent stressors [21,22], and thus post-surgical body weight reduction is common in mice [16,23–25]. However, as the experiment progressed, the mice recovered and gained stable weight over the next 3 weeks. Therefore, the early phase and the late experimental phase were chosen as time points to assess the distress using additional parameters. As seen in other studies on distress and weight change [23], when mice suffered severe distress, the body weight of the experimental animals started to decrease progressively. Although the surgery itself had an impact on the welfare of the

mice, the noticeable increase in body weight at the late phase indicated that the mice were in good condition, and that the AVF itself did not cause severe distress to the animals.

It is known that FCM levels positively correlate with distress [9,10]. The advantage of faeces samples over blood samples is that they can be easily collected without additionally stressing the animals [26]. In the present research, consistent with other experimental results [24,25,27], there was a moderate increase in FCM level after the respective intervention. However, there was no statistically significant difference compared to the preoperative phase. After AVF creation, FCM levels did not increase over the course of time, which indicates that the cervical fistula did not significantly increase distress in mice. It is noteworthy that one mouse had a particularly high FCM level in the early phase, corresponding to a loss of more than 10% body weight. Compared to other mice, this mouse had more intraoperative loss of blood, which may have contributed to its significant weight loss and stress [28]. This observation also indicates that the performance of the surgeon has the biggest effect on the animal's well- being.

Since not every type of stressor may be reflected in corticosterone levels [29], behavioural parameters were also detected in our research to assess animal distress. Numerous studies have demonstrated that burrowing behaviour and nesting activity are reduced by distress [12,30,31]. Similar to body weight, burrowing activity can also be assessed objectively, which is easy to perform. In order to induce minimal distress and unnecessary effects on the mice, burrowing and nesting behaviour were tested inside the home cage [32]. During fistula maturation, there was no decrease in burrowing activity observed. Mice actually burrowed more pellets in late phase. Since some mice pulled the nesting material into the burrowing tube, burrowing and nesting activity were assessed on different days. Unlike body weight, FCMs and burrowing activity, the nesting score is a subjective score; however, deficits of nest building also reflect a decline in animal welfare and impaired general condition [30]. In agreement with other studies [24,25,27], most mice were highly motivated to build nests in this study, but no significant difference between each time point was observed.

In addition, a distress score sheet was used to evaluate AVF-bearing mice. Our work group has used this distress score sheet several times to successfully analyse distress in experimental mice [16,23–25,27]. All mice showed low distress scores, no more than 2 out of 66 theoretically possible points. Consistent with the results of other parameters, the distress also reflected that this animal model only moderately increased distress. However, we want to mention that the distress score has a similar limitation to the nesting score in that it is not measured objectively but in a subjective manner.

We also want to describe other limitations of this study. Since the behavioural analysis of burrowing and nesting requires the mice to be housed separately, this separation may cause distress and might influence our analysis. However, we did not observe any obvious signs of distress on single housed mice before surgical intervention. Another limitation is the small number of mice tested in this experiment. This might prevent observing statistically significant differences between different time points. Since this is a new animal model, only a small number of animals was used to test the feasibility and validity of this animal model. However, distress of additional animals should be evaluated to further validate the feasibility and safety of this model.

5. Conclusions

The presented cervical AVF model matures successfully. The analysis of multiple distress parameters, such as body weight, FCMs, burrowing activity, nesting activity and a distress score, demonstrated that this model in mice can be established without causing severe distress. Therefore, it is a suitable model to study the pathophysiology of vascular remodeling in AVF. It should be noted that the mice in this study did not suffer renal insufficiency or uraemia, which are key factors affecting fistula maturation and neointima formation [33]. Therefore, kidney dysfunction should be added to this model, and the distress caused by renal insufficiency plus AVF should be carefully evaluated.

Supplementary Materials: The following are available online at https://doi.org/10.3390/ani9040145, Table S1: Distress score on mice [16]; Table S2: Consequences according to distress score [16].

Author Contributions: Individual author contributions were as follows: D.Z. and B.V. acquired the funding. D.Z., E.G. and B.V. developed the study concept. W.X. and E.G. developed the concept for experiments and data evaluation. W.X. carried out the experiments, and R.P. was responsible for FCM analysis. W.X. and D.Z. analysed data. W.X., C.S., D.Z. and E.G. wrote and reviewed the manuscript. All authors have read and agreed to the published version of the manuscript.

Funding: This study was supported by the Deutsche Forschungsgemeinschaft (DFG research group FOR 2591, ZE 712/1-1, ZE 712/1-2, VO 450/15-1 and VO 450/15-2).

Institutional Review Board Statement: All experiments were approved by the local ethics committee and the public authority (Landesamt für Landwirtschaft, Lebensmittelsicherheit und Fischerei Mecklenburg-Vorpommern, reference number: 7221.3-1-058/19).

Informed Consent Statement: Not applicable.

Data Availability Statement: The data presented in this study are available on request from the corresponding author. The data are not publicly available to preserve privacy of the data.

Acknowledgments: The authors kindly thank Edith Klobetz-Rassam for analysing FCM samples and Dorothea Frenz for HE staining.

Conflicts of Interest: The authors declare no conflict of interest.

References

1. Schmidli, J.; Widmer, M.K.; Basile, C.; de Donato, G.; Gallieni, M.; Gibbons, C.P.; Haage, P.; Hamilton, G.; Hedin, U.; Kamper, L.; et al. Editor's Choice—Vascular Access: 2018 Clinical Practice Guidelines of the European Society for Vascular Surgery (ESVS). *Eur. J. Vasc. Endovasc. Surg.* **2018**, *55*, 757–818. [CrossRef] [PubMed]
2. Vascular Access 2006 Work Group. Clinical Practice Guidelines for Vascular Access. *Am. J. Kidney Dis.* **2006**, *48* (Suppl. 1), S176–S247. [CrossRef] [PubMed]
3. Riella, M.C.; Roy-Chaudhury, P. Vascular access in haemodialysis: Strengthening the Achilles' heel. *Nat. Rev. Nephrol.* **2013**, *9*, 348–357. [CrossRef]
4. Hu, H.; Patel, S.; Hanisch, J.J.; Santana, J.M.; Hashimoto, T.; Bai, H.; Kudze, T.; Foster, T.R.; Guo, J.; Yatsula, B.; et al. Future research directions to improve fistula maturation and reduce access failure. *Semin. Vasc. Surg.* **2016**, *29*, 153–171. [CrossRef]
5. Kuwahara, G.; Hashimoto, T.; Tsuneki, M.; Yamamoto, K.; Assi, R.; Foster, T.R.; Hanisch, J.J.; Bai, H.; Hu, H.; Protack, C.D.; et al. CD44 Promotes Inflammation and Extracellular Matrix Production During Arteriovenous Fistula Maturation. *Arter. Thromb. Vasc. Biol.* **2017**, *37*, 1147–1156. [CrossRef] [PubMed]
6. Yang, B.; Shergill, U.; Fu, A.A.; Knudsen, B.; Misra, S. The Mouse Arteriovenous Fistula Model. *J. Vasc. Interv. Radiol.* **2009**, *20*, 946–950. [CrossRef]
7. Wong, C.Y.; De Vries, M.R.; Wang, Y.; Van Der Vorst, J.R.; Vahrmeijer, A.L.; Van Zonneveld, A.-J.; Hamming, J.F.; Roy-Chaudhury, P.; Rabelink, T.J.; Quax, P.H.A.; et al. A Novel Murine Model of Arteriovenous Fistula Failure: The Surgical Procedure in Detail. *J. Vis. Exp.* **2016**, *108*, e53294. [CrossRef] [PubMed]
8. Talbot, S.R.; Biernot, S.; Bleich, A.; Van Dijk, R.M.; Ernst, L.; Häger, C.; Helgers, S.O.A.; Koegel, B.; Koska, I.; Kuhla, A.; et al. Defining body-weight reduction as a humane endpoint: A critical appraisal. *Lab. Anim.* **2020**, *54*, 99–110. [CrossRef]
9. Möstl, E.; Palme, R. Hormones as indicators of stress. *Domest. Anim. Endocrinol.* **2002**, *23*, 67–74. [CrossRef]
10. Touma, C.; Palme, R.; Sachser, N. Analyzing corticosterone metabolites in fecal samples of mice: A noninvasive technique to monitor stress hormones. *Horm. Behav.* **2004**, *45*, 10–22. [CrossRef]
11. Gjendal, K.; Ottesen, J.L.; Olsson, I.A.S.; Sørensen, D.B. Burrowing and nest building activity in mice after exposure to grid floor, isoflurane or ip injections. *Physiol. Behav.* **2019**, *206*, 59–66. [CrossRef] [PubMed]
12. Deacon, R. Assessing Burrowing, Nest Construction, and Hoarding in Mice. *J. Vis. Exp.* **2012**, *59*, e2607. [CrossRef]
13. Lidster, K.; Owen, K.; Browne, W.J.; Prescott, M.J. Cage aggression in group-housed laboratory male mice: An international data crowdsourcing project. *Sci. Rep.* **2019**, *9*, 15–211. [CrossRef]
14. Touma, C.; Sachser, N.; Möstl, E.; Palme, R. Effects of sex and time of day on metabolism and excretion of corticosterone in urine and feces of mice. *Gen. Comp. Endocrinol.* **2003**, *130*, 267–278. [CrossRef]
15. Paster, E.V.; Villines, K.A.; Hickman, D.L. Endpoints for mouse abdominal tumor mod-els: Refinement of current criteria. *Comp. Med.* **2009**, *59*, 234–241.
16. Kumstel, S.; Tang, G.; Zhang, X.; Kerndl, H.; Vollmar, B.; Zechner, D. Grading Distress of Different Animal Models for Gastrointestinal Diseases Based on Plasma Corticosterone Kinetics. *Animals* **2019**, *9*, 145. [CrossRef]
17. Melenovsky, V.; Skaroupkova, P.; Benes, J.; Torresova, V.; Kopkan, L.; Cervenka, L. The Course of Heart Failure Development and Mortality in Rats with Volume Overload due to Aorto-Caval Fistula. *Kidney Blood Press. Res.* **2012**, *35*, 167–173. [CrossRef]

18. Ghanem, S.; Tanczos, B.; Deak, A.; Bidiga, L.; Nemeth, N. Carotid-Jugular Fistula Model to Study Systemic Effects and Fistula-Related Microcirculatory Changes. *J. Vasc. Res.* **2018**, *55*, 268–277. [CrossRef] [PubMed]
19. National Research Council. *Recognition and Alleviation of Distress in Laboratory Animals*; National Research Council: Washington, DC, USA, 2008; ISBN 9780309108171.
20. Morton, D.B.; Griffiths, P.H. Guidelines on the recognition of pain, distress and discomfort in experimental animals and an hypothesis for assessment. *Veter. Rec.* **1985**, *116*, 431–436. [CrossRef] [PubMed]
21. Desborough, J.P. The stress response to trauma and surgery. *Br. J. Anaesth.* **2000**, *85*, 109–117. [CrossRef]
22. McGUILL, M.W.; Rowan, A.N. Biological Effects of Blood Loss: Implications for Sampling Volumes and Techniques. *ILAR J.* **1989**, *31*, 5–20. [CrossRef]
23. Tang, G.; Seume, N.; Häger, C.; Kumstel, S.; Abshagen, K.; Bleich, A.; Vollmar, B.; Talbot, S.R.; Zhang, X.; Zechner, D. Comparing distress of mouse models for liver damage. *Sci. Rep.* **2020**, *10*, 19184. [CrossRef]
24. Tang, G.; Nierath, W.-F.; Palme, R.; Vollmar, B.; Zechner, D. Analysis of Animal Well-Being When Supplementing Drinking Water with Tramadol or Metamizole during Chronic Pancreatitis. *Animals* **2020**, *10*, 2306. [CrossRef]
25. Kumstel, S.; Vasudevan, P.; Palme, R.; Zhang, X.; Wendt, E.H.U.; David, R.; Vollmar, B.; Zechner, D. Benefits of non-invasive methods compared to telemetry for distress analysis in a murine model of pancreatic cancer. *J. Adv. Res.* **2020**, *21*, 35–47. [CrossRef] [PubMed]
26. Palme, R. Non-invasive measurement of glucocorticoids: Advances and problems. *Physiol. Behav.* **2019**, *199*, 229–243. [CrossRef]
27. Kumstel, S.; Janssen-Peters, H.; Abdelrahman, A.; Tang, G.; Xiao, K.; Ernst, N.; Wendt, E.H.U.; Palme, R.; Seume, N.; Vollmar, B.; et al. MicroRNAs as systemic biomarkers to assess distress in animal models for gastrointestinal diseases. *Sci. Rep.* **2020**, *10*, 16931. [CrossRef]
28. Whittaker, A.L.; Barker, T.H. The Impact of Common Recovery Blood Sampling Methods, in Mice (Mus Musculus), on Well-Being and Sample Quality: A Systematic Review. *Animals* **2020**, *10*, 989. [CrossRef]
29. Mallien, A.S.; Häger, C.; Palme, R.; Talbot, S.R.; Vogt, M.A.; Pfeiffer, N.; Brandwein, C.; Struve, B.; Inta, D.; Chourbaji, S.; et al. Systematic analysis of severity in a widely used cognitive depression model for mice. *Lab. Anim.* **2020**, *54*, 40–49. [CrossRef] [PubMed]
30. Arras, M.; Rettich, A.; Cinelli, P.; Kasermann, H.P.; Bürki, K. Assessment of post-laparotomy pain in laboratory mice by telemetric recording of heart rate and heart rate variability. *BMC Vet. Res.* **2007**, *3*, 16. [CrossRef]
31. Jirkof, P.; Cesarovic, N.; Rettich, A.; Nicholls, F.; Seifert, B.; Arras, M. Burrowing Behavior as an Indicator of Post-Laparotomy Pain in Mice. *Front. Behav. Neurosci.* **2010**, *4*, 165. [CrossRef] [PubMed]
32. Jirkof, P. Burrowing and nest building behavior as indicators of well-being in mice. *J. Neurosci. Methods* **2014**, *234*, 139–146. [CrossRef] [PubMed]
33. Brahmbhatt, A.; Misra, S. The Biology of Hemodialysis Vascular Access Failure. *Semin. Interv. Ridiol.* **2016**, *33*, 15–20. [CrossRef] [PubMed]

scientific reports

Check for updates

OPEN

3D-printed lightweight dorsal skin fold chambers from PEEK reduce chamber-related animal distress

Wentao Xie[1,2], Matthias Lorenz[3], Friederike Poosch[4], Rupert Palme[5], Dietmar Zechner[1], Brigitte Vollmar[1], Eberhard Grambow[1,6]✉ & Daniel Strüder[1,4]

The dorsal skinfold chamber is one of the most important in vivo models for repetitive longitudinal assessment of microcirculation and inflammation. This study aimed to refine this model by introducing a new lightweight chamber made from polyetheretherketone (PEEK). Body weight, burrowing activity, distress, faecal corticosterone metabolites and the tilting angle of the chambers were analysed in mice carrying either a standard titanium chamber or a PEEK chamber. Data was obtained before chamber preparation and over a postoperative period of three weeks. In the early postoperative phase, reduced body weight and increased faecal corticosterone metabolites were found in mice with titanium chambers. Chamber tilting and tilting-related complications were reduced in mice with PEEK chambers. The distress score was significantly increased in both groups after chamber preparation, but only returned to preoperative values in mice with PEEK chambers. In summary, we have shown that light chambers reduce animal distress and may extend the maximum dorsal skinfold chamber observation time. Chambers made of PEEK are particularly suitable for this purpose: They are autoclavable, sufficiently stable to withstand rodent bites, inexpensive, and widely available through 3D printing.

The dorsal skinfold chamber is an essential model for in vivo microcirculation analysis[1]. Researchers investigated inflammation[2–4], thrombogenesis[5–7], wound healing[8,9], angiogenesis, biomaterials[10] and tumor vascularisation[11–13] using the dorsal skinfold chamber[14–16]. Repetitive intravital visualisation of the microvascular dynamics is the major advantage of the model (Fig. 1).

Repetitive intravital microscopy without repetitive surgery requires the continuous exposition of the prepared vascular bed. The skinfold chamber on the back of the laboratory animal ensures optimal conditions for repetitive intravital microscopy[17]. The standard chamber comprises two titanium frames fixing the extended dorsal skin in the back's midline. During chamber implantation, the first frame is sutured to one side of the dorsal skinfold. The skin, the subcutaneous tissue, and the striated panniculus carnosus muscle on one side of the dorsal skinfold are removed. Then, microsurgery exposes the vessels of the opposite panniculus carnosus muscle. Finally, screws are punched through the dorsal skinfold to connect the second frame of the chamber and the observation window is filled with saline followed by sealing with a coverslip.

The major limitation of the model is the physical burden of the chamber, which leads to animal immobilization and distress. The titanium dorsal skinfold chamber is 4 cm long, 3 cm high, and weighs 3.8 g. The weight matches up to 20% of the mouse's body weight (20–30 g). Weight and skin stretching may lead to restricted breathing, immobilization, and pain. The severity of any dorsal skinfold chamber experiment is considered at least moderate. Therefore, the reputation of the model as a standard in microvascular research has been contested in the context of 3R (refinement, reduction, replacement)[18].

Lateral tilting of the dorsal skinfold chamber is another important limitation and strongly related to animal distress[17]. Weight, the chamber's high center-of-gravity, and overstretching of the skin (in particular at the fixation

[1]Institute for Experimental Surgery, Rostock University Medical Center, 18057 Rostock, Germany. [2]Department of Vascular and Thyroid Surgery, Department of General Surgery, The First Affiliated Hospital of Anhui Medical University, Hefei 230022, China. [3]Faculty of Engineering, Technology, Business and Design, University of Applied Sciences, 23966 Wismar, Germany. [4]Department of Otorhinolaryngology, Head and Neck Surgery "Otto Koerner", Rostock University Medical Center, 18057 Rostock, Germany. [5]Unit of Physiology, Pathophysiology and Experimental Endocrinology, Department of Biomedical Sciences, University of Veterinary Medicine Vienna, 1210 Vienna, Austria. [6]Department of General, Visceral, Thoracic, Vascular and Transplantation Surgery, Rostock University Medical Center, Schillingallee 35, 18057 Rostock, Germany. ✉email: eberhard.grambow@med.uni-rostock.de

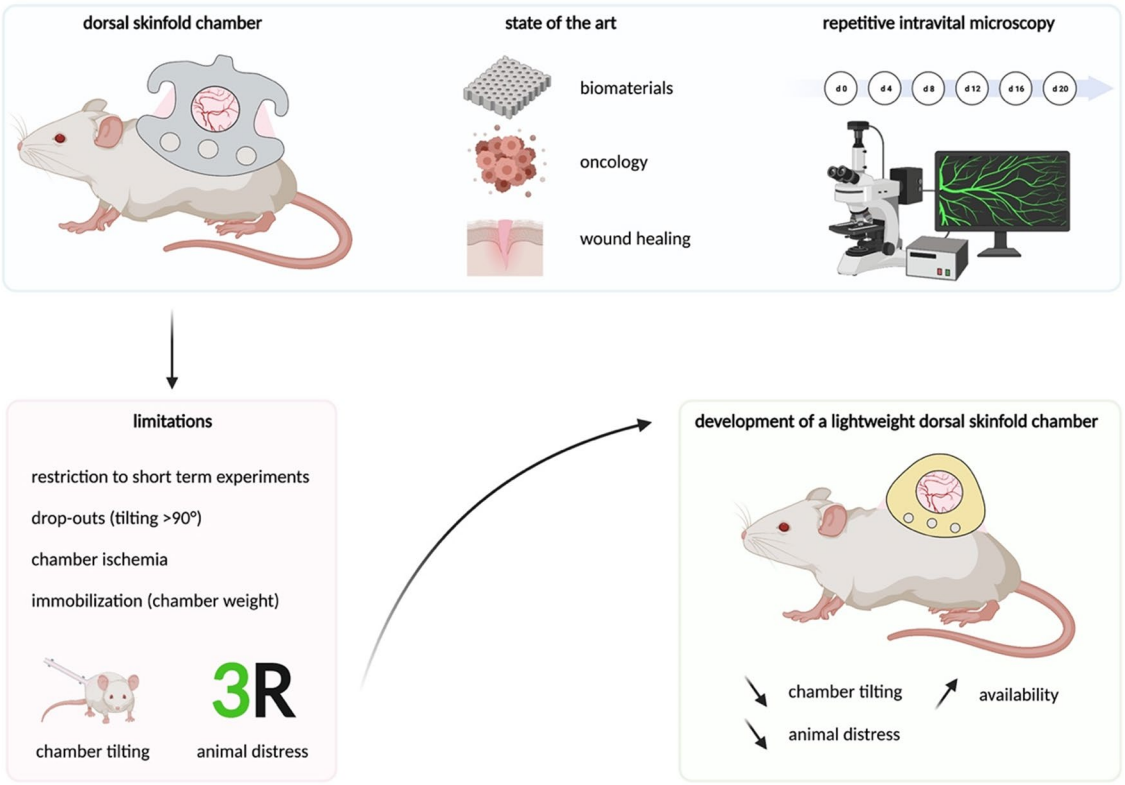

Figure 1. Application and limitations of the dorsal skinfold chamber. The model enables continuous observation of microvascular parameters by intravital microscopy. The major limitations are animal distress and restriction to short-term experiments. To improve animal welfare and extend the observation time, a lightweight, 3D-printable PEEK chamber was developed. Figure created with BioRender.com.

screws) lead to lateral tilting of the chamber in the second week after dorsal skinfold chamber preparation. Tilting comprises perfusion and causes animal distress (immobilization, pain). Chamber tilting of > 50° must be scored in the severity assessment and tilting of > 100° considered as an abort criterion. Therefore, experiments of up to 21 days are associated with high dropouts (20% in the third week) and low reliability (infections, ischemia). Experiments of longer than 21 days are impossible with standard chambers[19,20].

To overcome these limitations, the chambers were continuously revised. Schreiter et al. reviewed the developments until 2017[1]. While 63% of the dorsal skinfold chamber studies were from German-speaking countries and mostly used titanium chambers, smaller titanium chambers are already standard in the US[1]. Research groups from Sweden and Asia proposed more advanced plastic chambers made from plexiglass, dacron and polyetheretherketone (PEEK)[1].

For many years, PEEK has been used successfully in medicine as a replacement material for titanium to fabricate surgical devices, implants and prostheses[21,22]. PEEK is a linear, semi-crystalline polymer that exhibits excellent mechanical and thermal properties. PEEK is bioinert and durable (lack of thermal aging and chemical resistance).

Although many publications point out disadvantages of large titanium chambers, they are still used in most studies: Between 2017 and 2021, only four of 76 studies used non-titanium chambers (70 titanium, 3 plastic, 1 steel wire, 2 no information given; Suppl. Table S1)[23–26].

One factor in the limited distribution of improved dorsal skinfold chamber is that previous research on chamber refinement missed quantifying the actual impact on animal distress. Existing titanium chamber stocks and poor availability of plastic chambers are further factors, which hindered comprehensive implementation of refined dorsal skinfold chambers.

The goal of the present study was the design and evaluation of a lightweight PEEK dorsal skinfold chamber to reduce animal distress and preserve repetitive intravital microscopy quality. We introduce a 3D printed design with unrestricted access and evaluate animal distress compared with traditional chambers. Therefore, the pilot study assessed specific dorsal skinfold chamber parameters (intravital microscopy quality, chamber tilting) and general distress parameters (weight loss, corticosterone levels, behaviour, distress score). As bridging technology, the PEEK chamber may improve future in vivo research until sufficient in vitro and in virtuo models are established.

	Titanium chamber	PEEK chamber
Weigth (g)	3.8	1.5
Height (mm)	36 × 24	24 × 20
Transdermal screws	3	–
Price (€)	30–110	5

Table 1. Comparison of the titanium and PEEK chamber.

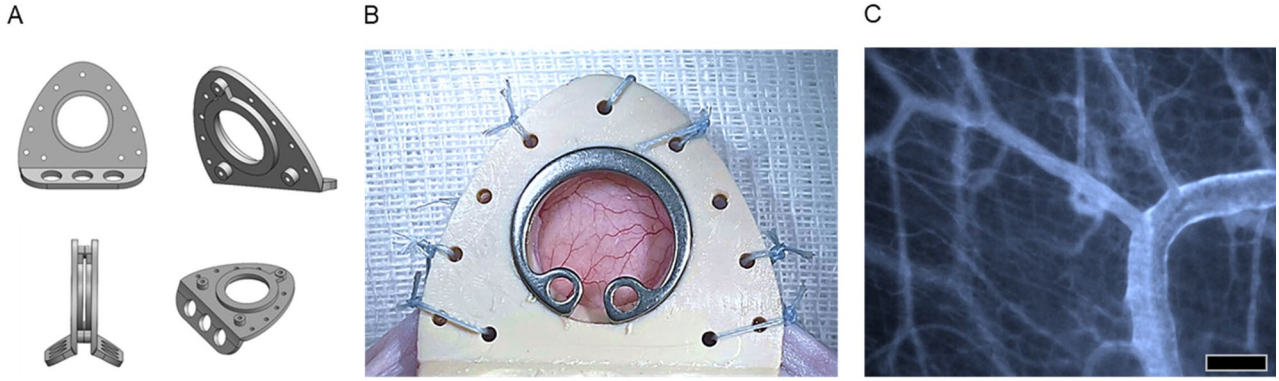

Figure 2. Exemplary design of the PEEK chamber. (**A**) Model of the scaled-down and 3D-printable PEEK chamber (created with SolidWorks). (**B**) The extrusion printed PEEK chamber was ground to remove superficial irregularities and implantated into the test animal. (**C**) Representative intravital microscopy image of a PEEK chamber on day 3. Bar represents 100 µm.

Results

This study examined animal distress of standard titanium dorsal skinfold chambers compared to a 3D printed design made of PEEK. Preparation of the chamber and intravital microscopy were comparable. PEEK chambers showed no signs of bites, chews or any other manipulation by the mice. In terms of lateral chamber tilting, animal weight loss and corticoid levels, the PEEK chamber was markedly superior.

The new PEEK chamber was designed lower and lighter than titanium chambers (approx. 1.5 g instead of 3.8 g). The chamber was 3D-printed cost-effectively according to a reproducible protocol (€5.30 /chamber). The costs were lower compared to milled titanium chambers (€30–€110). The design and the low weight allowed the PEEK chamber to be secured with sutures (Table 1). Robust suture material (FiberWire, Arthrex, Munich, Germany) attached with multiple knots reliably fixed the chamber for 21 days (Fig. 2). The traumatic transdermal insertion of titanium screws was obsolete. The duration and difficulty of chamber implantation was comparable to the titanium chamber (20 min). PEEK is bioinert and autoclavable; wound infections did not occur in the pilot study, even with repeated use of autoclaved chambers.

PEEK chambers significantly reduced lateral tilting in the third week (Fig. 3). In the first week, both preparations were stable in the median plane; the titanium group even showed slightly less tilting (PEEK: 15°/9°–35°; titanium: 5°/0°–28°, $p = 0.1688$; median/95% confidence interval). None of the chambers tilted by > 45° in the first week. In the second week, one PEEK chamber tilted moderately by 72° and one titanium chamber tilted severely by 102°. The other five of six chambers in the respective groups remained stable with less than 20° deviation. In the third week, the deviation of the moderately tilted PEEK chamber remained stable, and another PEEK chamber tilted likewise. Four of six PEEK chambers showed no deviation even after 21 days. In the titanium group, however, the tilting angle increased markedly in five of six animals. In three of six titanium chamber animals, the chamber deviated to about 90° and the skin around the screws had stretched to large defects. The median tilting of the titanium chambers was significantly greater than tilting of the PEEK chambers in the third week (PEEK: 8.5°/0°–62°; titanium: 67°/10°–129°, $p < 0.05$).

Postoperative weight loss was significantly reduced in PEEK chamber mice (Fig. 4A). While significant weight loss occurred postoperatively in all animals, weight loss was lower with PEEK chambers (PEEK: − 6.12%/− 14.46 to 1.06%; titanium: − 14.69%/− 18.95 to 8.77%; $p < 0.05$). The body weight of PEEK chamber mice recovered already in the middle phase (2.46%/− 0.47 to 9.07%). Titanium chamber animals did not fully recover from the high initial weight loss until the late phase (− 3.33%/− 25.68% to 5.10%). Additionally, the weight loss of titanium chamber approached 20%, which is considered as an abort criterium.

Similar beneficial results for the PEEK chamber were found for faeces corticosterone metabolites (FCMs; Fig. 4B). In the PEEK group, only two animals experienced a slight increase in FCMs during the early phase (147%/121–281% $p = 0.13$). In contrast, early phase FCMs in mice with titanium chambers increased fourfold compared to baseline (baseline: 100%, early phase: 368%/248–587%; $p < 0.05$). In the middle and late phase, FCM values in both groups returned to the baseline (Fig. 4B). The direct comparison between PEEK and titanium chambers revealed a significant increase of titanium chamber FCMs in the early phase (PEEK: 147%/121–281%;

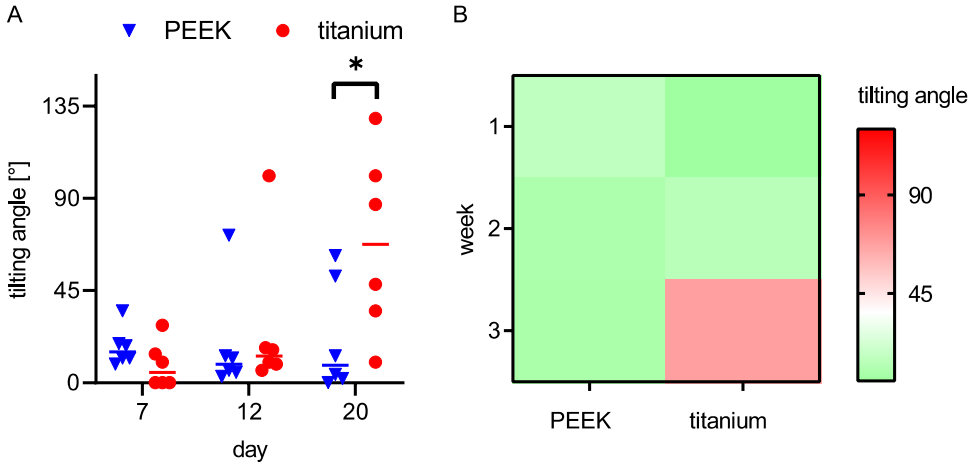

Figure 3. Lateral chamber tilting. PEEK and titanium chamber tilting angles over time are given as individual values (**A**) and as a heatmap indicating high risk for lateral chamber tilting (**B**). PEEK chambers significantly reduced lateral tilting in the third week, while tilting in both chambers was comparable for 12 days. This is further visualized in the heat map (**B**). Differences between the groups were analysed by multiple t-tests (Holm-Sidak), *p < 0.05, PEEK: n = 6, titanium: n = 6.

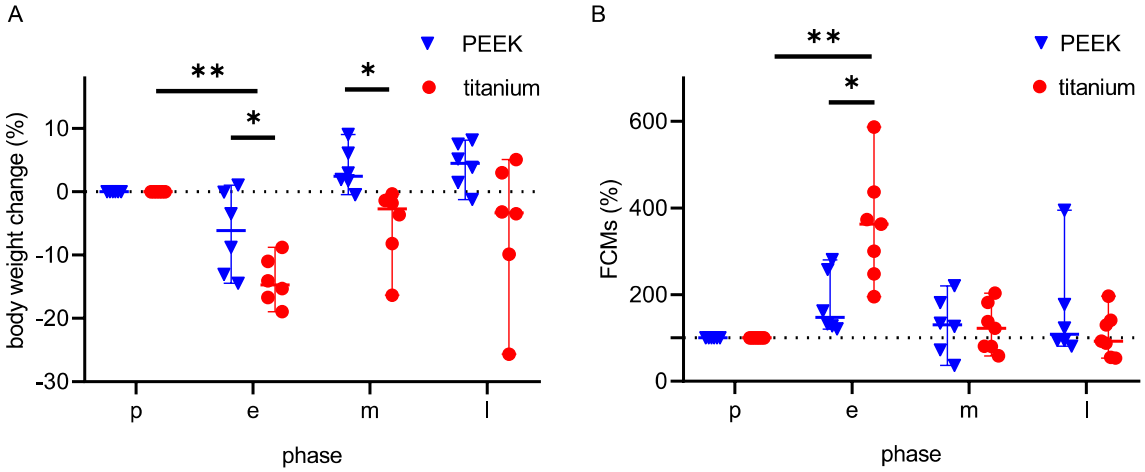

Figure 4. Changes in body weight and faecal corticosterone metabolite (FCM) concentrations after dorsal skinfold chamber implantation. Individual values are given over time in a preoperative phase (p), early postoperative phase (e), middle postoperative phase (m) and late postoperative (l) phase. Body weight change (**A**) between each time point was analysed by RM one-way ANOVA on ranks followed by Dunn's correction, and the difference between each group was analysed by unpaired t test followed by two-tailed P value tests. FCM concentrations (**B**) between each time point was analysed by Friedman test followed by Dunn's correction, and the difference between each group was analysed by unpaired t test followed by two-tailed P value tests. *p < 0.05; **p < 0.05; PEEK: n = 6, titanium: n = 6.

titanium: 368%/248–587%, p < 0.05), while FCMs were comparable in the middle (PEEK: 130%/37–220%; titanium: 101%/59–203%, p = 0.31) and late phase (PEEK: 108%/81–395%; titanium: 90%/54–196%, p = 0.85).

Specific distress scoring and burrowing assessment did not show differences between titanium and the PEEK chambers (Fig. 5). Distress values remained low, with maximum 7/66 points for PEEK and 6/66 points for titanium chambers (p > 0.8268). In both groups, the distress score increased slightly in the early phase and declined in the middle and late phase. Likewise, burrowing started with relatively high baseline values (PEEK: 108 g/57–195 g; titanium: 196 g/105–200 g, p = 0.06). Postoperative burrowing decreased significantly in both groups (PEEK: p < 0.05; titanium: p = 0.05, vs. baseline). Burrowing remained decreased markedly throughout the observation time in both groups (PEEK: 61 g/13–192 g; titanium: 36 g/20–56 g).

In summary, the PEEK chamber is easily available and maintains the high quality of intravital vascular imaging. The PEEK chamber's flat and lightweight design can reduce animal distress and prolong the maximum duration of the experiment.

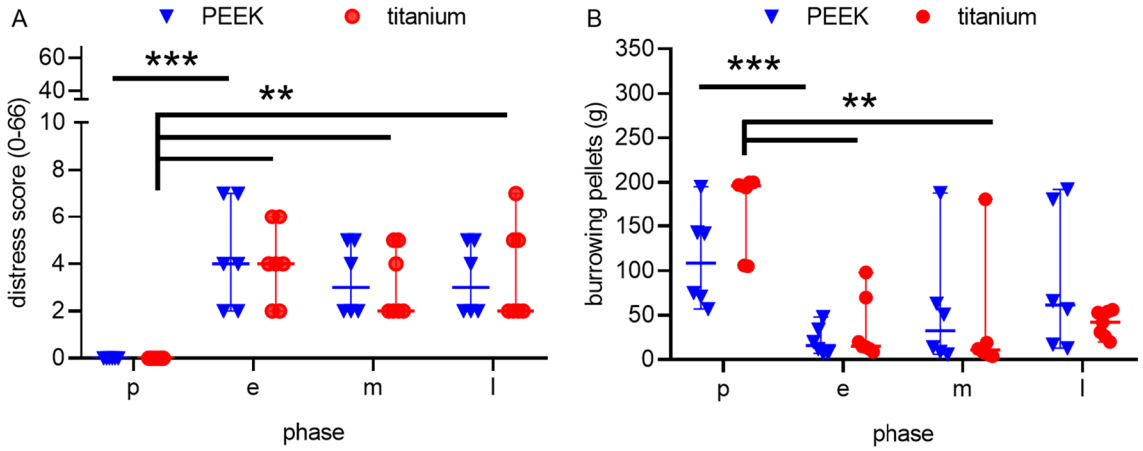

Figure 5. Distress Score and burrowing activity after dorsal skinfold chamber implantation. Individual values are given over time in a preoperative phase (p), early postoperative phase (e), intermediate postoperative phase (m) and late postoperative (l) phase. Specific distress scoring and burrowing assessment did not show differences between the titanium and the PEEK chamber. Distress score (**A**) and burrowing activity (**B**) at each time point were compared by Friedman test followed by Dunn's correction and the difference between each group was analysed by unpaired t test (Holm-Sidak). $^{**}p < 0.05$, $^{***}p < 0.05$; PEEK: n = 6, titanium: n = 6.

Discussion

The dorsal skinfold chamber is a major model for repetitive examination of vascular changes and inflammation. However, the dorsal skinfold chamber causes considerable stress for the test animals. Therefore, the model is not only criticized by animal welfare groups. This criticism is understandable, since many improved models have already been published, but mainly the classical titanium chamber is used[17,23,24,27–29]. For the widespread establishment of plastic chambers, a simple manufacturing protocol has been lacking on the one hand and proof of superiority in distress reduction on the other.

Here, we present a simple 3D-printed model made of PEEK. We show that the PEEK chamber reduces distress and extends maximum observation time.

The surgical demands and the quality of intravital microscopy are equivalent in PEEK and titanium chambers. When implanting the PEEK chamber, penetration of the skinfold with screws can be omitted, because of the chamber's light weight. In titanium chambers, screws cause penetrating holes at the base of the skinfold, which are associated with chamber tilting. The PEEK chamber is fixed by tear resistant sutures, which the test animal cannot reopen (FibreWire, Arthrex, Munich, Germany). These sutures cause less trauma than previously used screws. After chamber implantation, the experiments run without differences to titanium chambers. In particular, there are no differences in the quality of the repetitive intravital fluorescence microscopy.

The most common complication of dorsal skinfold chamber experiments is lateral tilting of the chamber during the second week[17]. By the third week, 50% of the titanium chambers tilt to a position of > 90°, which causes animal immobilization. In all PEEK chambers, tilting remained below 90° for three weeks. The only PEEK chamber that had a tilting of 50° in the second week remained constant in the following week. This is clearly because of the reduced weight. In contrast, titanium chambers continued tilting over time. Therefore, the stable position of PEEK chambers could extend the maximum duration of future experiments to four or five weeks.

Besides decreased tilting in the third week, the use of PEEK chambers also reduced distress for the experimental animals in the postoperative period. Postoperative weight loss is significantly higher in titanium chamber animals and does not return to baseline values over three weeks. With PEEK chambers, on the other hand, the test animals reach their original weight as early as the second week. Consistent with our data, previous research described up to 15% postoperative weight loss for titanium chambers and decreased weight loss for non-metal dorsal skinfold chambers[30–32].

This difference in stress was confirmed by FCM measurement, a non-invasive measure of adrenocortical activity[33]. FCMs increased significantly after implantation of a titanium chamber while only a slight increase in FCMs was observed for PEEK chambers. Therefore, postoperative stress was primarily related to the titanium chamber and not to the surgery itself. In the intermediate and late phase, FCMs returned to baseline values in both groups. The design of future titanium chamber experiments should consider increased postoperative stress as a potential bias[34].

In contrast to FCMs and body weight changes, mice in both groups did not differ in burrowing activity nor distress score. The distress score remained at a low level after the operation. The postoperative increase of 7/66 points in the distress score was statistically significant. However, the values remained in the lower range of the score.

To our knowledge, this study is the first to investigate the distress of laboratory animals with dorsal skinfold chambers. Despite the lack of data on animal distress, many chamber improvements have already been published. These improvements were supposed to reduce animal distress and to enable MRI imaging. A simple development is a smaller titanium frame with an equally large observation window[29]. These smaller titanium chambers are sold commercially in the United States (small dorsal kit SM100, APJ Trading Co., Ventura, CA, USA). Schreiter

et al. describe the advantages of a self-designed small titanium chamber: postoperatively no recovery period was necessary, younger animals could be used and their stress was supposed to be reduced[1]. However, titanium chambers are not MRI compatible and screw fixation is necessary. Furthermore, titanium is difficult to process and cannot be manufactured in life science facilities.

Innovative developments are chambers made of plastic, which have been used for years in Japan and the US. The first plastic chamber made of Duracon was described in 2003 by Ushiyama et al.[17]. The publication illustrated reduced tilting and supposed distress reduction, because of the lightweight Duracon material. However, quantification of tilting and distress was not performed. In addition, these early plastic chambers continued to use screw fixation[17,35]. These screws penetrate the skin and cause large wounds at the chamber basis.

A further weight reduction was achieved by using thermoplastic PEEK. PEEK is characterized by a high flexural modulus (3738 MPa) and tensile strength (100 MPa) compared to Duracon (2500 MPa, 87 MPa) and acrylic glass (3210 MPa, 75 MPa)[36]. PEEK can therefore resist the bite of rodents. Furthermore, PEEK can be fabricated with additive manufacturing processes, which results in further advantages such as a high degree of geometric freedom, low production costs and the flexibility regarding the unique or single-part production[37].

The first lightweight PEEK chambers were introduced by Gaustad et al. and Seynhaeve et al.[23,28]. The PEEK chamber weight was as low as 1 g and 1.1 g, respectively. The chambers were fixed using sutures (Gaustad) or small screws (Seyhaeve). Mice fitted with the chambers showed a full capacity of motion, climbed, and gained weight as mice without chambers. We observed similar positive effects for PEEK chambers (body weight, climbing, mobility). In addition, we verified reduced distress using a standardized protocol. We have repetitively measured chamber tilting and found that the PEEK chambers significantly reduce tilting in the third week of the experiment. Lightweight chambers with reduced lateral tilting enable increased observation times of up to one month[27]. This is especially relevant for biomaterial and oncology research: dorsal skinfold chamber observation times of three to five weeks could enable to study long-term biomaterial integration (fibrosis, giant cell formation, implant vascularization)[38]. In oncology, longer observation times could significantly improve the model, since the growth of tumor cells already preoccupies large parts of the current maximum observation time[39].

The reduction in tilting was significant, although the measurement method had limitations, as the chamber position depends on the body position. The measurement was performed on anaesthetized animals in an upright position with all feet on the ground. However, when positioning the animals, slight deviations of the angles occurred.

Another limitation of the study is that the standardized distress score does not focus on the immobilization of the test animals. However, the impediment of free movement, because of tilting and chamber weight, probably represents the main restriction for the experimental animals. Electronically recording of the animal mobility through tracking systems or recording of the time spent climbing the cage could increase the power of the stress analysis. However, using standardized distress scores enables comparisons to previous experiments.

The low number (n = 6) of test animals may be considered another limitation of the study. However, the PEEK chamber was significantly superior in major outcomes, such as tilting and weight loss. Therefore, no additional experimental animals had to be included. Another limitation related to the study design is that the PEEK and the titanium chambers have different sizes. Hence, all conclusions are related to the design (height, weight), but not to the material (PEEK vs. titanium). Low and lightweight titanium chambers may also decrease animal distress compared to large standard titanium chambers. Yet, we consider PEEK a more suitable material because it increases availability, enables imaging, and decreases costs. These main advantages render a light titanium group obsolete.

Conclusion. In experiments with dorsal skinfold chambers, the animals are particularly stressed by classical titanium chambers. This setup should be revised, in the context of 3R. Despite the development of smaller and lighter chambers, most dorsal skinfold chamber experiments in recent years have continued to use titanium chambers. We have shown that lighter chambers can significantly reduce animal distress and even extend the maximum experiment duration. Chambers made of PEEK are particularly suitable for this purpose: They are autoclavable, sufficiently stable to withstand rodents, inexpensive, and widely available through 3D printing.

Methods

PEEK chamber printing. The PEEK chamber was designed for geometric shape improvement, weight reduction, and optimization for additive manufacturing using SolidWorks (Dassault Systèmes, Waltham, MA, USA). The Fused Filament Fabrication (FFF) process and the printer Minifactory ultra (miniFactory Oy LTD, Seinäjoki, Finland) were used for chamber printing. The design (*.stl file) was imported to Simplify3d (Simplify3d, Ohio, US). Biocompatible and steam sterilizable PEEK filament Intamsys Funmat HT (INTAMSYS Technology Co. Ltd, Shanghai, China) with a flexural modulus of 3738 MPa and tensile strength of 100 MPa was chosen. The material-dependent printing parameters were 230 °C chamber temperature, 190 °C bed temperature, 420 °C nozzle temperature 0.4 mm nozzle diameter, and 18 mm/s printing speed. Slicing was done according to the manufacture settings with a corresponding layer thickness of 250 µm. A brim of 3 mm gave optimal hold to the chamber on the printer bed. To ensure a plane chamber surface for skin contact side, the bottom of the chamber was placed on the printer glass bed for slicing. An extrusion multiplexer of 1.02 was set to fill production-related gaps between the filaments in the x–y direction (see supplementary PEEK chamber 3D printing protocol). Irregularities on the top side (window side) were ground manually after the printing process (printed chamber before polishing shown in supplementary Figure S1 and polished surface shown in Fig. 2B). Seven holes of 1 mm diameter were drilled into the frames for suture chamber fixation using a template. Before experimental use, the chamber was visually proved and post processed by steam sterilization.

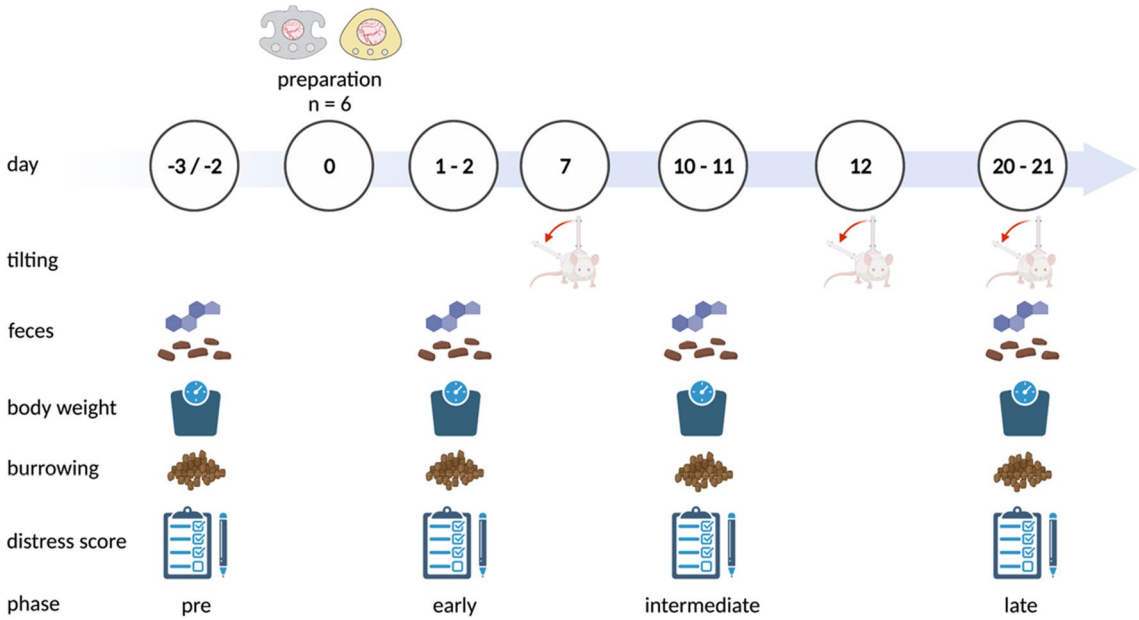

Figure 6. Experimental design. The dorsal skinfold chambers were implanted on day 0. Tilting angles were assessed on day 7, 12 and 21. Collection of faeces, body weight measurement, burrowing analysis and distress scoring were performed in a preoperative, early, intermediate, and late postoperative phase. Figure created with BioRender.com.

Animals and ethics statement. All in vivo experiments were conducted in accordance with the German legislation on protection of animals (7221.3-1-012/20) and the NIH Guide for the Care and Use of Laboratory Animals (Institute of Laboratory Animal Resources, National Research Council). Male hairless SKH1/hr mice (6–10 weeks of age and weight of 25–30 g) were used for all experiments. The animals were housed individually in a specific pathogen-free facility with a twelve-hour light–dark cycle and access to standard laboratory chow and water ad libitum.

Study design. Twelve mice were randomly allocated to two experimental groups: titanium chamber and PEEK chamber. Each animal was one experimental unit and examined independently using body weight, faecal corticosterone metabolites (FCMs), burrowing activity and clinical distress scores on days 1/2, 10/11 and 20/21 after dorsal skinfold chamber preparation. Following distress and tilting measurements on day 21, mice were sacrificed (Fig. 6).

Experimental procedures. Dorsal skinfold chamber implantation: Mice were anesthetized by an intraperitoneal (ip) injection of ketamine/xylazine (90/10 mg/kg bw) and positioned on a heating pad (37.8 °C). Microsurgery for dorsal skinfold titanium chamber implantation has been described before[5]. The significant change in the proposed model is the preparation without screws: After disinfection of the dorsal skin (Octeniderm, Schülke & Mayr GmbH, Norderstedt, Germany) and marking of the median line, a skin bilayer was stretched in the median line. Subsequently, the back of the PEEK chamber was sutured to the skin fold through the preformed holes (FiberWire, Arthrex, Munich, Germany). The preparation area was color-marked and the microsurgical preparation of the front side was performed. After completion of the preparation, the front of the chamber was placed congruently and fixed by three sutures connecting both chamber frames (Fig. 2).

Chamber tilting. For chamber tilting analysis, animals were sedated in an isoflurane chamber for approximately ten seconds on days 7, 12, and 20/21. The sedated animals were positioned upright, with all feet on the floor. In the upright position, the animals were photographed from behind. In Photoshop software (Adobe Inc., San José, U.S.), the lateral tilting angle was measured in degrees of deviation from a vertical line.

Body weight. The body weight was measured on a scale (EMB 200-2, Kern & Sohn, Balingen, Germany) at 9:00–9:30 am. Percent change in body weight was determined by comparison with body weight in the preoperative phase.

Distress score. Since handling may affect animal distress, the distress score was assessed before weighting. The distress score sheet comprises body weight, general condition, spontaneous behaviour, flight behaviour and process-specific criteria, as previously published[40]. (Suppl. Tables S2 and S3).

Burrowing. To quantify the burrowing activity, a tube (length: 15 cm, diameter: 6.5 cm) filled with 200 ± 1 g of food pellets (ssniff Spezialdiaeten GmbH, Soest, Germany) was placed in the left back corner of the cages 3 h before the dark phase at 04:00–04:10 pm. Despite the implanted chambers, mice had free access to these pellets throughout the whole observation time. The weight of the food pellets (g) left in the tube was measured on the next day.

Faecal corticosterone metabolites (FCMs). After weighting, the bedding with old faeces was removed and replaced by fresh beddings. After 24 h, at least 400 mg faeces were collected per cage. The faeces were dried for 4 h at 65 °C and kept at − 20 °C until further processing. 50 mg of homogenized, dried faeces were extracted with 1 mL of 80% methanol and FCMs analyzed with a 5α-pregnane-3β, 11β, 21-triol-20-one enzyme immunoassay[41,42]. FCMs were evaluated blinded, and the percentage of FCMs was determined by comparison to respective FCM concentrations in the pre-operative phase.

Intravital microscopy. Representative intravital microscopy was performed on day 3. Mice were anesthetized and placed on a plexiglass pad with integrated heating. For the visualization of the microvascular system fluorescein isothiocyanate–labeled (FITC)-dextran (0.05 ml, 5%, MW: 150 kD) was injected into the lateral tail vein (or into the retrobulbar venous plexus if tail vein injection failed). Intravital microscopy was performed with 50-, 100- and 200-fold magnification using an Axiotech vario microscope (Carl Zeiss AG, Oberkochen, Germany) with a 100-W HBO mercury lamp with a blue filter (excitation, 450–490 nm; emission, 520 nm) The microscopic images were recorded on DVD (DMR-EX99V, Panasonic, Kadoma, Japan) using a charge-coupled video camera (FK 6990A-IQ, Pieper, Berlin, Germany) for off-line evaluation.

Statistics. Data were graphed and analyzed with GraphPad Prism (version 8.0.1, GraphPad Software Inc., San Diego, CA, U.S.) and were presented as median and 95% confidence interval. The characteristics of data were assessed by Shapiro Wilk test. When analyzing the influence of time on the dependent variables, a Friedman Test was performed (corrections of multiple comparisons using Dunn test) in tilting angles, burrowing activity, percentage of FCMs and distress score, and a one-way repeated measure ANOVA was performed (corrections of multiple comparisons using Tukey test) in the percentage of body weight change analysis. When analyzing the influence of the chambers on the dependent variables, a Mann Whitney Rank sum test (for non-parametric data) or unpaired t test (for parametric data) was used. Differences with $p < 0.05$ were considered significant. Data are given as median/95% confidence interval.

Data availability

The datasets generated and analyzed during the current study are available from the corresponding author on reasonable request.

Received: 18 November 2021; Accepted: 30 May 2022
Published online: 08 July 2022

References

1. Schreiter, J., Meyer, S., Schmidt, C., Schulz, R. M. & Langer, S. Dorsal skinfold chamber models in mice. *GMS Interdiscip. Plast. Reconstr. Surg. DGPW* **6**, DOC10 (2017).
2. Pappelbaum, K. I. *et al.* Ultralarge von Willebrand factor fibers mediate luminal *Staphylococcus aureus* adhesion to an intact endothelial cell layer under shear stress. *Circulation* **128**, 50–59 (2013).
3. Butschkau, A. *et al.* Contribution of protein Z and protein Z-dependent protease inhibitor in generalized Shwartzman reaction. *Crit. Care Med.* **41**, e447–e456 (2013).
4. Hillgruber, C. *et al.* Blocking von Willebrand factor for treatment of cutaneous inflammation. *J. Invest. Dermatol.* **134**, 77–86 (2014).
5. Kram, L., Grambow, E., Mueller-Graf, F., Sorg, H. & Vollmar, B. The anti-thrombotic effect of hydrogen sulfide is partly mediated by an upregulation of nitric oxide synthases. *Thromb. Res.* **132**, e112–e117 (2013).
6. Grambow, E. *et al.* Effect of the hydrogen sulfide donor GYY4137 on platelet activation and microvascular thrombus formation in mice. *Platelets* **25**, 166–174 (2014).
7. Ampofo, E. *et al.* Role of protein kinase CK2 in the dynamic interaction of platelets, leukocytes and endothelial cells during thrombus formation. *Thromb. Res.* **136**, 996–1006 (2015).
8. Hergert, B., Grambow, E., Butschkau, A. & Vollmar, B. Effects of systemic pretreatment with CpG oligodeoxynucleotides on skin wound healing in mice. *Wound Repair Regen.* **21**, 723–729 (2013).
9. Sorg, H., Grambow, E., Eckl, E. & Vollmar, B. Oxytocin effects on experimental skin wound healing. *Innov. Surg. Sci.* **2**, 219–232 (2017).
10. Dau, M. *et al.* Collagen membranes of dermal and pericardial origin-In vivo evolvement of vascularization over time. *J. Biomed. Mater. Res. A* **108**, 2368–2378 (2020).
11. Hightower, C. M. & Intaglietta, M. The use of diagnostic frequency continuous ultrasound to improve microcirculatory function after ischemia-reperfusion injury. *Microcirculation* **14**, 571–582 (2007).
12. Püschel, A., Lindenblatt, N., Katzfuss, J., Vollmar, B. & Klar, E. Immunosuppressants accelerate microvascular thrombus formation in vivo: role of endothelial cell activation. *Surgery* **151**, 26–36 (2012).
13. Hillgruber, C. *et al.* Blocking neutrophil diapedesis prevents hemorrhage during thrombocytopenia. *J. Exp. Med.* **212**, 1255–1266 (2015).
14. Baron, V. T., Welsh, J., Abedinpour, P. & Borgström, P. Intravital microscopy in the mouse dorsal chamber model for the study of solid tumors. *Am. J. Cancer. Res.* **1**, 674–686 (2011).
15. Nesbitt, H. *et al.* The unidirectional hypoxia-activated prodrug OCT1002 inhibits growth and vascular development in castrate-resistant prostate tumors. *Prostate* **77**, 1539–1547 (2017).

16. Peng, W. *et al.* Targeted photodynamic therapy of human head and neck squamous cell carcinoma with anti-epidermal growth factor receptor antibody Cetuximab and Photosensitizer IR700DX in the mouse skin-fold window chamber model. *Photochem. Photobiol.* **96**, 708–717 (2020).
17. Ushiyama, A., Yamada, S. & Ohkubo, C. Microcirculatory parameters measured in subcutaneous tissue of the mouse using a novel dorsal skinfold chamber. *Microvasc. Res.* **68**, 147–152 (2004).
18. Russell, W. M. & Burch, R. L. *The Principles of Humane Experimental Technique* (Methuen, 1959).
19. Michael, S., Sorg, H., Peck, C.-T., Reimers, K. & Vogt, P. M. The mouse dorsal skin fold chamber as a means for the analysis of tissue engineered skin. *Burns* **39**, 82–88 (2013).
20. Alieva, M., Ritsma, L., Giedt, R. J., Weissleder, R. & van Rheenen, J. Imaging windows for long-term intravital imaging: General overview and technical insights. *Intravital* **3**, e29917 (2014).
21. Guo, F. *et al.* Biomechanical evaluation of a customized 3D-printed polyetheretherketone condylar prosthesis. *Exp. Ther. Med.* **21**, 348 (2021).
22. Alqurashi, H. *et al.* Polyetherketoneketone (PEKK): An emerging biomaterial for oral implants and dental prostheses. *J. Adv. Res.* **28**, 87–95 (2021).
23. Seynhaeve, A. L. B. & ten Hagen, T. L. M. Intravital microscopy of tumor-associated vasculature using advanced dorsal skinfold window chambers on transgenic fluorescent mice. *J. Vis. Exp.* **131**, e55115 (2018).
24. Gu, J.-M. *et al.* Blockade of placental growth factor reduces vaso-occlusive complications in murine models of sickle cell disease. *Exp. Hematol.* **60**, 73-82.e3 (2018).
25. Tong, F. *et al.* Hypo-fractionation radiotherapy normalizes tumor vasculature in non-small cell lung cancer xenografts through the p-STAT3/HIF-1 alpha signaling pathway. *Ther. Adv. Med. Oncol.* **12**, 1758835920965853 (2020).
26. Nawijn, C. *et al.* Multi-timescale microscopy methods for the characterization of fluorescently-labeled microbubbles for ultrasound-triggered drug release. *J. Vis. Exp.* **172**, e62251 (2021).
27. Axelsson, H., Bagge, U., Lundholm, K. & Svanberg, E. A one-piece plexiglass access chamber for subcutaneous implantation in the dorsal skin fold of the mouse. *Int. J. Microcirc. Clin. Exp.* **17**, 328–329 (1997).
28. Gaustad, J.-V., Brurberg, K. G., Simonsen, T. G., Mollatt, C. S. & Rofstad, E. K. Tumor vascularity assessed by magnetic resonance imaging and intravital microscopy imaging. *Neoplasia* **10**, 354–362 (2008).
29. Choi, M., Chung, T., Choi, K. & Choi, C. Dynamic fluorescence imaging for multiparametric measurement of tumor vasculature. *J. Biomed. Opt.* **16**, 046008 (2011).
30. Shan, S. *et al.* Preferential extravasation and accumulation of liposomal vincristine in tumor comparing to normal tissue enhances antitumor activity. *Cancer Chemother. Pharmacol.* **58**, 245–255 (2006).
31. Gelaw, B. & Levin, S. Wound-induced angiogenesis and its pharmacologic inhibition in a murine model. *Surgery* **130**, 497–501 (2001).
32. Leunig, M., Yuan, F., Gerweck, L. E. & Jain, R. K. Effect of basic fibroblast growth factor on angiogenesis and growth of isografted bone: Quantitative in vitro-in vivo analysis in mice. *Int. J. Microcirc. Clin. Exp.* **17**, 1–9 (1997).
33. Palme, R. Non-invasive measurement of glucocorticoids: Advances and problems. *Physiol. Behav.* **199**, 229–243 (2019).
34. Ibarguen-Vargas, Y., Surget, A., Touma, C., Palme, R. & Belzung, C. Multifaceted strain-specific effects in a mouse model of depression and of antidepressant reversal. *Psychoneuroendocrinology* **33**, 1357–1368 (2008).
35. Leung, H. M., Schafer, R., Pagel, M. M., Robey, I. F. & Gmitro, A. F. Multimodality pH imaging in a mouse dorsal skin fold window chamber model. *Proc. SPIE Int. Soc. Opt. Eng.* **8574**, 85740L (2013).
36. Roderick, R., Xavier, B., Philippe, B., Olli, P. & Riku, H. Semi-crystalline Kepstan® PEKK seals via fused filament fabrication on the miniFactory Ultra®. https://www.extrematerials-arkema.com/files/live/sites/arkema_extrematerials/files/downloads/brochures/kepstan-brochures/kepstan-br-semicrystalline-kepstan-pekk-seals-optimized.pdf (2021).
37. Vaezi, M. & Yang, S. Extrusion-based additive manufacturing of PEEK for biomedical applications. *Virtual Phys. Prototyp.* **10**, 123–135 (2015).
38. Laschke, M. W. & Menger, M. D. The dorsal skinfold chamber: A versatile tool for preclinical research in tissue engineering and regenerative medicine. *Eur. Cell. Mater.* **32**, 202–215 (2016).
39. Boucher, Y., Leunig, M. & Jain, R. K. Tumor angiogenesis and interstitial hypertension. *Cancer Res.* **56**, 4264–4266 (1996).
40. Xie, W. *et al.* Diagnostic ability of methods depicting distress of tumor-bearing mice. *Animals (Basel)* **11**, 2155 (2021).
41. Touma, C., Sachser, N., Möstl, E. & Palme, R. Effects of sex and time of day on metabolism and excretion of corticosterone in urine and feces of mice. *Gen. Comp. Endocrinol.* **130**, 267–278 (2003).
42. Touma, C., Palme, R. & Sachser, N. Analyzing corticosterone metabolites in fecal samples of mice: A noninvasive technique to monitor stress hormones. *Horm. Behav.* **45**, 10–22 (2004).

Acknowledgements

We thank the staff of the Rudolf-Zenker-Institute for Experimental Surgery for the care of the animals during the experiments and Edith Klobetz-Rassam for FCM analysis.

Author contributions

D.S., E.G., D.Z. and B.V. conceived and designed the experiments; W.X., M.L. and F.P. performed the experiments. R.P., W.X., D.S. and E.G. analyzed the data. M.L., and R.P. contributed materials/analysis tools; D.S., E.G. and W.X. wrote the paper. All authors approved the final version of the manuscript.

Funding

Open Access funding enabled and organized by Projekt DEAL. This joint research project HOGEMA is supported by the European Social Fund (ESF), reference: ESF/14-BM-A55-0012/18, and the Ministry of Education, Science and Culture of Mecklenburg-Vorpommern, Germany. Evaluation of distress was supported by the Deutsche Forschungsgemeinschaft (DFG research group FOR 2591, ZE 712/1-1, ZE 712/1-2, VO 450/15-1 and VO 450/15-2).

Competing interests

The authors declare no competing interests.

Additional information

Supplementary Information The online version contains supplementary material available at https://doi.org/10.1038/s41598-022-13924-5.

Correspondence and requests for materials should be addressed to E.G.

Reprints and permissions information is available at www.nature.com/reprints.

Publisher's note Springer Nature remains neutral with regard to jurisdictional claims in published maps and institutional affiliations.

Open Access This article is licensed under a Creative Commons Attribution 4.0 International License, which permits use, sharing, adaptation, distribution and reproduction in any medium or format, as long as you give appropriate credit to the original author(s) and the source, provide a link to the Creative Commons licence, and indicate if changes were made. The images or other third party material in this article are included in the article's Creative Commons licence, unless indicated otherwise in a credit line to the material. If material is not included in the article's Creative Commons licence and your intended use is not permitted by statutory regulation or exceeds the permitted use, you will need to obtain permission directly from the copyright holder. To view a copy of this licence, visit http://creativecommons.org/licenses/by/4.0/.

© The Author(s) 2022